Ultrafast Dynamics of Carotenoid Excited States−From Solution to Natural and Artificial Systems

Tomáš Polívka* and Villy Sundström

Department of Chemical Physics, Lund University, Box 124, SE−221 00 Lund, Sweden

Received June 10, 2003

Contents

1. Introduction

Carotenoids are, along with chlorophylls, the most abundant pigments found in nature. They are present in most organisms including humans but can be synthesized only by plants and microorganisms. While they are perhaps best known for their bright colors, they have well-documented multiple functions in nature: they serve as light-harvesting pigments in almost all photosynthetic organisms covering a region of the visible spectrum not accessible by (bacterio)chlorophylls ((B)Chl) and they protect against excessive light by quenching both singlet and triplet states of (B)Chls.[1−5] Outside photosynthesis, they are known as efficient quenchers of dangerous singlet oxygen and various reactive radicals by intercepting the chain of oxidative reactions.[6] There is accumulating evidence that this antioxidative function is a key mechanism of protection against various diseases including cancer, atherosclerosis, and macular degeneration in humans.[7,8] Yet, knowledge of the detailed molecular mechanism of such actions is so far very limited.

Most of the experimental and theoretical effort aiming for deeper knowledge of carotenoid excited-state dynamics performed in recent years was driven by the ability of carotenoids to transfer sunlight energy absorbed by their singlet excited states to (B)Chls, thereby actively participating in the light-harvesting process. The first study providing clear evidence of the light-harvesting function of carotenoids was performed more than 60 years ago.[9] It represented a milestone that promoted further interest in studies of carotenoid excited states. Due to the absence of spectroscopic methods allowing one to follow the excited-state dynamics of carotenoids, the time period until the late 1980s was characterized by studies relying mostly on measurements of fluorescence excitation spectra. Experiments carried out during this period, which are reviewed, for example, by Govindjee,[10] established the involvement of carotenoid excited states in energy transfer between carotenoids and (B)Chls and demonstrated that quantum yields of carotenoid−(B)Chl transfer are not far from unity in some cases. Along with the efforts to understand details behind the light-harvesting function of carotenoids, a number of studies of carotenoids and their close relatives polyenes in solution were performed. In 1972, an important breakthrough in the field of carotenoid photophysics was reported; it was demonstrated that the absorbing state of longer polyenes is not the lowest excited state but that an additional, 'dark' state is located between the ground state and the absorbing state.[11,12] This discovery radically affected further research on caro-

* To whom correspondence should be addressed. Fax: +46-46-222-4119. E-mail: tomas.polivka@chemphys.lu.se.

10.1021/cr020674n CCC: $48.50
Published on Web 02/18/2004

Tomáš Polivka was born in the Czech Republic in 1968, and he is currently a senior researcher at the Department of Chemical Physics, Lund University. He received his M.Sc. degree in Physics (1992) and his Ph.D. degree in Chemical Physics (1996) from Charles University in Prague, where he worked in the optical spectroscopy group at the Department of Chemical Physics and Optics. Since 1997 he has been working in the group of Professor Villy Sundström at Lund University. His research interests focus on studies of excited-state dynamics of photosynthetic pigments and on functions of carotenoids in various biological systems. He is also working on studies of energy and electron transfer in artificial systems mimicking processes in natural photosynthesis.

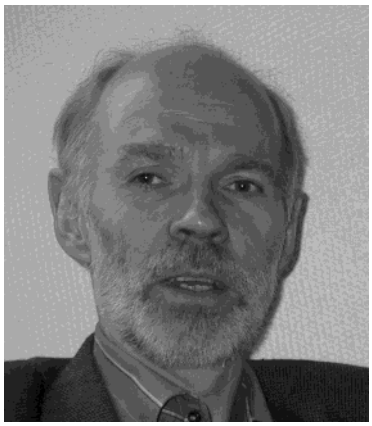

Villy Sundström is presently professor of Chemical Physics at Lund University, Sweden. He received his Ph.D. degree in 1977 at Umeå University, also in Sweden, after studies at Bell Labs, Murray Hill, NJ. In 1978 he introduced the field of ultrafast spectroscopy to Scandinavia by establishing the first picosecond laboratory in Umeå, Sweden. In 1994 he moved to Lund University to initiate a new research group and the Department of Chemical Physics. Today the group consists of ~20 students, postdoctoral fellows, and senior scientists, working on a range of related topics: energy and electron transfer in natural and artificial photosynthesis, photophysics, excited-state dynamics, and functions of carotenoid molecules, interfacial electron transfer in sensitized semiconductor systems, excited-state and charge dynamics in conjugated polymers, and reaction dynamics.

tenoid photophysics, as a major part of the experimental and theoretical studies was directed toward localization of this dark state and elucidation of its role in light harvesting and photoprotection. Further theoretical investigations of polyenes showed that other dark states occur in the vicinity of the absorbing state,[13] and these additional dark states were only recently tackled by experimental methods.[14,15] The studies on polyenes are vitally important for understanding carotenoid photophysics, and the reader is referred to reviews by Orlandi[16] or Hudson[17] for a more detailed account.

Another turning point in carotenoid photophysics came in the late 1980s with the availability of spectroscopic methods enabling investigation the dynamics of excited states on (sub)picosecond time scales. Since the pioneering experiment performed by Wasielewski and Kispert, who were the first to measure the S_1 lifetime of β-carotene,[18] a large number of successive experiments, often supported by theoretical investigations, attempted to disentangle the complicated picture of carotenoid excited-state dynamics in both solution and various light-harvesting complexes. The initial period of the time-resolved studies of carotenoid excited states was reviewed a few years ago[2,3,19] and therefore will not be described here in detail. This review focuses predominantly on the last six years of research on carotenoid excited states. This period is characterized mainly by various experimental approaches to locate the dark S_1 state of carotenoids and to reveal its role in light-harvesting processes. Besides the localization of the S_1 state, a number of other important discoveries were made that again significantly changed the picture of carotenoid excited-state dynamics. First, other dark excited states were experimentally found,[15,20] and their roles in relaxation and energy-transfer pathways are still a matter of debate. Second, unique properties of excited states of carotenoids having a conjugated carbonyl group were discovered, exhibiting solvent-dependent relaxation schemes.[21−23] This family of carotenoids exhibits polarity-driven excited-state dynamics, and exact relaxation patterns and their relation to the polarity of the environment are still unclear. The first part of the review focuses on excited states of carotenoids in solution, as knowledge of relaxation pathways in isolated carotenoids is a necessary prerequisite to understand carotenoid dynamics in complex systems. The second part deals with carotenoids in light-harvesting systems, reviewing the progress in understanding of mechanisms and pathways of carotenoid−B(Chl) energy transfer in the past few years. The new discoveries made for carotenoids in solution were naturally reflected in studies of their light-harvesting function, and the purpose of this part of the review is to summarize our current knowledge of light harvesting by carotenoids in various antenna systems. We focus here mainly on singlet−singlet energy transfer between carotenoids and (B)Chls. The complete patterns of energy-transfer pathways including energy transfer between (B)Chls and/or triplet−triplet energy transfer were already summarized in specialized reviews focusing on bacterial light-harvesting complexes[24−27] or light-harvesting complexes from higher plants.[5,28] Similarly, a review by Britton[29] gives an excellent overview of steady-state spectroscopic properties of carotenoids, and the details will not be repeated here. Although theoretical investigations of carotenoid−(B)Chl energy transfer are included in the review, details about theoretical methods are omitted. These details can be found in the particular references or in a recent review by Ritz et al.[4] that summarizes various factors controlling the efficiency of energy transfer between carotenoids and (B)Chls on a theoretical level. Unlike these more specialized reviews,

our main purpose is to summarize the current knowledge of excited-state dynamics of carotenoids in a broader context by directly comparing investigations of carotenoids in solution, protein complexes, and artificial systems.

2. Theoretical Background

The diversity of carotenoid functions is unmatched by any other class of natural pigments. The functional variety is directly related to their unique spectroscopic properties resulting from the structure of the carotenoid molecule (Figure 1). The central pattern repeated in all carotenoids is a backbone consisting of alternating single and double carbon bonds that form a conjugated π-electron system responsible for most of the spectroscopic properties of carotenoids. Until recently, most of our knowledge of the properties of carotenoid excited states was largely based on spectroscopic studies of polyenes that belong to the same idealized C_{2h} point symmetry group as carotenoids. In terms of C_{2h} symmetry labels, the two low-lying singlet excited states denoted $2^1A_g^-$ and $1^1B_u^+$, are responsible for most of the spectroscopic properties of carotenoids. Since the ground state of carotenoids is of A_g^- symmetry, the one-photon transition between the ground state and the $2^1A_g^-$ state is symmetry forbidden while that between the ground state and the $1^1B_u^+$ state is allowed. In 1972, experiments on the polyene diphenyloctatetraene,[12] supported by calculations,[11] established that the lowest excited state in this polyene is located below the strongly allowed $1^1B_u^+$ state, making the lowest energy transition symmetry forbidden. This discovery aroused a number of experimental and theoretical studies of polyenes, which established that the forbiddenness of the lowest energy transition is a common feature of all polyenes having conjugation length $N > 3$.[13] This 'reverse' ordering of the excited states is also a central feature of all carotenoids occurring in nature, since most of them have a conjugation length between 7 and 13 (Figure 1).

While the $1^1B_u^+$ state, in terms of molecular orbitals, is described by a simple HOMO → LUMO transition, the theoretical explanation for the fact that the $2^1A_g^-$ state lies below the $1^1B_u^+$ state requires involvement of highly excited configurations that are able to take into account electron−electron interactions.[13,30−32] To properly describe the properties of the $2^1A_g^-$ state, at least doubly excited configurations must be used because this state represents a mixture of singly and doubly excited configurations. In terms of molecular orbitals, the singly excited configurations correspond to (HOMO-1) → (LUMO) and (HOMO) → (LUMO+1) transitions while the most important doubly excited configuration is the (HOMO, HOMO) → (LUMO, LUMO) transition.[16] Using doubly excited configurations is usually enough to push the $2^1A_g^-$ state below the $1^1B_u^+$, but quantitative agreement between experimental and theoretical $2^1A_g^-$ energies required even higher configuration interaction.[13,30−32] The doubly excited character of the $2^1A_g^-$ state can be rationalized as involving two 1^3B_u triplet excitations that are coupled to an overall singlet state, which explains the fact that the energy of the $2^1A_g^-$ state is about twice the energy of the lowest triplet state.[13] Besides these two states of ionic (B_u^+) and covalent (A_g^-) nature, other covalent states formed by various combinations

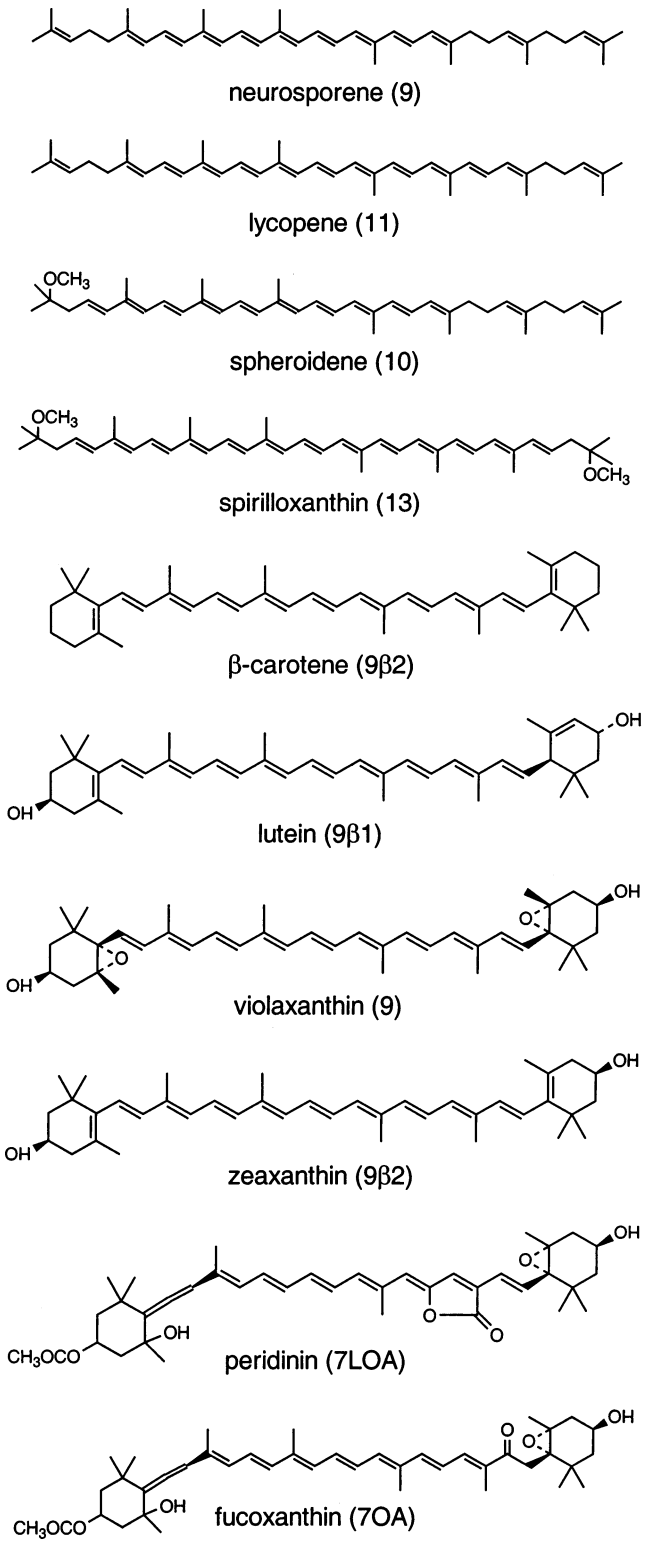

Figure 1. Molecular structures of carotenoids frequently used for studies of excited-state dynamics. Conjugation length is denoted in parentheses as follows: *N*, number of conjugated C=C bonds in the linear conjugated backbone; *βn*, conjugation extended to *n* C=C bonds located at a terminal ring; O, conjugation extended to a carbonyl group; LO, conjugation extended to a carbonyl group located at a lactone ring; A, conjugation extended to an allene moiety.

of triplet excitations coupled to a singlet state exist in the excited-state manifold of polyenes and carotenoids. From a spectroscopic point of view, the most interesting ones are the $1^1B_u^-$ and $3^1A_g^-$ states that are formed as a combination of 1^3B_u and 1^3A_g and 1^3A_g and 1^3A_g triplet states, respectively,[13] because the energies of these states approach the energy of the absorbing $1^1B_u^+$ state as the conjugation length increases to $N \approx 11$.[13] Detailed descriptions of the electronic properties of the excited states of polyenes can be found elsewhere.[16,17,33]

Throughout this review we use the following notation to describe excited states of carotenoids. In the symmetry notation, we will omit the spin index for singlet states. For description of excited states, we will follow the conventional notation used throughout literature about carotenoid excited states to date, thus, the absorbing $1B_u^+$ state will be called the S_2 state and the dark $2A_g^-$ state the S_1 state. When other states are discussed, they will be designated by their symmetry label.

3. Excited States in Solution

Knowledge of the properties of excited states of carotenoids in solution is a necessary prerequisite for understanding their functions in more complex natural and artificial systems. Most of the features of the excited states that have been recognized as important for the functioning of carotenoids in more complex systems have been established by experiments performed in solution. Studies of the energetics and dynamics of carotenoid excited states in various solvents during the past few years have extended our knowledge of their properties inferred from polyenes, leading to discoveries of new states and their dependencies on solvent parameters. This revealed new, previously unknown, relaxation pathways that are of high importance for functionality of carotenoids in more complex systems. An energy-level scheme of a carotenoid molecule together with transitions that will be used to describe the dynamics of excited states in the following sections is depicted in Figure 2.

3.1. S_2 State

The strong absorption of carotenoids (extinction coefficients on the order of 10^5) in the blue-green spectral region is caused by the strongly allowed S_0-S_2 transition.[29] The S_0-S_2 transition of carotenoids usually exhibits a characteristic three-peak structure corresponding to the lowest three vibrational levels of the S_2 state (Figure 3). The energy gap between vibrational peaks of $\sim$1350 cm^{-1} results from the combination of two symmetric vibrational modes with energies of $\sim$1150 (C−C stretch) and $\sim$1600 cm^{-1} (C═C stretch). The resolution of vibrational peaks in the absorption spectrum is an important spectroscopic measure as it reflects certain structural properties of a carotenoid molecule. The vibrational structure is well resolved for linear carotenoids such as lycopene or spheroidene, while a clear loss of resolution of vibrational bands is observed for carotenoids having conjugation extended to various end groups. A typical example is β-carotene, for which

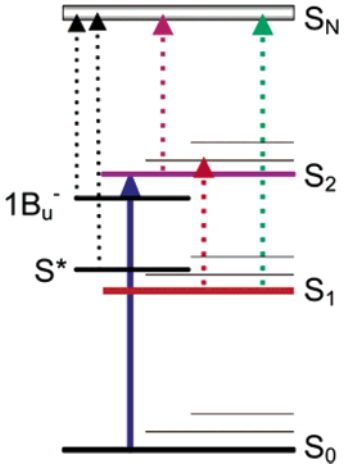

Figure 2. Simplified energy-level scheme of a carotenoid molecule including transitions corresponding to transient signals occurring after excitation (blue arrow). The S_N state in this scheme represents only a symbolic final state for S_1-S_N (green), S_2-S_N (purple), $1B_u-S_N$ (black), and S^*-S_N (black) transitions. In reality, the final states of these transitions must be of different symmetry, and therefore, the S_N state in the scheme consists actually of four different states.

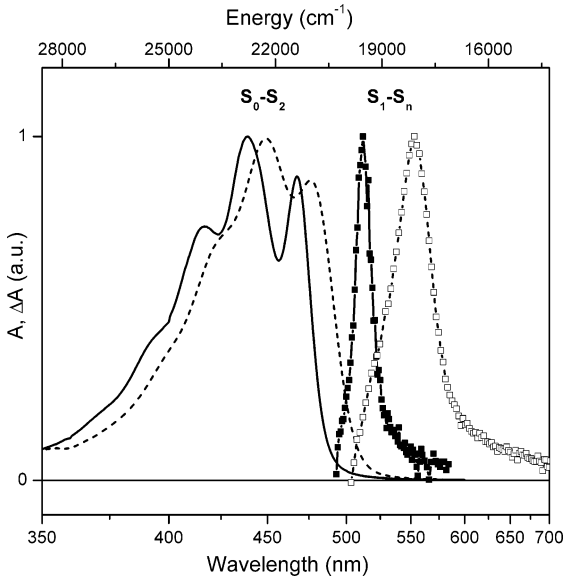

Figure 3. S_0-S_2 (ground-state absorption) and S_1-S_N (excited-state absorption) transitions of violaxanthin (solid line and full symbols) and zeaxanthin (broken line and open symbols) having conjugation lengths of 9 and 11 (9β2), respectively. The S_1-S_N spectra were recorded 3 ps after excitation at 480 nm (violaxanthin) and 490 nm (zeaxanthin). All data were obtained in methanol solution at room temperature.

the conjugation extends to the terminal β-ionylidene rings. The conjugated double bonds located on the β-ionylidene ring are in *s-cis* orientation with respect to the main conjugated backbone (Figure 1), because, as shown recently by density functional calculations, the *s-cis* configuration is more stable.[34] The loss of vibrational resolution is attributed to the repulsion between methyl groups on the β-ionylidene ring and hydrogen atoms on the conjugated backbone that forces the conjugated double bond of the β-ionylidene ring out of plane.[35−37] This situation leads to a broader distribution of conformers, which causes the

Table 1. Energies of the S_2 and S_1 States of Carotenoids[a]

			S_1 energy			
carotenoid[b]	N[c]	S_2 energy	fluorescence	Raman[d]	S_1-S_2	2-photon
spirilloxanthin	13	19 000 (51)	11 900 (51)	11 780 (15)	11 560 ± 200 (67)	
anhydrorhodovibrin	12	19 400 (51)	12 500 (51)	12 195 (15)		
lycopene	11	19 900 (51)	13 300 (51)	13 200 (14) 12 920 (15)	12 500 ± 150 (91)	
rhodopin glucoside	11	20 000 (92)			12 800 ± 200 (92) 12 550 ± 150[e] (92)	
spheroidenone	10O	19 500 (46)			13 200 ± 100 (46)	
spheroidene	10	20 700 (92)	14 200[f] (50)	14 200 (89)	13 400 ± 90[g] (62, 92)	13 900 ± 150[e] (176)
β-carotene	9β2	20 840 (39)	14 200 ± 500 (39) 14 500[h] (52)	14 670 (14) 14 500 (88)		~14 500 (95)
zeaxanthin	9β2	21 010 (84)	14 550 ± 90 (84) 14 610 ± 40[i] (85)		14 030 ± 90 (81) 13 850 ± 200[j] (198)	
lutein	9β1	21 200 (293)			14 050 ± 300[j] (198)	<15 100 (95) ~15300[k] (201)
violaxanthin	9	21 230 (84)	14 880 ± 90 (84) 15 580 ± 60[i] (85)		14 470 ± 90 (81) 13 700 ± 300[j] (198)	
nonaene*	9	21 510 (40)	15 120 ± 220 (40)			
neurosporene	9	21 300 (50)	15 300 (50)			
m9-β-carotene*	7β2	22 500 (39)		15 750 (14)		
siphonaxanthin	8O	20 870 (46)	~16 200 (73)		16 610 ± 200 (46)	
fucoxanthin	7OA	20 960 (46)	~16 200 (73)		16 520 ± 200 (46)	
peridinin	7LOA	20 620 (23)	16 200 (45) 16 700 (23 106)		16 100 ± 200 (23)	18 500–18 850 (43) ~16 200 (45)
octaene*	8	22 420 (40)	16 840 ± 170 (40)			
heptaene*	7	23 530 (40)	18 160 ± 40 (40)			

[a] The values correspond to room-temperature measurements unless stated otherwise. Numbers in parentheses are references. Solution measurements were performed in *n*-hexane except for the following cases: violaxanthin, zeaxanthin (81), lutein (293), and rhodopin glucoside (92) in methanol; fucoxanthin and siphonaxanthin in CS_2 (73); lutein in octanol (95); β-carotene in octane (95). [b] Carotenoids marked by asterisk are synthesized molecules that do not occur naturally. [c] Conjugation length. See caption of Figure 1 for explanation. [d] All resonance Raman measurements were carried out with crystalline carotenoid microcrystals deposited on KBr disks. [e] In LH2 complex. [f] At both room temperature and 170 K. [g] In both LH2 complex and *n*-hexane solution. The same value was obtained also in solution at 185 K. [h] At 170 K. [i] At 77 K in EPA glass. [j] In LHCII complexes reconstituted with a single carotenoid species. [k] In native LHCII complexes containing lutein, violaxanthin, and neoxanthin with stoichiometry approximately 1.8:1:0.2.

observed reduction of vibrational structure of the S_0-S_2 transition (Figure 3).

While the resolution of vibrational structure is very little affected by the conjugation length,[38] the energy of the S_0-S_2 transition decreases with the conjugation length. A few recent studies on analogues of the same carotenoid having different conjugation lengths demonstrated that the dependence of the S_2 state energy on conjugation length (N) can be in the first approximation expressed as $E = A + B/N$, where A and B are adjustable parameters.[38–40] While the parameter B is related to the slope of the energy dependence on the conjugation length, parameter A is the energy of the 0–0 vibrational band of the S_0-S_2 transition for an infinite carotenoid. Earlier works on spheroidene and β-carotene analogues suggested that A is ~11 000 cm^{-1} (910 nm),[38,39] but more recent results established it to be around 14 000 cm^{-1} (700 nm) for open chain carotenoids,[40] in good agreement with studies of polyenes.[41] For naturally occurring carotenoids having conjugation lengths in the range 7–13, the 0–0 band of the S_0-S_2 transition is located between 475 and 525 nm (21 200–19 000 cm^{-1}, see Table 1), which gives the bright colors of carotenoids varying from yellow to red. Besides the number of conjugated double bonds, the 0–0 energy is also affected by the structure of a particular carotenoid. For example, the nonplanarity of the conjugated C=C bond located at the β-ionylidene ring discussed above leads to a decrease of the effective conjugation length. This results in higher S_2 energy of β-carotene and zeaxanthin than for their linear counterpart lycopene, which also possesses 11 conjugated double bonds (Table 1).

The energy of the S_0-S_2 transition of carotenoids also depends on the refractive index of the solvent and, consequently, on the polarizability of the solvent. Therefore, in a solvent with high polarizability such as CS_2, the spectral shift of the S_2 state can be as high as 40 nm toward the red.[22,39,42] On the other hand, the polarity of the solvent has only a small effect on the excited states of carotenoids, with the exception of carotenoids possessing a conjugated carbonyl group in their structure. In this case the polarity of the solvent has a dramatic effect on the properties of the excited states.[22] The electron-withdrawing character of the conjugated carbonyl group has a significant effect on the spectroscopic properties since it leads to a pronounced charge-transfer character of both the ground and excited states of a carotenoid.[21–23,43–46] While in nonpolar solvent the shape of the S_0-S_2 transition of a carbonyl carotenoid usually exhibits a typical three-peak character, in polar solvent the vibrational structure is lost and the absorption spectrum is asymmetrically broadened toward longer wavelengths (Figure 4). It was shown that this effect is mostly due to the charge-transfer character of the ground state, while the properties of the S_2 state remain rather unaffected by solvent polarity.[44,45] Stabilization of a negative charge on the carbonyl oxygen in polar solvents enhances the ground-state charge-transfer character

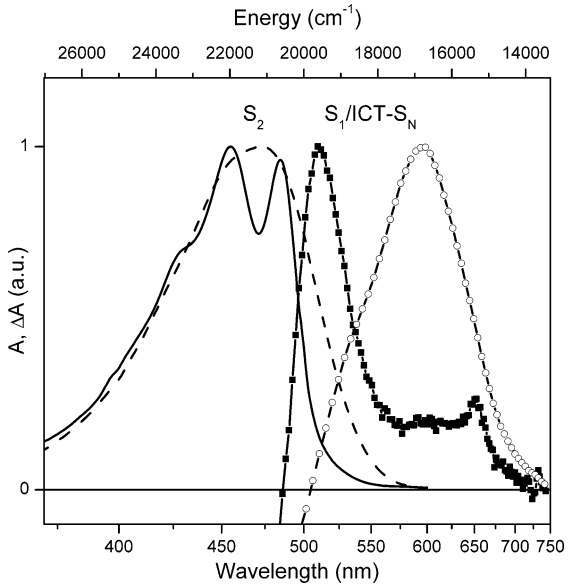

Figure 4. Room-temperature absorption spectra of the carbonyl carotenoid peridinin in *n*-hexane (solid line) and methanol (dashed line). Transient absorption spectra corresponding to the $S_1/ICT-S_N$ transition of peridinin in *n*-hexane (full squares) and methanol (open circles) recorded 1 ps after the excitation at 490 nm are also shown. All spectra are normalized to their absorption maximum.

and leads to the presence of several ground-state conformations, leading to the observed loss of vibrational structure and spectral broadening.[22,44−46] In addition, it was shown that the asymmetric broadening of the peridinin absorption spectrum is enhanced in protic solvents,[44] which are capable of forming a hydrogen bond via the carbonyl oxygen, further stabilizing the charge-transfer character of the ground state. All the carbonyl carotenoids studied so far exhibit a dependence on solvent polarity,[21−23,43−47] although subtle changes in carotenoid structure cause large variation in the magnitude of these changes: while rather small effects are observed for the linear carotenoid spheroidenone containing a carbonyl group in a *s-cis* configuration at the end of the carbon−carbon conjugated backbone,[48,49] the highly substituted carotenoid peridinin having a carbonyl group in the middle of the conjugated chain attached via a lactone ring (see Figure 1) exhibits significant changes of the spectroscopic properties when switched from nonpolar to polar solvent.[22,46]

Longer carotenoids violate Kasha's rule as they exhibit emission from the S_2 state.[37−40] The critical conjugation length for which the S_1 emission, which dominates for shorter conjugation, changes to S_2 emission is around eight conjugated C=C bonds. Studies of a series of open-chain carotenoids demonstrated that those with a conjugation length of eight exhibited dual emission from both the S_1 and S_2 states.[40] A very similar result was obtained for a series of β-carotene analogues, although it was shown that in solvents with high polarizability such as CS_2 the maximal dual emission is observed for an analogue having a conjugation length of nine as a result of the smaller S_2-S_1 energy gap, leading to a decreased S_2 emission quantum yield.[39] The S_2 emission constitutes almost a mirror image of the absorption spectrum with a Stokes shift of 150−300 cm^{-1}, almost independent of conjugation length for carotenoids with conjugation lengths 9−13.[37,38,40,50−52]

While the radiative lifetime of the S_2 state as calculated by the Strickler−Berg equation[53] is in the range of nanoseconds, measured quantum yields of the S_2 emission on the order of 10^{-5} showed that the internal conversion on the subpicosecond time scale governs the S_2 dynamics.[38,40,42] Thus, information about the dynamics of the S_2 state relies solely on ultrafast time-resolved techniques, particularly on fluorescence up-conversion and transient absorption data. Application of these techniques to a number of carotenoids employed in photosynthetic light harvesting established that the S_2 lifetime is in the range of 100−300 fs[42,54−56] and dependent on both conjugation length and solvent parameters. A detailed fluorescence up-conversion study of the effect of solvent properties on the S_2 dynamics of β-carotene[42] demonstrated that increasing the polarizability of solvent decreased the S_2 lifetime of β-carotene from 180 fs in *n*-hexane to 130 fs in CS_2 due to the polarizability shift of the S_2 state, making the S_2-S_1 gap smaller and thus facilitating the internal conversion. For all solvents, the S_2 decay was successfully fitted by a monoexponential decay with no rise component, signaling that no dynamical Stokes shift is present, although the authors detected a slight dependence on probing wavelength for β-carotene in *n*-hexane—the S_2 lifetime was prolonged by about 20 fs at longer detection wavelengths. Similar results were obtained with excitation of β-carotene into higher vibrational levels[56] and were further confirmed also for the linear carotenoid neurosporene.[55] The effect was explained in terms of sub-100 fs vibrational relaxation in the S_2 state (see section 3.4). Interestingly, Ricci et al. observed opposite wavelength dependence of the S_2 emission when the carotenoid spheroidene was excited into the 0−1 vibrational band of the S_2 state.[54] While the dependence on solvent polarizability matches well that observed for β-carotene,[42,56] the S_2 decay is fastest when probed in the red tail of the S_2 emission band. Thus, the excitation into higher vibrational levels of the S_2 state makes the situation more complicated as vibrational relaxation contributes to the dynamics, which was further underlined by the fact that for spheroidene in CS_2 the S_2 decay did not fit well to a single-exponential decay when the S_2 state was excited into the 0−1 vibrational transition. An explanation involving formation of a CS_2−spheroidene exciplex was proposed to justify this anomalous behavior.[54] The fact that more polarizable solvents need a second component for the fitting of S_2 decay was also recognized by Macpherson et al.,[42] implying more complicated interaction with these solvents.

While the solvent effect on the S_2 lifetime was successfully explained using the S_2-S_1 energy gap, the effect of conjugation length and carotenoid structure on the S_2 lifetime is more complicated. The S_2 lifetimes for a series of β-carotene[39] or spheroidene[38] analogues, having conjugation lengths varying from 5 to 13 for β-carotene and 7−13 in the case of spheroidene, were calculated from the S_2 emission

quantum yield and the S_2 radiative lifetimes. A similar approach was used for a series of three open-chain carotenoids.[40] Although the trends of the S_2 lifetime dependence on conjugation length were not consistent in these works, it was obvious that the conjugation length has no dramatic effect on the S_2-S_1 internal conversion rate. This result cannot be explained by the energy gap law since the S_2-S_1 energy gap increases with conjugation length and reaches nearly 10 000 cm^{-1} for the β-carotene analogue with 19 conjugated C=C bonds,[57] while a value of 3340 cm^{-1} was observed for the carotenoid phytoene with 5 C=C bonds.[58] Thus, a ca. 2-fold change of the S_2-S_1 internal conversion rate in the above-mentioned series of carotenoids appears to be inconsistent with such a large narrowing of the S_2-S_1 energy gap. Frank et al. proposed that a higher density of accepting vibrational modes could compensate for the large S_2-S_1 energy gap for longer carotenoids, counteracting the decrease of S_2-S_1 internal conversion rate due to energy gap.[40]

Direct measurements of the S_2 lifetime for carotenoids with different conjugation lengths and structures provide further support to the hypothesis that the S_2-S_1 energy gap is not the only crucial factor that determines the S_2-S_1 internal conversion rate. On the basis of the S_2-S_1 energy gap, the S_2 lifetimes should increase with conjugation length. However, fluorescence up-conversion experiments on three linear carotenoids neurosporene ($N = 9$),[55] spheroidene (10),[54] and rhodopin glucoside (11)[59] revealed S_2 lifetimes of ~230, 170, and 130 fs, respectively. Thus, the S_2 lifetimes exhibit an opposite trend than expected from the S_2-S_1 energy gap. The S_2 lifetimes of β-carotene (11) in various solvents obtained by fluorescence up-conversion fall into the range 130−180 fs, confirming the pattern of increased S_2-S_1 internal conversion rate with conjugation length.[42,56] The effect of carotenoid structure on S_2 lifetimes was investigated by fluorescence up-conversion measurements on β-apo-8′-carotene with different end groups, yielding S_2 lifetimes in range 95−180 fs depending on the structure.[60] Similar results were obtained from transient absorption data. Although the direct measurement of the S_2 lifetime by fitting the rise of the S_1-S_N excited-state absorption (Figure 2) usually suffers by an error as vibrational relaxation in the S_1 state also contributes to the S_1-S_N rise (see section 3.4), this problem was successfully treated by global analysis of kinetics recorded over the whole S_1-S_N band.[61] In addition, a recently discovered S_2-S_N excited absorption band occurring in the near-infrared region provided another possibility to study the S_2 dynamics.[62,63] On the basis of the transient absorption method, it was found that the S_2 lifetime decreases in the order neurosporene ($N = 9$, 320 fs) > spheroidene (10, 250 fs) > lycopene (11, 130 fs).[4] Although these values differ slightly from those obtained by fluorescence up-conversion, the 'reverse' trend is apparent. Similar results were recently obtained for various series of both natural and synthetic carotenoids having conjugation lengths in the range of 7−15.[64−66] Global analysis of both S_1-S_N[20] and S_2-S_N[67] kinetics of spirilloxanthin ($N = 13$) gave a S_2 lifetime of ~90 fs, and fluorescence up-conversion yielded a spirilloxanthin S_2 lifetime of 70 fs.[68] These results further confirmed the unusual trend of the S_2-S_1 internal conversion rate. A consistent explanation of these observations is still missing. Besides higher density of accepting vibrational modes that facilitates the S_2-S_1 internal conversion for longer carotenoids used to explain virtually identical S_2 lifetimes for a series of open-chain carotenoids,[40] involvement of intermediate states in the S_2-S_1 internal conversion was recently proposed,[14,15,64,69−72] resulting in complicated relaxation schemes that will be discussed in section 3.5.

Nevertheless, it is worth noting that not all carotenoids follow the trend of S_2 lifetime decreasing with conjugation length: for peridinin, a highly substituted carotenoid having a conjugated carbonyl group, allene group, and seven conjugated C=C bonds, the S_2 lifetime of 56 fs was measured in methanol.[44] Although no direct measurements of S_2 lifetimes of other carotenoids containing conjugated carbonyl group are available to date, the fact that this family of carotenoids does not exhibit any appreciable S_2 emission[49,73] suggests that the very short lifetime is likely common to all these carotenoids. This observation, showing that the carbonyl carotenoids do not follow the trend of other types of carotenoids, can be understood in terms of a more complicated structure of the excited states of these carotenoids, involving appreciable charge-transfer character.[21−23,43−46] Recent two-photon absorption experiments demonstrated that this also leads to a significant mixing of the S_1 and S_2 states,[43,45] which is most likely the cause of the observed short S_2 lifetimes of carbonyl carotenoids.

3.2. S_1 State

As described in the previous section, after being promoted to the S_2 state, a carotenoid molecule undergoes fast relaxation on a time scale 50−300 fs (depending on environment and structure of carotenoid) to the lowest singlet excited-state S_1, implying that properties of the S_1 state are crucial for understanding photophysics of carotenoids. Because of the forbidden nature of the S_0-S_1 transition, knowledge about energetics and dynamics of this key excited state was very limited. Since the theoretical prediction in 1972 of the $2A_g^-$ state being the lowest excited state in longer polyenes and carotenoids,[11] it took more than 20 years until the energy of this state could be determined experimentally for longer carotenoids.

3.2.1. Energy of the S_1 State

The first attempt to localize the S_1 state experimentally was carried out in 1977 by Thrash et al., who analyzed the Raman excitation profile of β-carotene and located its S_1 energy above 17 000 cm^{-1}.[74] However, this rather high value was questioned by subsequent studies of polyenes[75] and carotenoids[76] that utilized the S_1 emission of shorter polyenes/carotenoids. On the basis of a theoretical analysis of excited states of polyenes,[13] one can deduce that the

S_1 energy of carotenoids decreases with conjugation length, and this decrease is slightly steeper than for the S_2 state, making the S_2-S_1 gap larger for longer carotenoids. As described above, this is the reason for the characteristic switch between S_2 and S_1 emission observed for conjugation lengths around 8. Thus, carotenoids with $N \leq 8$ exhibit appreciable S_1 emission with a maximum corresponding to the 0−2 vibrational band of the S_1-S_0 transition, signaling a substantial displacement of the S_0 and S_1 potential surfaces.[37,40] Consequently, spectral analysis of the S_1 emission spectra enabled determination of the 0−0 origin of the S_1-S_0 transition. Both Cosgrove[75] and DeCoster[9] used knowledge of the spectral origin of the S_1-S_0 transition for shorter polyenes/carotenoids to extrapolate the S_1 energy of longer ones. They showed that for a carotenoid having 11 C=C bonds such as β-carotene, the S_1 energy must lie substantially lower than the 17 000 cm^{-1} proposed by Thrash et al.,[74] and on the basis of the extrapolation they concluded that the S_1 state of β-carotene is located between 13 000 and 14 000 cm^{-1}.[75,76] With knowledge of S_1 lifetimes of longer carotenoids (see below), the extrapolation method was further improved by application of the energy-gap law for radiationless transitions,[77] which led to refinement of the β-carotene S_1 energy to 14 100 cm^{-1}.[78] In addition, the energy-gap law was used to estimate S_1 energies of a number of biologically important carotenoids such as spheroidene, zeaxanthin, violaxanthin, antheraxanthin, canthaxanthin, diatoxanthin, and diadinoxanthin.[78−80] Nevertheless, experimental verification of these extrapolations was necessary, and the quest for a reliable experimental method that would enable the determination of the S_1 energy became one of the dominating streams in carotenoid photophysics in recent years.

Some properties of the S_1 state can be monitored via its characteristic, strong S_1-S_N excited-state absorption (ESA) occurring in the visible spectral range; the spectral profile is shown in Figure 3. Due to symmetry reasons, the final S_N state must be of B_u^+ symmetry to account for such a strong transition. Consequently, it must be present also in the ground-state absorption spectrum. Inspection of the UV part of the absorption spectra of carotenoids reveals rather broad absorption bands below 300 nm[45,81] that were assigned to states of B_u^+ symmetry.[45] Then, knowing the energies of the S_1-S_N and S_0-S_N absorption bands from transient absorption and steady-state experiments, it would be possible to calculate the energy of the S_1 state. However, attempts to determine the S_1 energy by this method failed due to two reasons. First, higher B_u^+ states in the absorption spectrum are rather structureless. Therefore, assessment the 0−0 origin of the S_0-S_N transition suffers from a significant error. Second, the S_1-S_N ESA band overlaps with ground-state bleaching; thus, the S_1-S_N ESA band observed in experiment does not correspond to the full spectral profile of the S_1-S_N transition as the bleaching cuts its higher-energy part (Figure 3). Nevertheless, the shape and position of the S_1-S_N band is, similarly to the ground-state absorption spectrum, a fingerprint of a carotenoid molecule. As shown in Figure 3, dependence of the S_1-S_N maximum on conjugation length always follows that of the S_0-S_2 transition, but the shift of the S_1-S_N band is usually larger. Even though no clear vibrational structure of the S_1-S_N band was observed so far (with exception of a 'compensated' S_1-S_N spectrum of lycopene in CS_2[82]), the vibrational structure of the absorption spectrum is imprinted into the shape of the S_1-S_N ESA band. Linear carotenoids with highly resolved vibrational peaks in their ground-state absorption spectrum have a sharp, narrow S_1-S_N ESA band, while significant broadening of the S_1-S_N ESA is observed for carotenoids with a less-structured absorption spectrum (Figure 3). Thus, although S_1-S_N ESA can give information about certain properties of the S_1 state (especially about the lifetime as described below), different techniques are needed to determine the S_1 energy.

Until the late 1990s, experimental studies to locate the S_1 energy relied on progress in fluorescence detection techniques that enabled detection of weak S_1 emission even for carotenoids with $N > 9$. Due to very low quantum yields of the S_1 emission, on the order of $10^{-5}-10^{-7}$ [38,40] and to substantial overlap with the dominating S_2 emission for longer carotenoids, these measurements required extremely precise detection to analyze the spectral profile of the S_1 emission. The first room-temperature fluorescence spectrum of β-carotene reported by Bondarev[83] displayed a weak, distinct band that was assigned to S_1 emission, with its 0−0 spectral origin being located at 13 200 ± 300 cm^{-1}. This value is significantly below the values predicted by extrapolations,[78] but as shown later, this inconsistency was mainly due to a rather poor signal/noise ratio that did not allow resolution of the vibronic structure of the S_1 emission and, consequently, separation of vibronic bands from overlapping contributions of S_2 and S_1 emissions. Nevertheless, the important conclusion of this experiment was that the S_1 energy is much less sensitive to solvent polarizability than the S_2 state: while S_2 emission shifts significantly going from *n*-hexane to CS_2, the weak S_1 emission is very little affected.[83] Later, more accurate measurements of β-carotene S_1 emission revealed the vibronic structure of the S_1 emission band[39] that enabled a more detailed analysis of the vibronic transitions. On the basis of the fact that the maximum of the S_1 emission corresponds to the 0−2 vibrational band, these authors concluded that the 0−0 origin of the S_1-S_0 transition must be completely hidden under the red tail of the strong S_2 emission band, and the low S_1 energy reported by Bondarev et al.[83] was concluded to be one vibronic band (~1300 cm^{-1}) too low due to their wrong assignment of vibronic bands. Spectral analysis performed by Andersson et al.[39] positioned the S_1 energy of β-carotene in CS_2 at 14 200 ± 500 cm^{-1}, which, despite rather high error, was in good agreement with the energy-gap law extrapolations. A slightly higher value of 14 500 ± 150 cm^{-1} was reported on the basis of analysis of S_1 emission of β-carotene in *n*-hexane at 170 K.[52]

Motivated by the key importance of the S_1 energy for understanding energy-transfer pathways, the S_1

energy of carotenoids playing a role in photosynthetic light harvesting was also located by measurements of weak S_1 emission. The S_1 emission analysis of neurosporene ($N = 9$) and spheroidene ($N = 10$) in *n*-hexane placed the S_1 energy at 14 200 cm^{-1} for spheroidene, while the S_1 state of the shorter neurosporene was correspondingly higher at 15 300 cm^{-1}, again in a good agreement with the energy-gap law predictions.[50] Decrease of temperature from 293 to 170 K exposed more pronounced vibrational structure of the S_1 emission, and the quantum yield of S_1 emission was lower at low temperature, but no shift of the S_1 emission spectrum with temperature was revealed, suggesting that the S_1 energy is temperature independent.[50] However, fluorescence measurements of violaxanthin ($N = 9$) and zeaxanthin ($N = 11$), two carotenoids involved in the xanthophyll cycle in higher plants,[79] showed different results. At room temperature, the S_1 energies of violaxanthin and zeaxanthin were determined to be 14 880 ± 90 and 14 550 ± 90 cm^{-1}, respectively,[84] in fact much more similar than predicted from the energy-gap law.[79] Different values, however, were obtained at 77 K in EPA glass, where better resolution of vibrational bands was achieved. While the S_1 energy of zeaxanthin at 77 K was only a little higher than at room temperature (14 610 cm^{-1}), a significant shift of the violaxanthin S_1 state was observed; it was located at 15 580 ± 60 cm^{-1}, 700 cm^{-1} higher than at room temperature.[85] Since the room-temperature S_1 energy of violaxanthin was determined to be significantly below 15 000 cm^{-1} also by other methods,[81] this observation is quite intriguing and remains unexplained.

Recently, fluorescence spectroscopy was used to resolve the S_1 energy of even longer carotenoids. Fujii et al.[51] recorded fluorescence spectra of lycopene ($N = 11$), anhydrorhodovibrin ($N = 12$), and spirilloxanthin ($N = 13$) in *n*-hexane, concluding that their S_1 energies are 13 300, 12 500, and 11 900 cm^{-1}, respectively, and independent of temperature. For these long carotenoids the extremely weak S_1 emission does not exhibit any pronounced vibrational structure. The determination of the 0−0 spectral origin therefore relies on estimation of the width of vibrational bands and assumption of the 0−2 vibrational band being the maximum of the S_1 emission. Although such fitting can suffer from a considerable error, on the basis of spectral analyses of S_1 emissions of shorter carotenoids this procedure usually generates reasonable results. For the study by Fujii et al.,[51] fitting is further complicated by the presence of another state claimed by the authors, which contributes to the fluorescence spectrum (see section 3.3). Thus, the vibrational bands of the three states overlap significantly, which makes the fitting rather ambiguous. However, despite all these complications the extracted S_1 energies are in good agreement with the energy-gap law predictions and also fit the extrapolations made from shorter carotenoids whose S_1 energies were determined by fluorescence spectroscopy.[78] The S_1 energies of various carotenoids are summarized in Table 1.

Another steady-state technique aiming to determine the energy of a one-photon forbidden state is based on Raman spectroscopy, and its application to locate the S_1 state of carotenoids was developed mainly by Koyama and co-workers. The ground-state Raman spectrum of carotenoids in the frequency region 1000−1800 cm^{-1} is dominated by two Raman lines at ~1500 and ~1150 cm^{-1} (the exact frequencies of these lines depend on carotenoid), which correspond to symmetric stretching C═C and C−C vibrations of the conjugated backbone.[86] Under resonance Raman conditions, when the excitation light is in resonance with an electronic transition of the studied molecule, the intensities of the Raman lines are greatly enhanced. Thus, tuning the detection to the frequency of either C═C or C−C stretching modes and scanning the excitation light over a broad spectral range, a resonance Raman profile can be obtained. The high sensitivity of Raman line intensities to the resonance conditions enables detection of even dark states with very low transition dipole moments.

The first resonance Raman profile of a carotenoid S_1 state was recorded for the C−C and C═C stretching modes of β-carotene, detecting a peak at 14 600 cm^{-1}.[87] However, the dominating peak contained a high-energy shoulder that was ascribed to contamination by an infrared-active mode at 966 cm^{-1}. Consequently, analysis of this profile gave an 0−0 energy of the S_0-S_1 transition of 13 600 cm^{-1}.[87] Later, a better resonance Raman profile of β-carotene was recorded by Hashimoto et al.,[88] placing the S_1 energy of β-carotene at 14 500 cm^{-1}. Given the reasonable agreement with both theoretical predictions and earlier fluorescence results, measurements of resonance Raman profiles were extended to other carotenoids. Resonance Raman profiles of crystalline spheroidene at 100 K displayed a pronounced vibrational progression of the S_1 state.[89] Both C−C and C═C stretching modes had a common origin at 14 200 cm^{-1} that was assigned to the 0−0 origin of the S_0-S_1 transition. Since the vibrational progression of the resonance Raman profile reflects the vibrational bands of the S_1 state, the different spacings between the vibrational peaks assigned to the C−C and C═C stretching modes could be used to obtain frequencies 1150 and 1500 cm^{-1} for C−C and C═C stretches, respectively.[89] While in the case of the C−C stretching mode this result agrees with known S_1 state stretching frequencies measured by means of time-resolved Raman spectroscopy, it contradicts the known fact that the C═C stretching frequency is significantly higher in the S_1 state, reaching nearly 1800 cm^{-1}.[90] The same problem with the C═C stretching frequency in the S_1 state being too low appeared when resonance Raman profiles of lycopene ($N = 11$), β-carotene ($N = 11$), and mini-9-β-carotene were measured.[14] Although both stretching modes have the same 0−0 origins of the S_0-S_1 transition located at 13 200 (lycopene), 14 670 (β-carotene), and 15 750 cm^{-1} (mini-9-β-carotene), the spacing of vibrational bands in the S_1 state failed to reproduce the higher frequency of the C═C stretching mode in the S_1 state. Explanation of this discrepancy

waits for further experimental and theoretical analysis. It is also worth noting that this technique suffers a similar problem as with the detection of S_1 fluorescence; because the S_0-S_2 transition is strongly allowed, the intensity of Raman lines will be several orders of magnitude higher when the excitation is in resonance with the allowed S_0-S_2 transition than when in resonance with the forbidden S_0-S_1 transition. Accordingly, similar to fluorescence, the S_0-S_1 profile could be completely superimposed on the red wing of the S_0-S_2 transition preventing reliable analysis. Contrary to fluorescence detection, however, for resonance Raman profiles a particular transition could be suppressed by self-absorption, causing the intensity of bands in the resonance Raman profile to be strongly dependent on the concentration of the sample and the optical geometry of the experiment.[69] Thus, by a proper choice of sample concentration and experimental arrangement, the strong S_0-S_2 transition can be filtered out from the resonance Raman profile, allowing observation of the S_0-S_1 profile.[69] Despite problems to reproduce vibrational frequencies in the S_1 state, resonance Raman profiles proved to be a useful method to locate the 0−0 origin of the carotenoid S_1 state. Extracted values match well those recorded by fluorescence (although the values for longer carotenoids are systematically lower than those obtained from fluorescence as seen in Table 1), and they also fit into the range of S_1 energies predicted by the energy-gap law. In addition, varying the concentration of the sample in a wide range led to detection of other dark carotenoid states lying between the S_1 and S_2 states (see section 3.3).

A different approach employing femtosecond time-resolved spectroscopy to locate the S_1 energy of carotenoids, based on the fact that the S_1-S_2 transition is symmetry allowed, emerged in 1999.[81] A femtosecond excitation pulse populates the lowest vibrational band of the well-characterized S_2 state to avoid contribution from vibrational relaxation within this state. The excited molecule then relaxes to the S_1 state on the time scale of 50−300 fs as described in section 3.1. By scanning the wavelength of the probe pulse within the time window dictated by the lifetime of the S_1 state, the S_1-S_2 resonance can be found. Given the known spectral profile of the S_2 state and lifetime of the S_1 state, the S_1-S_2 transition must (1) reflect the spacing between the S_2 vibrational bands; (2) decay with the S_1 lifetime. If these two conditions are fulfilled, the energies of the vibrational bands of the S_1-S_2 transition can be determined. The location of the carotenoid S_1 state can then be obtained, since its 0−0 spectral origin can be calculated from the spectral origins of S_0-S_2 and S_1-S_2 transitions.[81] Although this approach is quite straightforward, its application was complicated by the necessity to have tunable femtosecond pulses in the 1−2 μm spectral range where the S_1-S_2 transition is expected. Along with availability of sources generating such pulses in the late 1990s, this method became a powerful tool to study the properties of the S_1 state of carotenoids. Typical S_1-S_2 profiles of two carotenoids with different conjugation lengths are shown in Figure 5.

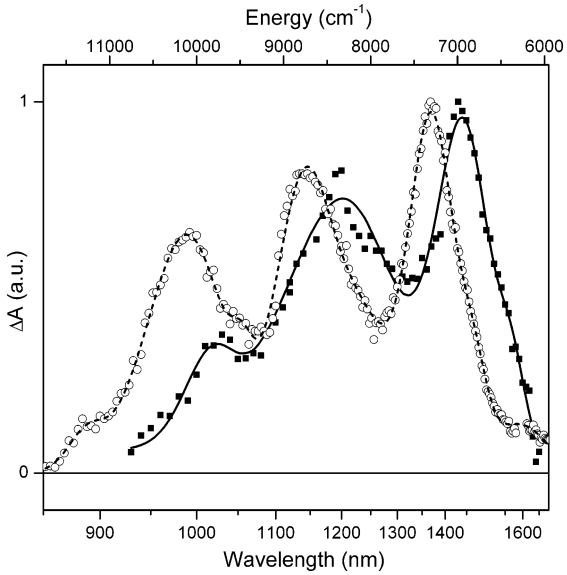

Figure 5. Transient absorption spectra of spheroidene in *n*-hexane (open circles) and violaxanthin in methanol (full squares) in the spectral region 850−1750 nm representing the spectral profile of the S_1-S_2 transition. The spectra were recorded 3 ps following excitation at 490 (spheroidene) and 480 nm (violaxanthin). The solid and broken lines are results of fitting the spectra to a sum of Gaussian profiles.

The first application of this method was used to locate the S_1 energies of two carotenoids, violaxanthin and zeaxanthin, that participate in the xanthophyll cycle of higher plants.[81] Transient absorption spectra recorded for both carotenoids in the spectral region 900−1600 nm resembled well the characteristic three-peak structure of the S_2 state, with vibrational spacing matching perfectly that observed in the ground-state spectrum (see Figure 5 for the S_1-S_2 spectrum of violaxanthin). In addition, the whole near-infrared transient absorption spectrum decayed with a time constant of 8.8 ps for zeaxanthin and 25 ps for violaxanthin, thus agreeing with the known S_1 lifetimes of these carotenoids (see below). Consequently, it was concluded that the recorded transient absorption spectrum indeed reflected the spectral profile of the S_1-S_2 transition and the well-resolved vibrational bands allowed for the location of the 0−0 origin of the S_1-S_2 transition, peaking at 7010 (zeaxanthin) and 6950 cm^{-1} (violaxanthin). Then, with the knowledge of the S_1-S_2 and S_0-S_2 transition energies, the position of the S_1 level of both carotenoids was determined by simple subtraction. To improve the precision, both the 0−0 and 0−1 transitions of the steady-state and transient absorption spectra were used, leading to an S_1 energy of 14 030 $\pm$ 90 cm^{-1} for zeaxanthin and 14 470 $\pm$ 90 cm^{-1} for violaxanthin.[81] Although these values fall into the range of energies expected for carotenoids with these conjugation lengths, using an experimental approach exploiting the allowed S_1-S_2 transition (while the methods used before relied exclusively on detection of weak signals originating from the forbidden S_1-S_0 transition) revealed a number of interesting new features that ignited lively discussions about the S_1 state of carotenoids.

First, the S_1-S_2 spectra of violaxanthin ($N = 9$) and zeaxanthin ($N = 11$) are almost the same, indicating

that the S_1-S_2 energy gap is not much affected by the conjugation length, and both the S_1 and S_2 states are shifted by about the same energy with increased conjugation. In addition, the difference between the S_1 energies of these two carotenoids is significantly smaller than predicted by extrapolations using the energy-gap law; while the S_1 energy of zeaxanthin is close to the expected one, for violaxanthin having a conjugation length of 9, the extrapolations predict an S_1 energy above 15 000 cm^{-1},[79] substantially higher than the 14 470 cm^{-1} extracted from the S_1-S_2 spectra. Thus, this new approach demonstrated that extrapolations from the energy-gap law are not straightforward when carotenoids with different structures are compared. This conclusion was later confirmed by detecting S_1 emissions of violaxanthin and zeaxanthin.[84]

Since recording of S_1-S_2 spectra proved to be a very useful technique to establish S_1 energies of carotenoids, subsequent studies of various carotenoids followed. A more detailed study, including temperature dependence, was performed on spheroidene ($N = 10$) and revealed additional subtleties of the S_1-S_2 spectra.[62] The analysis of the S_1-S_2 spectrum supported by simulations proved that the observed bands correspond to three vibrational levels of the S_2 state, with the 0−0 transition being the strongest one (Figure 5), suggesting only a small shift between the S_1 and S_2 potential surfaces. Interestingly, the energy of the 0−0 spectral origin of the S_1-S_2 transition at 7300 cm^{-1} put the spheroidene S_1 state at 13 400 ± 90 cm^{-1}, about 800 cm^{-1} lower than the energy obtained from fluorescence and resonance Raman measurements. This intriguing result was explained as a result of different carotenoid configurations occurring in the S_1 state. It was proposed that the crucial difference leading to different results when different techniques are used lies in the fact that while the S_1-S_2 technique probes an allowed transition, fluorescence and resonance Raman monitors a forbidden transition. With a statistical distribution of conformers in the S_1 state, fluorescence and resonance Raman techniques detect predominantly the conformations deviating from the idealized C_{2h} symmetry, since these have the S_1-S_0 transition least forbidden. An exactly opposite situation holds for the allowed S_1-S_2 transition, because the least distorted conformations give the dominant contribution to the S_1-S_2 spectrum. The difference in S_1 energies obtained by the different techniques is consequently a result of the fact that each technique probes a different subset of S_1 state conformations.[62] This implies that the spheroidene S_1 energy of 13 400 cm^{-1} obtained from the S_1-S_2 spectra corresponds to the S_1 energy of the *all-trans* configuration, while the higher energy of 14 200 cm^{-1} was assigned to conformations deviating from the ideal C_{2h} symmetry. This hypothesis is further supported by the fact that the 0−0 band of the S_1-S_2 transition exhibited a clear asymmetry, having a shoulder on the low-energy side. If the S_1 energy is calculated on the basis of this shoulder, a nearly perfect match with the energies determined from S_1 fluorescence and resonance Raman was found. Accordingly, it was concluded that the low-energy shoulder in the S_1-S_2 spectra is due to the distorted S_1 conformations.[62]

To date, S_1-S_2 spectra of violaxanthin,[81] zeaxanthin,[81] spheroidene,[62] lycopene,[91] rhodopin glucoside,[92] spirilloxanthin,[67] peridinin,[23,44] spheroidenone,[46] siphonaxanthin,[46] and fucoxanthin[46] have been reported. The resulting S_1 energies, together with those obtained by other techniques, are summarized in Table 1. Except for rhodopin glucoside, for which emission or resonance Raman data are not available so far, the S_1 energies extracted from S_1-S_2 spectra are systematically lower than those determined by fluorescence and/or resonance Raman spectroscopy, with the difference depending on carotenoid structure. The difference is almost negligible for the carbonyl carotenoids peridinin, fucoxanthin, and siphonaxanthin,[46,49] but the S_1 state properties of these carotenoids are markedly different from those without a carbonyl group (see below). The difference found for the linear carotenoids spheroidene and lycopene (800 cm^{-1}) is about twice that revealed for violaxanthin (400 cm^{-1}) and zeaxanthin (500 cm^{-1}). The latter have a more complicated structure, leading to a more restricted ability to form conformers than for their linear counterparts. The 'conformational' hypothesis is further supported by measurements on the long ($N = 13$), linear carotenoid spirilloxanthin. For this carotenoid, the 0−0 band of the S_1-S_2 transition is significantly broader, signaling a much wider distribution of S_1 conformers.[67] In addition, spirilloxanthin is known to isomerize spontaneously on a time scale of minutes.[93] Thus, ground-state conformers are inevitably present in measurements of both S_1-S_2 spectra[67] and fluorescence.[51] Therefore, the actual difference between these two techniques is slightly smaller than for other linear carotenoids (Table 1).

Besides these three techniques, which are currently the most widely used to locate the carotenoid S_1 state in solution, a few studies using other approaches were also reported. First, an approach based on two-photon excitation spectra is a promising tool, since the S_0-S_1 transition is two-photon allowed.[13] However, use of this technique in solution is rather limited, since it relies on detection of the S_1 fluorescence. Thus, the two-photon absorption was successfully used for the carbonyl carotenoid peridinin that exhibits substantial S_1 emission.[43,45] An alternative approach to measure two-photon excitation spectra that requires combination with time-resolved techniques was developed.[94,95] To overcome complications with detection of weak fluorescence, the two-photon excitation spectra were measured using detection of the strong S_1-S_N ESA. Two-photon excitation profiles of the S_1 state of β-carotene and lutein were recorded,[95] demonstrating the feasibility of such measurements. However, a poor signal/noise ratio did not allow evaluation of the 0−0 origin of the S_1 state with high enough precision; the low-energy onset of the two-photon excitation spectrum is around 13 400 cm^{-1}, suggesting an S_1 energy in the range 14 000−15 000 cm^{-1} for both carotenoids. The real power of the two-photon excitation spectra is manifested for locating the S_1 state in light-harvesting complexes,

where emission from (B)Chls occurring as a consequence of energy transfer is detected (see section 4.1). It must be noted that much earlier a technique called consecutive two-photon absorption spectroscopy was applied to find the S_1 state of a double carbonyl carotenoid canthaxanthin (9β2O2), but the reported energy of 15 267 ± 100 cm^{-1} is clearly too high for such a long carotenoid.[96]

To complete the list of various techniques to assess the S_1 energy of carotenoids, two more approaches must be mentioned. First, Bettermann et al. applied intracavity absorption spectroscopy on carotenoids.[97] This technique employs a specially designed ring dye laser with the sample cuvette placed directly into the laser resonator. In this arrangement, small changes of sample absorbance will cause strong reductions in laser amplification and, consequently, a significant decrease of intensity of the laser light, enabling detection of very weak transitions. The intracavity absorption measurements were employed to study the properties of a model carotenoid having conjugation length 9 (702). The extracted S_1 energy was 15 200 cm^{-1}, and based on the analysis of patterns of the promoting vibrational modes, it was also concluded that the second triplet state T_2 occurs in the vicinity of the S_1 state.[97] Second, a method based on pulsed near-edge X-ray absorption spectroscopy (NEXAFS) was introduced recently.[98,99] A sharp peak below the carbon K-edge in the NEXAFS spectrum gives the energy of the first excited state with respect to the ionization potential of the molecule. Together with application of photoelectron spectroscopy, which enables estimation of the energy of the HOMO orbital, and quantum chemical calculations, the authors placed the energy of the β-carotene S_0-S_1 transition at 15 400 cm^{-1}.[98] This energy is about 1000 cm^{-1} higher than that determined by other methods (Table 1), and it is not easy to trace the origin of this discrepancy. However, the complicated nature of the experiment and uncertainty caused by calculations, together with sample preparation including the high-temperature (180 °C) deposition of β-carotene on Si_3N_4 foils that are measured in an ultrahigh vacuum, makes a direct comparison with other methods rather difficult.

Comparing all the methods used to locate the S_1 energy of carotenoids, it is clear that all of these methods have their own advantages and disadvantages, and success of their application depends on the studied system. While fluorescence and resonance Raman methods are useful tools for measurements of the S_1 energy of shorter carotenoids in solution, their use is rather limited for carotenoids having more than 10 C=C bonds, since the signals become extremely weak, putting constraints on a reliable data analysis. On the other hand, the S_1-S_2 spectra are more reliable for longer carotenoids, since the longer carotenoids exhibit a larger S_1-S_2 energy gap, shifting the S_1-S_2 profile toward higher energies, thus making the detection easier. For carotenoids with $N \leq 9$, the 0−0 band of the S_1-S_2 transition can extend below 5000 cm^{-1}, where vibrational overtones originating from solvent may occur. Although higher vibrational bands of the S_1-S_2 transition can be used to calculate the S_1 energy,[23,46] the precision is certainly lower in such a case. For S_1-S_2 spectra, another complication arises from the fact that the extinction coefficient of the S_1-S_2 transition is about 10 times smaller than that of the S_1-S_N transition, setting strong requirements on the signal/noise ratio. This, together with more complicated detection in the near-infrared region, prevents recording S_1-S_2 spectra with diode-array detection, which is nowadays standard for measurements of the S_1-S_N transition. Despite these complications, the S_1-S_2 method is the only one providing information about both the energy and lifetime of the S_1 state, which makes it very useful in establishing excited-state properties. In addition, if future experiments confirm the validity of the 'conformational' hypothesis, the S_1-S_2 method together with two-photon absorption are the only techniques enabling determination of the S_1 energy of the *all-trans* conformation. For the intracavity absorption and NEXAFS methods, the limited amount of reported data prevents direct comparison with other methods, and assessment of their usefulness for measurements of the S_1 energy therefore awaits future experiments.

Beyond solution, in the protein environment of various carotenoid-binding proteins, application of these methods is more restrictive (see section 4). For light-harvesting complexes containing (B)Chls in addition to carotenoids, utilization of fluorescence and resonance Raman techniques is not technically possible. For fluorescence, a much stronger emission from (B)Chls covers the weak S_1 emission, making it impossible to detect. For the measurements of resonance Raman profiles, which requires high-concentrated crystalline samples to achieve the required sensitivity,[14,69] it is not feasible to perform measurements on protein complexes. Measurements of S_1-S_2 spectra can be applied without serious restrictions to carotenoids in both solution and protein complexes, making this technique very universal, although spectral analysis of the S_1-S_2 profile is more complicated due to the presence of excited-state absorption signals from (B)Chls. The two-photon technique is very useful for light-harvesting complexes. Due to carotenoid−(B)Chl energy transfer, two-photon excitation profiles can be detected via (B)Chl emission, provided that the S_1 state is involved in energy transfer. Applications of these methods to carotenoids in the protein environment will be described in more detail in section 4.

3.2.2. S_1 Lifetime

Although not directly useful for determination of the S_1 energy, measurements of the S_1-S_N ESA signals have been widely used to obtain S_1 lifetimes. The first work in the late 1980s by Wasielewski and Kispert gave the S_1 lifetimes of β-carotene ($N = 11$, 8.4 ps), canthaxanthin ($N = 13$, 5.2 ps), and β-apo-8′ carotenal ($N = 10$, 25.4 ps).[18] This pioneering work was followed by a number of studies on various carotenoids that established not only the S_1 lifetimes but also their dependence on conjugation length, carotenoid structure, and environment (Table 2 and Figure 6). A systematic dependence of the S_1 lifetime

Table 2. S_1 Lifetimes of Carotenoids without a Conjugated Carbonyl Group[a]

carotenoid[b]	N[c]	τ_{S1} (ps)	ref
dodecapreno-β-carotene*	17β2	0.5	57
decapreno-β-carotene*	13β2	1.1	57
tetradehydrospheroidene*	13	1.1	38
spirilloxanthin	13	1.4	20,72
anhydrorhodovibrin	12	2.2	72
didehydrospheroidene*	12	2.7	38
didehydrospheroidene*	11	3.9	38
lycopene	11	4−4.7	72, 100, 178
rhodopin glucoside	11	4.2−4.8	59, 92
15,15-*cis*-spheroidene	10	7	103
β-carotene	9β2	9−11	100, 101, 165
zeaxanthin	9β2	9	79, 81, 100
spheroidene	10	8−9.5	22, 38, 62, 178
diatoxanthin	9Aβ1	13.3	80
lutein	9β1	14	102, 293
antheraxanthin	9β1	14.4	79
nonaene*	9	18	40
neurosporene	9	21.2	178
diadinoxanthin	9A	22.8	80
violaxanthin	9	24	79, 81
dihydrospheroidene*	9	25.4	38
neoxanthin	8A	35	22
m9-β-carotene*	7β2	52	39
octaene*	8	68	40
tetrahydrospheroidene*	8	85	38
m8-β-carotene*	6β2	96	39
m7-β-carotene*	5β2	282	39
heptaene*	7	290	40
tetrahydrospheroidene*	7	407	38
m5-β-carotene*	3β2	2700	39

[a] All values refer to measurements at room temperature. [b] Carotenoids marked by asterisk are synthesized carotenoids that do not occur naturally. [c] Conjugation length. See caption of Figure 1 for description.

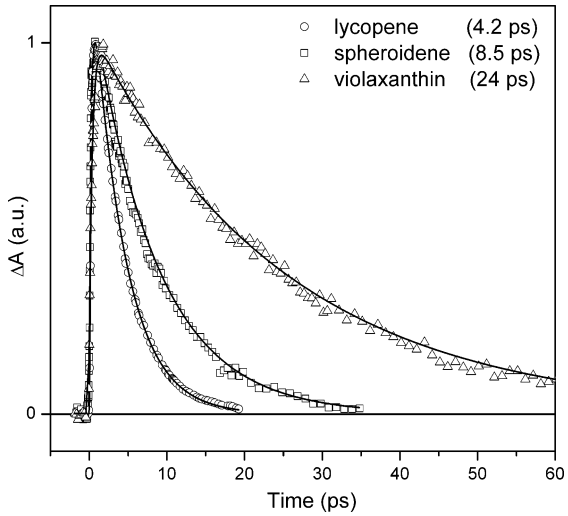

Figure 6. Kinetics representing decay of the S_1 state recorded at the maximum of the S_1-S_N transition of lycopene ($N = 11$) in *n*-hexane (circles), spheroidene (10) in *n*-hexane (squares), and violaxanthin (9) in methanol (triangles). Solid lines represent monoexponential fits of the decays yielding S_1 lifetimes of 4.2 (lycopene), 8.5 (spheroidene), and 24 ps (violaxanthin). Excitation wavelengths were 480 (violaxanthin), 490 (spheroidene), and 510 nm (lycopene).

on conjugation length was demonstrated for a few series of carotenoid analogues. For example, measurements on spheroidene analogues yielded lifetimes of 400 ($N = 7$), 85 (8), 25 (9), 8.7 (10), 3.9 (11), 2.7 (12), and 1.1 ps (13).[38] A similar dependence was found for a β-carotene series, although the actual lifetimes were slightly different: 282 (7), 96 (8), 52 (9), and 8.1 ps (11).[39] Apart from the conjugation lengths 7−13 that are characteristic of carotenoids occurring in natural systems, a few studies of carotenoids with both shorter and longer conjugation lengths added more experimental data to the conjugation length dependence of the S_1 lifetimes. A S_1 lifetime of 2.7 ns was found for a very short β-carotene analogue with $N = 5$,[39] and an even longer S_1 lifetime was estimated for the naturally occurring *cis*-phytofluene ($N = 5$) on the basis of the quantum yield of the S_1 emission.[58] On the longer conjugation side, S_1 lifetimes of 2.5, 1.1, and 0.5 ps were obtained for β-carotene analogues with 13,[66] 15, and 19[57] conjugated C=C bonds, respectively, confirming the decrease of the S_1 lifetime with conjugation length as was successfully explained by the energy-gap law.[38,78]

The effect of carotenoid structure on S_1 lifetimes can be evaluated from a number of studies measuring S_1 lifetimes of various carotenoids. In fact, observed changes of the S_1 lifetime can be in most cases rationalized as a deviation of carotenoid structure from the ideal polyene C_{2h} symmetry, causing a decrease of the effective conjugation length. As an example, one can consider carotenoids having $N = 11$. For the linear unsubstituted carotenoid lycopene, the S_1 lifetime is ∼4 ps.[72,82,100] For spheroidenone, a linear carotenoid containing 10 C=C bonds and one C=O group, the S_1 lifetime is prolonged to 6 ps,[22,46] because the conjugated carbonyl group that is in a *s-cis* position relative to the C=C conjugated backbone makes the effective conjugation length slightly shorter than that for the full 11 C=C conjugation in lycopene. Further prolongation of the S_1 lifetime to 9 ps is noticed for β-carotene,[100,101] in which two C=C bonds are located in the terminal β-ionylidene rings, leading to even shorter effective conjugation. The carotenoid diatoxanthin has an even longer S_1 lifetime of 13 ps, because its 9 C=C conjugation is terminated by a β-ring at one side and the 11th C=C bond of the conjugated chain at the opposite end is an allene moiety, leading to further shortening of the effective conjugation length.[80] The observed lifetime of 13 ps is in fact almost the same as for its counterpart without the allene moiety, lutein, which has an S_1 lifetime of 14 ps,[102] signaling only a minor extension of conjugation to the allene moiety in the case of diatoxanthin. A similar effect of a terminal allene moiety occurs for neoxanthin having 8 C=C bonds and the allene moiety. The neoxanthin S_1 lifetime of 35 ps[22] is shorter than the ∼70 ps expected for $N = 8$, but it is clearly longer than 20−25 ps anticipated for a carotenoid having $N = 9$.[40]

In contrast, various substituents that are not in contact with the conjugated backbone have no effect on S_1 lifetime (see Table 2). Rhodopin glucoside ($N = 11$), possessing a glucoside ring at the end of the linear conjugated chain, has the same S_1 lifetime of 4 ps as its nonsubstituted counterpart lycopene. Similarly, violaxanthin ($N = 9$), with its terminal rings containing epoxy groups decoupled from the conjugated backbone, has a lifetime of 24 ps, the same as that observed for the unsubstituted $N = 9$

carotenoid neurosporene. It is worth noting, however, that although substituents decoupled from conjugation have no effect on S_1 lifetime, introduction of a large group into the carotenoid structure can cause formation of a wider distribution of ground-state conformers. Rhodopin glucoside is a good example as the large glucoside group at the end of the conjugated backbone makes the molecule highly asymmetric; the vibrational bands in the rhodopin glucoside absorption spectrum are much less resolved than those of lycopene.[92,100] For symmetric substituents, as in the case of violaxanthin, this effect is less pronounced.[81,84] The presence of small groups (such as hydroxyl) has no effect on either the S_1 lifetime or absorption spectrum: from a photophysical point of view, β-carotene and zeaxanthin are virtually identical molecules.[100] Interestingly, although isomerization in the middle of the conjugated chain could be viewed also as a decrease of effective conjugation, a shortening of the S_1 lifetime was reported for a locked spheroidene isomer.[103] The observed effect is small, but a clearly shorter S_1 lifetime of 7.1 ± 0.1 ps for the 15,15′-*cis*-spheroidene was observed, as compared with 8−9 ps for its *all-trans* counterpart (Table 2).

While there is in fact no information about the temperature dependence of the S_2 lifetime, a few studies of the temperature effect on S_1 lifetime were performed. Single-photon counting measurements of the S_1 emission of mini-9-β-carotene ($N = 9$) revealed a significant increase of the S_1 lifetime from 60 ps at 293 K in toluene to 130 ps at 77 K in 3-methylpentane.[39] A comparable increase of the S_1 lifetime was observed for a shorter mini-8-β-carotene (100 ps at 293 K and 280 ps at 77 K).[39] A markedly smaller effect was reported for spheroidene, yielding an S_1 lifetime of 8 ps at room temperature and 9.5 ps at 186 K in *n*-hexane.[62]

For the carotenoids without a conjugated carbonyl group there is almost no solvent effect on the S_1 lifetimes. Frank et al.[22] performed a systematic study showing the dependence of the S_1 lifetime on solvent parameters. The S_1 lifetime of spheroidene was, within experimental error, the same (8−9 ps) in all investigated solvents, ranging from the nonpolar *n*-hexane to the polar solvents methanol and acetonitrile. The same lifetime of 9 ± 1 ps was also recorded in the highly polarizable CS_2, and no effect of hydrogen-bonding solvents was detected,[22] confirming that solvent parameters have no effect on S_1 lifetime. Similar results, although for a smaller range of solvents, were reported for neoxanthin,[22] zeaxanthin,[79,81,100] lycopene,[82,100] β-carotene,[100] and apo-β-carotene.[47] In all cases, the S_1 lifetime remains, within experimental error, the same regardless of solvent parameters. Nonetheless, a few recent studies have demonstrated that this rule is dramatically violated for carbonyl carotenoids,[21−23,44−47] whose unique S_1 state properties are described in the next section.

3.2.3. S_1 State of Carbonyl Carotenoids

Carbonyl carotenoids attracted attention mainly due to their specific occurrence in light-harvesting antennae of algae.[104] The three most abundant, fucoxanthin, siphonaxanthin, and peridinin (Figure 1), were investigated in the early 1990s by fluorescence spectroscopy.[49,73] Comparison of absorption and emission properties of these three carbonyl carotenoids in CS_2 with those observed for their counterparts having similar structure but lacking the carbonyl group suggested that the carbonyl group markedly changes the spectroscopic properties. Although fucoxanthin and neoxanthin have very similar structures, introduction of the carbonyl group into fucoxanthin causes a slight red shift of the absorption spectrum. In terms of the effective conjugation length, this red shift is rather surprising, since exchange of one C=C bond by a C=O group should create shorter effective conjugation and, accordingly, a blue-shifted absorption spectrum. In addition, contrary to neoxanthin that emits predominantly from its S_2 state, fucoxanthin exhibits solely S_1 emission.[49,73] The S_1 emission is characteristic of the carbonyl carotenoids studied so far, with an exception of the long spheroidenone (10O).[49] This makes location of their S_1 energies quite straightforward. The S_1 fluorescence spectra of fucoxanthin, siphonaxanthin, and peridinin are nearly identical, putting their S_1 energy in the range of 16 000−16 500 cm^{-1}, regardless of their different structures.[49]

The first measurement of the S_1 lifetime for carbonyl carotenoids was performed on peridinin in CS_2 yielding a time constant of 103 ps,[105] which was in the range expected for a carotenoid with S_1 energy above 16 000 cm^{-1}. However, a transient absorption spectroscopy study of peridinin in two solvents with different polarity,[106] followed by a systematic investigation of the dependence of peridinin properties on solvent parameters,[21] showed that the peridinin excited-state properties differ significantly from those known for non-carbonyl carotenoids (Table 3). While in nonpolar solvents the S_1 lifetime was about 160 ps, an increase of solvent polarity in middle-polarity solvents such as tetrahydrofuran or propanol caused a shortening to 50−80 ps. In the polar solvents methanol and acetonitrile, the S_1 lifetime was more

Table 3. S_1 Lifetimes of Carotenoids Having a Conjugated Carbonyl Group[a]

		τ_{S1} (ps)		
carotenoid[b]	N[c]	nonpolar[d]	polar[e]	ref
peridinin	7LOA	160−170	10[f]	21−23
uriolide acetate	8LO	70−77	26−46	22
fucoxanthin	7OA	60−70	23-35	22, 46
siphonaxanthin	8O	58	20	46
apo-β-caroten-8-al*	8Oβ1	26.4[g]	8.4	47
apo-β-caroten-6-al*	9Oβ1	12[g]	6.3	47
okenone	10Oβ1	8	n.m.	151
spheroidenone	10O	6	6	22, 46
hydroxyechinenone	9β2O	6	6	284
canthaxanthin	9β2O2	5.2[h]	n.m.	18

[a] All values refer to measurements at room temperature. n.m. = not measured. [b] Carotenoids marked by asterisk are synthesized carotenoids that do not occur naturally. [c] Conjugation length. See caption of Figure 1 for description. [d] *n*-Hexane or CS_2. [e] Methanol or acetonitrile. [f] Value refers to the excitation close to absorption maximum. Shorter lifetimes can be observed after excitation of the red wing of the absorption spectrum in protic solvents. See text for details. [g] In 3-methylpentane. [h] In toluene.

than 1 order of magnitude shorter than in nonpolar solvents (12 and 7 ps, respectively).[21] By comparing with time-resolved studies on other molecules, a model was proposed in which the presence of a new state with charge-transfer character in the excited-state manifold plays a crucial role in polar solvents. In some solvents, the intramolecular charge-transfer (ICT) state was suggested to lie below the S_1 state of peridinin, resulting in quenching of the S_1 state and hence to a shorter S_1 lifetime. This interpretation was recently supported by ab initio calculations using time-dependent density functional theory.[107] As shown in Figure 7, these data were also later confirmed by

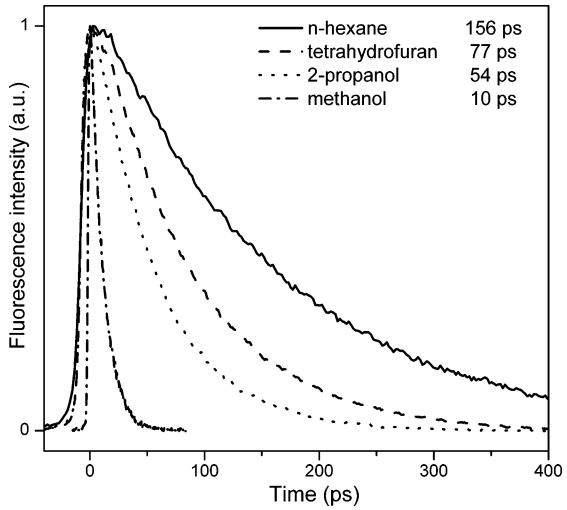

Figure 7. Decays of peridinin fluorescence in solvents with different polarity taken at the emission maximum at 730 nm after excitation of the S_2 state of peridinin at 470 nm. All traces are normalized. Adapted with permission from ref 23. Copyright 2001 American Chemical Society.

measurements of the S_1 emission lifetime by means of a streak camera.[23] Initially, the ICT state was ascribed to the presence of a lactone ring, but a subsequent study of other carotenoids showed similar (but less pronounced) behavior for fucoxanthin, which has an allene moiety and a carbonyl group but lacks the lactone ring, and for uriolide acetate, which has the lactone ring and carbonyl group but lacks allene moiety, leading to the conclusion that the carbonyl group is responsible for the polarity-dependent S_1 lifetime.[22] Recent quantum chemical calculations on peridinin using time-dependent density functional theory showed that the ICT state is characterized by a substantial transfer of electron density from the terminal ring containing an epoxy group to the polyene chain and the carbonyl group localized at the lactone ring.[107] Thus, it is the interaction of the carbonyl group with the solvent that leads to a stabilization of the ICT state in a polar solvent. It was also proposed that stabilization of the ICT state might include a twisting of the molecule, forming a twisted ICT (TICT),[21] but later experiments on viscosity dependence showed that it is not likely.[44]

Transient absorption spectra of peridinin in the region corresponding to the S_1-S_N transition further confirmed the markedly different behavior of peridinin in solvents with different polarity (Figure 4). In nonpolar solvent, the S_1-S_N spectrum is dominated by a sharp narrow band at 510 nm and is thus comparable with other non-carbonyl carotenoids of similar conjugation length,[21−23,44] although additional weak bands in the 550−700 nm range were proposed to be due to some charge-transfer character even in nonpolar solvent.[21,22] In methanol, the transient absorption spectrum is markedly different, consisting of a broad band extending from 500 to 700 nm with a peak at around 630 nm. This change was ascribed to a stabilization of the charge-transfer state in polar solvent, and the observed spectrum was explained as being due to an ICT$-S_N$ transition with a shoulder at 530 nm due to the 'normal' S_1-S_N band.[21−23] Extending the transient absorption spectra toward the infrared spectral region revealed further differences between polar and nonpolar solvents (Figure 8). For peridinin in *n*-hexane, the spectral region

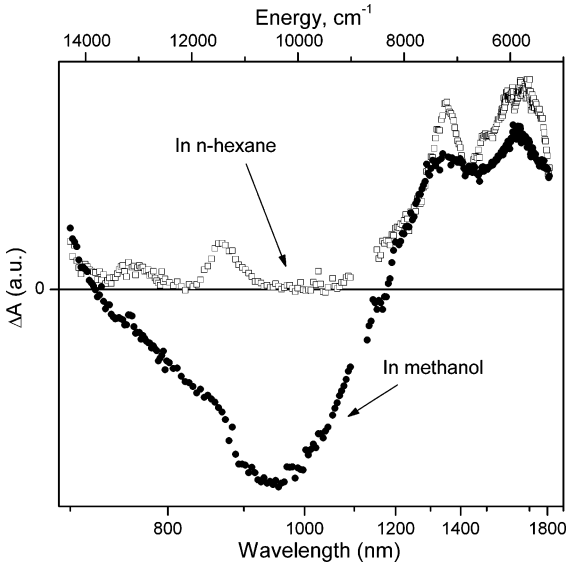

Figure 8. Peridinin near-IR transient absorption spectra in *n*-hexane (open symbols) and methanol (full symbols). In both solvents, peridinin was excited at 490 nm and transient absorption spectra were measured 1 ps after the excitation. Adapted with permission from ref 23. Copyright 2001 American Chemical Society.

750−1900 nm is dominated by the ESA signal above 1200 nm, characteristic of the S_1-S_2 transition of carotenoids. In methanol, a new negative spectral band located at 950 nm appears[23] and was assigned to stimulated emission from the peridinin ICT state, showing that probing the infrared spectral region permits a study of the ICT state without interference with signals from other excited states. The kinetics measured at the maximum of the ICT emission revealed a 1 ps rise component. This 1 ps dynamics, present also in the visible spectral region as a shift of the broad excited-state absorption band, was a clear sign of the richer dynamics in polar solvents and ascribed to a relaxation process between the S_1 and ICT states.[23] Several models were proposed to explain the complicated behavior of the peridinin excited states,[21−23] but none of them could consistently explain all the observed dynamical features.

Later experiments that focused on different polar solvents and included also dependence on viscosity, temperature, and excitation wavelength suggested

that it is not possible to consistently explain all experimental data unless the S_1 and ICT states merge to form one state called S_1/ICT that has a rather complicated solvent-dependent potential-energy surface.[44] The fact that the S_1 and ICT states actually form one state was also demonstrated by two-photon absorption measurements.[43,45] Measurements of peridinin in different polar solvents disclosed another interesting feature of the peridinin molecule. First, the asymmetric broadening of the absorption spectrum (section 3.1) in polar solvents varied from solvent to solvent. Moreover, even in the same solvent, the peridinin S_1/ICT lifetime varied with excitation wavelength: when excited below 500 nm, the lifetime in methanol was 10 ps, in agreement with previous results, but excitation into the red wing of the absorption spectrum at 550 nm gave a lifetime of 5 ps.[44] Interestingly, this effect was observed only in the protic solvents methanol and ethylene glycol, while the aprotic polar solvent acetonitrile did not cause any excitation wavelength dependence of the peridinin S_1/ICT lifetime. Consequently, it was proposed that the asymmetric broadening of absorption spectra toward longer wavelengths in polar protic solvents was due to a mixture of two forms of peridinin: a 'normal' peridinin without involvement of the C═O group in hydrogen-bonding absorbing predominantly in the spectral region below 500 nm and a 'red' form that was assigned to peridinin molecules actively participating in hydrogen bonding via the carbonyl group. The hydrogen bonding causes enhancement of the charge-transfer character, leading to an even shorter S_1/ICT lifetime. Within this model, the 1 ps dynamics are due to a small structural change of peridinin (most likely movement of the carbonyl group) in the S_1/ICT state, resulting in stabilization of charge-transfer character.[44]

Despite better understanding of the unique properties of peridinin, details behind its energetics and dynamics are still tenuous. On the basis of both time-resolved and two-photon absorption spectroscopy, it can be concluded that there are no distinct S_1 and ICT states as proposed earlier.[21−23] Instead, these states are strongly mixed, forming only one S_1/ICT state having charge-transfer character.[44,45] However, proposed explanations of the polarity dependence of the S_1/ICT lifetime state are not in accord. A model based on time-resolved spectroscopy data proposes large polarity-dependent changes of the S_1/ICT potential surface that are accompanied by corresponding changes of its charge-transfer character, concluding that these changes are primarily responsible for the observed S_1/ICT lifetime variations.[44] On the other hand, polarized two-photon excitation spectroscopy supported by quantum chemical calculation led to the conclusion that the charge-transfer character of the S_1/ICT state is not changed by solvent polarity and that the solvent-dependent S_1/ICT lifetime is due to a large change of ground-state charge-transfer character.[45] Thus, a consistent picture of the peridinin dynamics is still lacking. However, it seems that to consistently explain experimental data from different techniques, one must consider rather large polarity-dependent changes of both the ground and S_1/ICT states, since significant changes of the S_1-S_N excited-state absorption and the rich polarity-dependent dynamics of the S_1/ICT state[23,44] clearly require polarity-dependent changes of the S_1/ICT state.

Significant consensus exists for determination of the 0−0 origin of the S_1/ICT state. Spectral analysis of the peridinin S_1 emission placed the 0−0 origin at about 16 700 cm^{-1} in *n*-hexane, whereas a slightly lower value of 16 300 cm^{-1} was established in methanol.[21,23] An energy of 16 100 cm^{-1} was obtained in both solvents from S_1-S_2 spectra, although for methanol an error of 500 cm^{-1} was reported due to a complication to read the 0−0 origin of the S_2 state with sufficient precision.[23] A similar value of 16 200 cm^{-1} was determined from two-photon excitation spectra of peridinin in CS_2,[45] in a good agreement with emission data for peridinin in CS_2,[21,49,73] showing that the S_1/ICT energy is not or only very little affected by solvent, in accord with recent density functional theory calculations.[107] While the experiments described above established the 0−0 origin of the S_1/ICT state in the range 16 100−16 700 cm^{-1} depending slightly on solvent, the two-photon excitation study of peridinin in benzene reported an S_1/ICT energy in the range 18 500−18 900 cm^{-1} (530−540 nm), since no signal was detected above 600 nm.[43] The striking similarity between the one-photon and two-photon absorption spectra was explained in terms of mixing of S_2 and S_1/ICT states, making them both allowed in the two-photon absorption experiment.[43] Shima et al. made a similar observation,[45] but measurements of two-photon excitation spectra with linearly and circularly polarized light allowed regions of S_2-like and S_1/ICT-like signals to be separated, confirming that the S_1/ICT state lies indeed at around 16 200 cm^{-1}. Performing MNDO−PSDSCI calculations, the authors confirmed the S_2-S_1/ICT mixing, explaining the extremely weak signals from two-photon absorption in the region above 600 nm, as a result of the S_1/ICT state acquiring significant B_u^+ character.[45]

The carotenoid peridinin is the most extensively studied carbonyl carotenoid. Comparing its properties with those of other carbonyl carotenoids studied so far, it is obvious that the general pattern of the observed features is common for all of them, although the magnitude of the polarity-induced changes does not reach that of peridinin for other carbonyl carotenoids.[22,46] The asymmetric broadening and lack of pronounced vibrational structure of absorption spectra are similar for all carbonyl carotenoids. The change of the S_1/ICT lifetime, however, depends strongly on the structure of the particular carbonyl carotenoid (Table 3). When switching from nonpolar to polar solvents, the S_1/ICT lifetime changes from 60 to 20 ps (siphonaxanthin), 60 ps to 30 ps (fucoxanthin), 70 ps to ∼40 ps (uriolide acetate) but is unchanged for the longer spheroidenone, whose S_1/ICT lifetime remains 6 ps for all solvents.[22,46] Similar trends were observed for the S_1/ICT$-S_N$ transition in the visible spectral range and the polarity-induced S_1/ICT emission peaking at ∼950 nm. All the features characteristic of polarity-induced changes for

peridinin can also be detected for other carbonyl carotenoids, with their magnitudes in order siphonaxanthin > fucoxanthin ≈ uriolide acetate > spheroidenone. An analogous polarity-induced behavior was also revealed for a modified apo-β-carotene, for which the conjugated carbonyl group was introduced by adding an aldehyde group at the end of the conjugated backbone.[47] Moreover, broadening of the absorption spectrum and shortening of the lifetime in polar solvents was also observed for apo-β-carotene modified with two cyano groups, demonstrating that introducing an electron acceptor into the carotenoid structure also leads to peridinin-like behavior.[108] In naturally occurring carotenoids, however, no other electron acceptor than the carbonyl group has been found to date, making the carbonyl carotenoids a separate family having unique properties of excited states playing a key role in light-harvesting complexes of algae (see section 4.3).

3.3. Other States

Calculations on polyenes predicted additional states besides the S_1 and S_2 states. From extrapolations of state energies to longer polyenes it became apparent that two other excited states of $1B_u^-$ and $3A_g^-$ symmetry are of interest in carotenoids, since especially the $1B_u^-$ state approaches the S_2 state for $N \approx 9$ and it should be located between the S_1 and S_2 states for $N > 10$.[13] As a result, for most of the naturally occurring carotenoids, this state can be involved in the excited-state dynamics. The $3A_g^-$ state was predicted to be in the vicinity of the S_2 state for $N \approx 13$[13] and thus above the S_2 state for most of carotenoids, but it could affect the dynamics of the longest carotenoids such as spirilloxanthin. Since transition from the ground state to both $3A_g^-$ and $1B_u^-$ states is forbidden (for $1B_u^-$ it is both one- and two-photon forbidden),[13] location of these states suffered from the same problems as the S_1 state. However, for the $3A_g^-$ and $1B_u^-$ states, the experimental difficulties are further enhanced by the fact that these states, if populated, will relax quickly to the S_1 state, limiting their lifetime to the hundred femtosecond time scale.

As described above, the success of resonance Raman spectroscopy to locate the S_1 state relies on proper sample concentration and detection geometry, allowing separation of resonance Raman profiles originating from S_1 and S_2 states. By setting an appropriate concentration and using a back-scattering geometry, Sashima et al. obtained a resonance Raman profile of spheroidene that corresponded to a new electronic state located between the S_1 and S_2 states.[69] The 0−0 spectral origin had an energy of 17 600 cm^{-1}, and the new state was ascribed to the $1B_u^-$ state. The same technique was applied to other carotenoids, and the $1B_u^-$ state was detected for mini-9-β-carotene (19 700 cm^{-1}),[14] β-carotene (16 550 cm^{-1}),[14] lycopene (15 770 cm^{-1}),[14] anhydrorhodovibrin (14 500 cm^{-1}),[15] and spirilloxanthin (13 330 cm^{-1}).[15]

On the basis of these findings, the $1B_u^-$ state was included in fitting fluorescence spectra of a few carotenoids. Spectral deconvolution of fluorescence profiles of lycopene, anhydrorhodovibrin, and spirilloxanthin led to $1B_u^-$ energies of 16 000, 14 900, and 13 600 cm^{-1}, respectively.[51] Although the $1B_u^-$ energies extracted from fluorescence profiles are close to those revealed by resonance Raman spectroscopy, it is necessary to point out that the appearance of $1B_u^-$ emission is not easy to explain. The intensity of the $1B_u^-$ emission together with the presumably short lifetime of the $1B_u^-$ state led to a conclusion that the transition dipole moment of the $S_0-1B_u^-$ transition is 4−5 D, thus significantly larger than that of the S_0-S_1 transition.[51] Since the $S_0-1B_u^-$ transition is both one- and two-photon forbidden, such a large dipole moment is quite surprising. Moreover, a transition dipole moment of 4−5 D should be visible in the absorption spectrum, which is obviously not the case. Despite these problems, the $1B_u^-$ energies detected both by resonance Raman and fluorescence fit well to the predicted dependence of the $1B_u^-$ energy on conjugation length.[15] Further investigations of resonance Raman profiles made it possible to find sample concentrations, for which a resonance Raman profile corresponding to the $3A_g^-$ state was found.[15] The $3A_g^-$ energies of 19 990 (spheroidene), 18 020 (lycopene), 16 450 (anhydrorhodovibrin), and 14 556 cm^{-1} (spirilloxanthin) were determined. Although reading of the $3A_g^-$ energies from resonance Raman profiles is more complicated because of overlapping contributions from nearby states, they fall reasonably into the range predicted by theoretical calculations on polyenes.[13] It is worth noting, however, that semiempirical MNDO−PSDCI calculations on rhodopin glucoside ($N = 11$) in pentane placed the $3A_g^-$ state above the S_2 state at 22 200 cm^{-1}, thus significantly higher than was determined by resonance Raman profiles for lycopene having the same conjugation length.[109]

Significant improvement of both time and spectral resolution in time-resolved techniques in the past few years has also allowed for searching of the $1B_u^-$ and $3A_g^-$ states by means of these methods. Using singular value decomposition and global fitting of data recorded in the 840−1040 nm spectral region after excitation of the neurosporene S_2 state by 130 fs pulses, Zhang et al. identified spectral changes that were attributed to excited-state absorption from the S_2 and $1B_u^-$ states, respectively.[70] This result, together with a subsequent study of neurosporene by means of time-resolved Raman spectroscopy,[71] suggested direct involvement of $1B_u^-$ in relaxation processes taking place in neurosporene. While the time-dependent spectral changes in excited-state absorption observed for neurosporene were quite subtle, a study performed using 15 fs pulses on β-carotene showed a distinct separation of excited-state absorption bands.[110] The excited-state absorption band located around 800 nm that appeared immediately after excitation was in ∼50 fs replaced by another ESA band centered at 1000 nm, which then decayed to form the known S_1-S_N band peaking at 560 nm. Similar to the study of neurosporene,[70] these spectral changes were explained in terms of an additional state located below the absorbing S_2 state that produces the 1000 nm ESA band, while the 800 nm band is due to the S_2 excited-state absorption. A

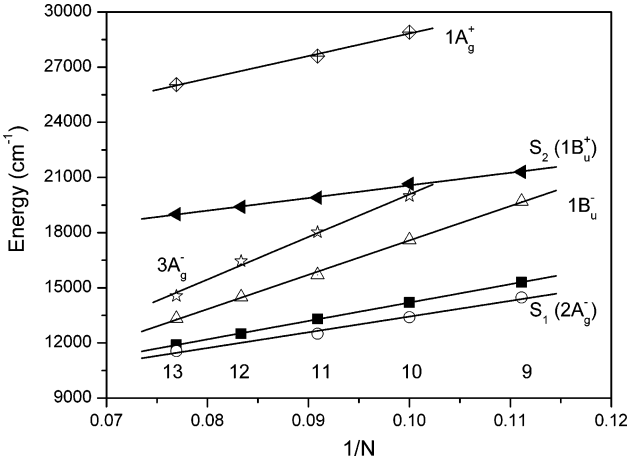

Figure 9. Dependence of energies of the five low-lying singlet excited states of carotenoids on their conjugation length: S_1 energy as determined from the S_1-S_2 spectral profiles (open circles); S_1 energy obtained from fluorescence measurements (full squares); $1B_u^-$ (open triangles) and $3A_g^-$ (open stars) energies obtained from resonance Raman profiles; $1B_u^+$ (full triangles) and $1A_g^+$ (diamonds) energies determined from absorption spectra. To avoid effects of carotenoid structures on state energies, only the linear carotenoids spirilloxanthin (13), anhydrorhodovibrin (12), lycopene (11), and spheroidene (10) are used. For $N = 9$, values for neurosporene are used in the case of the S_1 energy from fluorescence and the S_2 energy, violaxanthin for the S_1 energy from the S_1-S_2 profile, and m9-β-carotene for the $1B_u^-$ energy.

subsequent study by Fujii et al.[72] went further as they studied time-dependent changes of excited-state absorption in the 850−1040 nm region of five carotenoids with different conjugation lengths. Distinct spectral shifts of the excited-state absorption on the time scale of 50−300 fs were attributed to contributions from the S_2 and $1B_u^-$ states in the case of neurosporene ($N = 9$) and spheroidene ($N = 10$), while for the longer carotenoids lycopene ($N = 11$), anhydrorhodovibrin ($N = 12$), and spirilloxanthin ($N = 13$), they were assigned to excited-state absorption from the S_2 and $3A_g^-$ states, respectively.[72] This conclusion was based on slightly different patterns of spectral shifts observed for neurosporene and spheroidene and on the resonance Raman data putting the $3A_g^-$ state below the S_2 state for linear carotenoids with $N \geq 11$.[15] These experimental observations triggered a number of discussions about involvement of these states in relaxation processes in carotenoids, and various models will be reviewed in section 3.5. Locations of the $1B_u^-$ and $3A_g^-$ states for carotenoids with different conjugation wavelengths are summarized in Figure 9 and Table 4.

In addition to the $1B_u^-$ and $3A_g^-$ states that were predicted by calculations on polyenes, another state lying between the S_1 and S_2 states, called S*, was recently discovered. Using global analysis of data in the spectral region 470−720 nm, it was shown that the S_1-S_N band of spirilloxanthin (peaking at 590 nm) possessed a distinct shoulder at ~540 nm. While the 590 nm band decayed with 1.4 ps corresponding to the S_1 lifetime of spirilloxanthin, the 540 nm shoulder exhibited a much longer decay of ~6 ps.[20] This result was explained in terms of two parallel pathways of S_2 depopulation; a major part (70%) decays to form the S_1 state, while the minor pathway (30%) leads to population of the new S* state, which then decays to the ground state with a 6 ps lifetime. Interestingly, as shown in several studies,[111−113] the S* state is formed with much higher yield when carotenoids are incorporated into light-harvesting proteins. While no S* state was detected for spheroidene in solution, it is populated with about 20% efficiency for spheroidene in the bacterial light-harvesting complex LH2.[111] It was also recently shown that the S* is populated when carotenoids are covalently bound to an energy acceptor in artificial antenna systems (see section 5.1).[114] In light-harvesting protein complexes, the S* state was also found to be a precursor of ultrafast singlet−triplet homofission (for details, see section 4.1).[20,111−113] For carotenoids in solution, population of the S* state is probably limited to only long carotenoids, and spirilloxanthin was until recently the only carotenoid for which involvement of the S* state in solution was demonstrated.[20] The most recent experiments employing pump−dump−probe spectroscopy, however, revealed spectral features characteristic of the S* state also for lycopene, zeaxanthin, and β-carotene.[115] It is worth mentioning that a distinct shoulder at the high-energy side of the S_1-S_N spectrum with similar dynamical properties (slower decay than the S_1-S_N band) was observed much earlier for synthetic long analogues of β-carotene having conjugation lengths of 15 and 19.[57] For both conjugation lengths, this band was observed to decay on the 5−15 ps time scale, somehow dependent on solvent. This feature

Table 4. Energies of Other Singlet Excited States of Certain Carotenoids[a]

		$1B_u^-$				
carotenoid[b]	N[c]	fluorescence	Raman	2-photon	$3A_g^-$	$1A_g^+$ (*cis*-peak)
spirilloxanthin	13	13 600 (51)	13 330 (15)		14 556 (15)	26 050 (93)
anhydrorhodovibrin	12	14 900 (51)	14 500 (15)		16 450 (15)	
lycopene	11	16 000 (51)	15 770 (14)		18 020 (15)	27 600 (120)
			15 630 (15)			
spheroidene	10		17 600 (69)		19 990 (15)	28 900 (119)
β-carotene	9β2		16 550 (14)			29 400 (118)
m9-β-carotene*	7β2		19 700 (14)			
peridinin	7LOA			22 000 (45)		30 500 (45)

[a] The values of the $1B_u^-$ energies determined by fluorescence and energies of the $1A_g^+$ state obtained from absorption spectra of isomers were taken from carotenoids dissolved in *n*-hexane. For recording resonance Raman profiles to determine the $1B_u^-$ and $3A_g^-$ energies, crystalline samples were used. The $1B_u^-$ energy of peridinin was measured in CS_2. Numbers in parentheses are references. [b] Carotenoids marked by asterisk are synthesized carotenoids that do not occur naturally. [c] Conjugation length. See caption of Figure 1 for description.

was assigned to a transition from the 'hot' ground state populated by the S_1-S_0 internal conversion. The possibility of the S* state being the vibrationally hot ground state was also considered by Gradinaru et al.,[20] but the absence of a shift and narrowing of the spectrum expected as a result of vibrational cooling led to the conclusion that the S* signal is due to a relaxed state. The finding that S* participates in carotenoid-to-BChl energy transfer[111-113] confirmed that the S* state must be at higher energy (or at least similar) than the S_1 state. Thus, the hypothesis of S* as a hot vibrational ground state was ruled out for the S* state in carotenoids incorporated in light-harvesting complexes. However, recent pump−dump−probe experiments suggested that the S* states in light-harvesting complexes and in solution could be of different origins,[115] and the S* state in solution was proposed to be a vibrationally hot ground state (see also section 4.1).

Yet another state, labeled as $S^‡$, was revealed using pump−dump−probe spectroscopy on β-carotene in solution.[116] This state is populated only when β-carotene is excited into the higher vibrational levels of the S_2 state at 400 nm, most likely by opening a new relaxation channel that is not accessible when the 0−0 transition of the S_2 state is excited. The spectral characteristics of the $S^‡$ state resemble those of the S* state, but the global analysis of the recorded data revealed that the $S^‡$ state is slightly blue-shifted from the S* state.[116] In addition, the $S^‡$ state in β-carotene exhibits double-exponential decay with time constants of 10 and 65 ps, thus significantly longer than the S* state.[20] Origin and symmetry properties of the $S^‡$ state remain unknown.

To finish the listing of the singlet excited states involved in various spectroscopic studies, the $1A_g^+$ state must be mentioned. The lowest state of A_g^+ symmetry in the manifold of carotenoid excited states is the *cis*-peak usually located 7000−8000 cm^{-1} above the 0−0 origin of the S_2 state. Because the ground state is of A_g^- symmetry, the transition from the ground state to the $1A_g^+$ state is symmetry forbidden for *all-trans* carotenoids, but it becomes allowed for various *cis*-isomers.[29] Since the shift of the S_2 state due to isomerization is rather small (on the order of a few nanometers), appearance of the *cis*-peak is a reliable control of the presence of isomers in the sample. The position and relative intensity of the *cis*-peak and S_2 absorption are characteristics of a particular isomer. For spheroidene, the 0−0 origin of the *cis*-peak is at 345 nm for all possible isomers, but its intensity relative to the S_2 absorption varies markedly from 0.08 to 0.45.[117] Similar to the other excited states, the *cis*-peak shifts to the red with conjugation length, being located at 340 nm for β-carotene,[118] at 345 nm for spheroidene,[117,119] at 362 nm for lycopene,[120] and at 384 nm for spirilloxanthin[93] (Table 4 and Figure 9).

3.4. Vibrational Relaxation

Because of very fast dynamics of carotenoid excited states, studies attempting to address questions regarding relaxation within the vibrational manifold of particular electronic states were less frequent. In the past few years, emerging new techniques such as time-resolved Raman spectroscopy enabled the study of vibrational relaxation of carotenoids in detail.

Although the absorbing S_2 state is strongly allowed and easily accessible by direct excitation, knowledge of vibrational relaxation in the S_2 state is more vague than that of the S_1 and S_0 states, mainly because this relaxation is extremely fast, challenging the current limits of time-resolved spectroscopy. This was first demonstrated on spheroidene in a few different solvents, for which up-conversion measurements did not show any differences when excited in the range 427−490 nm with ∼150 fs time resolution. Even after excitation to higher vibrational levels, the up-converted S_2 emission did not exhibit any appreciable rise attributable to S_2 vibrational relaxation, and it was concluded that S_2 vibrational relaxation should be faster than 50 fs.[54] This was further confirmed by means of up-conversion measurements on β-carotene with ∼60 fs time resolution. In addition to the same decay kinetics regardless of excitation wavelengths in the range 400−485 nm, no 'hot' emission bands due to fluorescence occurring prior to vibrational relaxation were observed, setting the upper limit for the time scale of S_2 vibrational relaxation to about 20 fs.[42] A similar value of ∼40 fs was obtained from up-conversion measurements of neurosporene excited into the second vibrational level of the S_2 state at 420 nm.[55] The same authors studied S_2 vibrational relaxation of β-carotene and β-apo-8′-carotenal, concluding that the active Franck−Condon mode (C═C) relaxes on 40−80 and ∼30 fs for β-carotene and β-apo-8′-carotenal, respectively.[56] On the basis of temporal evolution of fluorescence spectra, they also concluded that low-frequency modes exhibit a slower (220 fs) S_2 relaxation for β-carotene.[56]

Contrary to the sub-100 fs vibrational relaxation in the S_2 state, S_1 vibrational relaxation occurs on a slower time scale. Using analysis of time-dependent changes in S_1-S_N excited-state absorption of lycopene in CS_2, Zhang et al. concluded that vibrational relaxation in the S_1 state occurs on the same time scale as S_1-S_0 internal conversion, i.e., ∼3 ps.[82] However, this conclusion was later shown to be likely due to limited time resolution, and it was demonstrated by recording the time-dependent changes of the spectral profile of the S_1-S_N transition (Figure 10) that the vibrational relaxation in the S_1 state of lycopene actually takes place on a subpicosecond time scale.[100] The subpicosecond time scale for S_1 vibrational relaxation has up to date been established for a few different carotenoids. A study of the excited-state dynamics of β-carotene excited by 7 fs pulses demonstrated thermalization of the S_1 state with a time constant of 620 fs.[121] A similar time constant of 700 fs for S_1 vibrational relaxation was determined from fitting of kinetics recorded at the red edge of the S_1-S_2 spectrum at 1450 nm for spheroidene at 185 K.[62] Later, on the basis of a detailed analysis of the time-dependent spectral profiles of the S_1-S_N transition of the three structurally different carotenoids β-carotene, zeaxanthin, and lycopene (all having 11 conjugated C═C bonds), it was concluded

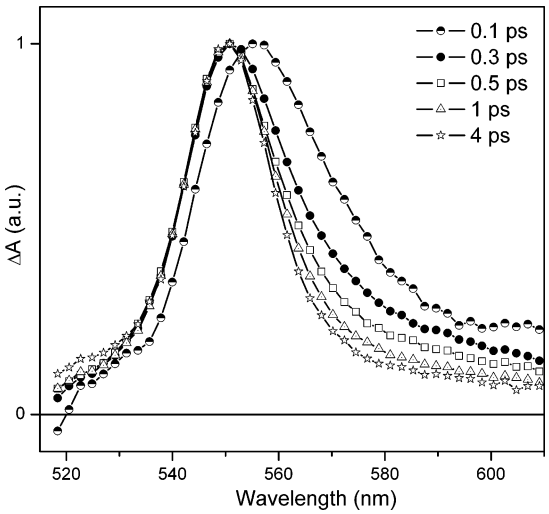

Figure 10. Transient absorption spectra of the S_1-S_N transition of lycopene in *n*-hexane recorded at different time delays. To demonstrate the time-dependent changes of the spectral profile of the S_1-S_N transition, the transient spectra are normalized at their maxima. Excitation at 510 nm. Reprinted with permission from ref 100. Copyright 2002 Elsevier Science.

that the vibrational relaxation in the S_1 state is not affected by the structure of the carotenoid and that it takes place on the ~500 fs time scale in the polar solvent methanol. A slightly slower vibrational relaxation was observed in the nonpolar solvent *n*-hexane, yielding time constants of 650 (*β*-carotene) and 800 fs (zeaxanthin).[100] In addition, Gaussian deconvolution of the S_1-S_N ESA band reveals that the low-energy tail observed at early decay times extends approximately 1500 cm^{-1} toward lower energies from the maximum of the S_1-S_N band (Figure 10), suggesting that rather low-frequency vibrational modes are involved. This fact is in accord with measurements of the S_1-S_2 spectra, showing that the relative shift of the S_1 and S_2 potential surfaces is small,[62] thus preventing population of high-energy vibrational modes by the S_2-S_1 internal conversion. A time constant of 700 fs for the vibrational cooling in the S_1 state of *β*-carotene was also revealed by time-resolved transient grating.[122] Slightly shorter relaxation time constants were determined in another transient absorption study of *β*-carotene, yielding values of 0.3 ps in ethanol and 0.4 ps in *n*-hexane and benzyl alcohol.[101] Contrary to the work of Billsten et al.,[100] these authors proposed a different mechanism for the relaxation in the S_1 state. It was suggested that *β*-carotene might undergo a small structural change upon excitation, followed by relaxation of the twisted conformers to the S_1 state. The observed time constant of 0.3−0.4 ps is ascribed to this conformational change, during which the twisted conformation relaxes to the *all*-trans form.[101] It is worth mentioning that although this mechanism is similar to the 'conformational' hypothesis described in section 3.2, these two hypotheses are qualitatively different. While de Weerd et al. proposes the conformational change to occur in the S_1 state,[101] the hypothesis suggested by Polívka et al. has the view that twisted conformers still exist in the relaxed S_1 state and that the conformational change toward the *all-trans* form takes place during the S_1-S_0 internal conversion.[62]

The subpicosecond time scale of vibrational relaxation in the S_1 state of *β*-carotene was also confirmed by femtosecond time-resolved Raman spectroscopy as a 0.6 ps component found in kinetics of the 1800 cm^{-1} C=C stretching mode in the S_1 state.[123] Interestingly however, these authors assigned the 0.6 ps component to a relaxation between the $v = 2$ and 1 vibrational levels of the S_1 state since it appeared as a rise in the kinetics corresponding to this mode. The decay of these kinetics was characterized by a time constant of 8.8 ps, very close to that of the S_1-S_0 internal conversion. Consequently, a model was proposed in which the $v = 1$ vibrational level of the S_1 state is the initial state for the S_1-S_0 internal conversion, preventing any population of the $v = 0$ vibrational level of the S_1 state.[123] Later, using a series of *β*-carotene analogues, Yoshizawa et al. suggested that such a storage of energy in the C=C stretching mode is characteristic of carotenoids with $N < 13$.[66] This model was, however, questioned by McCamant et al., who also used time-resolved Raman spectroscopy to follow vibrational relaxation in *β*-carotene.[124] Despite a limited time resolution of ~2 ps, these authors concluded on the basis of detailed analysis of the anti-Stokes/Stokes intensity ratio for different vibrational modes that the 0.6 ps component indeed corresponds to a full vibrational relaxation to the $v = 0$ vibrational level of the S_1 state.[124] The same research group further refined this conclusion by improving both the time resolution (~100 fs) and signal/noise ratio of their time-resolved stimulated Raman experiment.[125] By analyzing decays of the C=C stretching mode in the S_1 state, it was concluded that vibrational relaxation in the S_1 state of *β*-carotene in cyclohexane consist of two separate processes. The energy in the vibrationally hot C=C mode is first distributed to the strongly coupled vibrations in ~200 fs and then follows an intramolecular vibrational energy distribution to the complete set of normal modes within 450 fs.[125] An interesting new insight into the vibrational relaxation in the S_1 state was recently provided by the femtosecond time-resolved transient grating technique. Using this nonlinear spectroscopic method, Siebert et al. suggested that a fraction of higher vibrational states of the S_1 state of *β*-carotene could relax to the ground state directly, making a new channel competing with vibrational relaxation.[122]

Vibrational relaxation in the ground state was studied almost exclusively by means of time-resolved anti-Stokes Raman scattering.[126] Contrary to the mode-averaged relaxation obtained from transient absorption spectroscopy, this technique enables the determination of relaxation times for specific vibrational modes. Two comprehensive studies of the ground-state vibrational relaxation of *β*-carotene were recently performed. Using anti-Stokes resonance Raman spectroscopy with picosecond time resolution, McCamant et al. investigated ground-state relaxation of the C=C (1523 cm^{-1}), C−C (1157 cm^{-1}), and $C-CH_3$ (1004 cm^{-1}) vibrational modes, concluding that their relaxation times differ substan-

tially. While relaxation of the C=C stretching mode was beyond the time resolution of the detection system (<1 ps), the other modes exhibited longer relaxation times of 5 (C−C) and 12 ps (C−CH_3), respectively.[124] This result contradicts, however, the results obtained by femtosecond coherent anti-Stokes Raman scattering (CARS), where three pump and one probe beams are used to generate the CARS signal.[127] In this study, two more vibrational modes (the C−H bending mode at 1269 cm^{-1} and the C=C−C bending mode at 872 cm^{-1}) were studied in addition to those studied by McCamant et al. Although the observed trend of relaxation times for different vibrational modes follows that obtained by McCamant et al., the actual time constants are markedly different. The fastest relaxation is observed for the C=C stretching mode with a time constant of 8.5 ps, while ∼9 ps relaxation was obtained for both C−C and C−CH_3 stretches; the C=C−C and C−H bending modes relaxed with time constants of 10.9 and 13.4 ps, respectively.[127] The apparent contradiction in the relaxation time of the C=C stretching mode is further underlined by another time-resolved anti-Stokes Raman study, in which a time constant of 15 ps was determined for β-carotene.[123] The same time constant of 15 ps for ground-state vibrational relaxation was obtained for the carotenoids spirilloxanthin[128] and canthaxanthin.[129] Regardless of this contradiction, these studies confirmed that mode-averaged vibrational relaxation in the ground state occurs on the time scale of 8−15 ps, in agreement with data obtained by transient absorption spectroscopy on long (N = 15 and 19) synthesized analogues of β-carotene, yielding ground-state relaxation time constants of 5−15 ps.[57]

In summary, it is clear that even though detailed studies of vibrational relaxation emerged only recently and the results obtained from different groups are still contradictive in certain aspects, the time scales of vibrational relaxation in the S_2, S_1, and S_0 states of carotenoids have been established. Thus, vibrational relaxation in the S_2 state is extremely fast, taking place on a time scale faster than 80 fs. A slower, 300−800 fs vibrational relaxation characterizes the S_1 state, and ground-state vibrational relaxation is clearly the slowest one, occurring on the 5−15 ps time scale. No studies addressing vibrational relaxation in other excited states of carotenoids have been reported so far.

3.5. Relaxation Schemes of Carotenoid Excited States in Solution

Knowledge of the properties of carotenoid excited states summarized in previous sections allowed for construction of models of relaxation pathways within the manifold of excited states after excitation to the absorbing S_2 state. Discovery of new states below the S_2 state made the simple $S_2 \rightarrow S_1 \rightarrow S_0$ model used for nearly two decades no longer appropriate, and new models depicted in Figure 11 were proposed.

The last S_1-S_0 relaxation step is the best understood so far. With knowledge of S_1 energies and lifetimes it was recognized that the S_1-S_0 internal conversion follows well that predicted by the energy-gap law for radiationless transitions.[77,78] To explain the rather short S_1 lifetime of carotenoids, as compared with lifetimes observed for most organic dyes, a mechanism involving a strong vibrational coupling was proposed for S_1-S_0 internal conversion. Since the S_0 and S_1 states have the same A_g^- symmetry, they can be vibrationally coupled through the totally symmetric a_g stretching modes, which would result in a large difference in frequencies of these modes in the S_0 and S_1 states.[130] This effect was known from short polyenes, for which the ∼1550 cm^{-1} frequency of the C=C stretching mode in the S_0 state increased to ∼1700 cm^{-1} in the S_1 state.[16] About the same difference in the C=C stretching frequency was later revealed for carotenoids by means of picosecond time-resolved resonance Raman,[90] suggesting that vibrational coupling through the C=C stretching mode plays a central role in S_1-S_0 internal conversion in carotenoids. This proposal was confirmed by femtosecond transient absorption spectroscopy combined with picosecond transient Raman spectroscopy on isotope-labeled β-carotene.[131] It was shown that ^{13}C-labeled β-carotene had a longer S_1 lifetime of 14.3 ps, while shorter and nearly identical S_1 lifetimes (9.9 and 10.7 ps, respectively) were observed for nonlabeled and ^{2}H-labeled β-carotene, confirming that skeletal vibrational modes are crucial for S_1-S_0 internal conversion. A corresponding decrease of the frequency of the C=C stretching mode for ^{13}C-labeled β-carotene in the S_1 state proved that vibrational coupling through the C=C stretching mode is responsible for the fast S_1-S_0 internal conversion of carotenoids.[131]

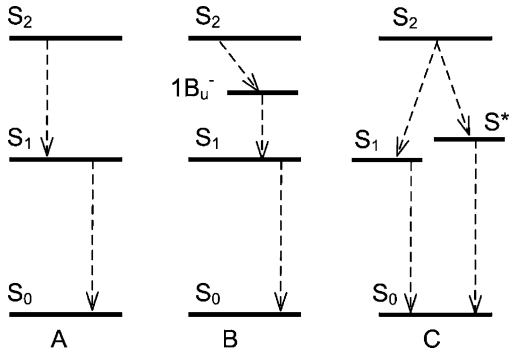

Figure 11. Three possible relaxation pathways that can take place after excitation of a carotenoid into the S_2 state. (A) The direct $S_2 \rightarrow S_1 \rightarrow S_0$ pathway operating most likely for shorter carotenoids. (B) The $S_2 \rightarrow 1B_u^- \rightarrow S_1 \rightarrow S_0$ (or $S_2 \rightarrow 3A_g^- \rightarrow S_1 \rightarrow S_0$ in some cases, see text for details) pathway including an intermediate state. (C) The relaxation pathway involving branching of the S_2 population into S_1 and S* states. See text for analysis of the particular cases.

While the mechanism of the S_1-S_0 internal conversion is well understood, considerably less is known about mechanisms and pathways driving a carotenoid from the excited S_2 state toward the S_1 state. Until experimental data suggesting the presence of additional states between S_1 and S_2 states were reported, a direct S_2-S_1 relaxation as shown in Figure 11A was assumed. Since the S_1 and S_2 states have A_g^- and B_u^+ symmetry, respectively, vibronic coupling via totally symmetric a_g modes is symmetry forbidden.[69] Thus, to explain the very fast (50−200

fs) S_2-S_1 internal conversion, a conical intersection between the S_1 and S_2 potential surfaces was invoked.[33] However, the proposed existence of the conical intersection requires a substantial shift between the S_1 and S_2 potential surfaces. This is not supported by the S_1-S_2 spectra that display an intensity of their vibrational bands in the order $0-0 > 0-1 > 0-2$, suggesting a rather small displacement between the S_1 and S_2 potential minima (Figure 5).[62] Out-of-plane bending vibrational modes of b_u symmetry resulting from intensity borrowing between A_g^- and B_u^+ states were in addition proposed to play a role in the S_2-S_1 internal conversion of polyenes.[132] Although the vibrational coupling via the totally symmetric a_g modes is symmetry forbidden, a mixing of the S_2 and S_1 states allows vibrational coupling through nontotally symmetric b_u modes. This mechanism may be important especially for shorter polyenes and carotenoids with a small S_2-S_1 energy gap, facilitating the S_2-S_1 mixing. Therefore, the relaxation scheme depicted in Figure 11A is most likely valid for carotenoids with $N < 9$, which have the $1B_u^-$ and $3A_g^-$ states above the S_2 state, but the S_1-S_2 gap is narrower to enhance the S_1/S_2 mixing (Figure 9).

When the existence of additional states between S_2 and S_1 was experimentally confirmed,[14,15,69] these states were incorporated into the relaxation schemes of carotenoid excited states. In the first paper showing the resonance Raman profile of the $1B_u^-$ state of spheroidene,[69] it was suggested that the location of the $1B_u^-$ state below the S_2 state can mediate the S_2-S_1 internal conversion process (model B in Figure 11). Because the B_u^- and S_1 (A_g^-) states both have 'minus' Pariser's label, a strong vibronic coupling is allowed,[14,69] while vibronic coupling between the S_2 (B_u^+) and B_u^- states was justified by the small $S_2-B_u^-$ energy gap ($\sim$2100 cm^{-1}), for which the pseudoparity selection rule can be broken.[69] Thus, to overcome difficulties in explaining the ultrafast S_2-S_1 internal conversion rate, it was proposed that the $1B_u^-$ state is crucial for facilitating the S_2-S_1 internal conversion, making a 'vibrational coupling bridge' between the S_2 and S_1 states.[14] This $S_2 \rightarrow 1B_u^- \rightarrow S_1 \rightarrow S_0$ model was further supported by time-resolved data. Spectral changes that appeared in excited-state absorption in the 840−1060 nm spectral region for neurosporene were attributed to the $S_2-1B_u^-$ internal conversion. In this scheme, the S_2 and $1B_u^-$ lifetimes were 40−80 and 190−270 fs, respectively.[70] Further refinement of this model for neurosporene was achieved by application of subpicosecond time-resolved Raman spectroscopy.[71] By recording Raman spectra in the time window up to 20 ps with time resolution of about 0.16 ps, these authors distinguished Raman spectra of the S_2, $1B_u^-$, and S_1 states, concluding that internal conversion between S_2 and $1B_u^-$ states occurs to the $v = 1$ vibrational level of the $1B_u^-$ state. The following relaxation between the $1B_u^-$ and S_1 states then occurred predominantly to the $v = 3$ vibrational level of the S_1 state.[71] The same group later recorded time-resolved absorption in the 840−1060 nm region for five carotenoids with different conjugation length[72] and proposed two different relaxation pathways. For longer carotenoids, the $1B_u^-$ state drops too low below the S_2 state to allow efficient vibrational coupling necessary to explain the fast S_2-S_1 relaxation for longer carotenoids.[4,72] To resolve this contradiction, the authors proposed, on the basis of slightly different patterns of spectral changes in transient absorption spectra, that the $S_2 \rightarrow 1B_u^- \rightarrow S_1 \rightarrow S_0$ is valid only for neurosporene ($N = 9$) and spheroidene ($N = 10$). For the longer lycopene, anhydrorhodovibrin, and spirilloxanthin, the $S_2 \rightarrow 3A_g^- \rightarrow S_1 \rightarrow S_0$ pathway was proposed to operate, since the $3A_g^-$ state is pushed below the S_2 state for these carotenoids. The S_2 lifetimes determined by this study were much shorter (10−20 fs) than previously reported. While the temporal resolution in that study was $\sim$130 fs and these extremely short lifetimes suffered by a relatively large error as they were extracted by a global fitting analysis and subsequent deconvolution with response function, a study of excited-state dynamics of β-carotene and lycopene using 15 fs pulses[110] allowed determination of lifetimes with much higher precision. The data further supported the $S_2 \rightarrow 1B_u^- \rightarrow S_1 \rightarrow S_0$ model depicted in Figure 11B, and S_2 lifetimes of 10 ± 2 and 9 ± 2 fs were determined for β-carotene and lycopene, respectively.[110] Even more complicated schemes were proposed by Rondonuwu et al., who suggested the $1B_u^-$ state to be a precursor of an ultrafast singlet−triplet conversion to the second triplet state, $1^3A_g^-$, which further decays to the lowest triplet state on the picosecond time scale for carotenoids with conjugation lengths in the range of 9−13.[64] This model, however, does not include any vibrational relaxation, and the spectral profile of the $1B_u^-$ state extracted from global fitting analyses is nearly identical with the spectral profile assigned previously to the vibrationally hot S_1 state.[100,101] Taking into account the complicated branching schemes proposed by these authors, the uncertainty in assignment of the spectral profiles represents a serious problem, which is further complicated by the fact that the only known mechanism for the ultrafast singlet−triplet conversion in carotenoids, a singlet homofission, is energetically unfavorable for some of the studied carotenoids. Thus, the validity of these complicated relaxation schemes remains to be verified by further experimental and theoretical investigations of carotenoid excited states.

In brief, experimental evidence suggesting involvement of an intermediate state that facilitates S_2-S_1 internal conversion has recently been obtained. However, the proposed extremely fast internal conversion from the S_2 state to the intermediate ($1B_u^-$, $3A_g^-$) state occurring at a time scale of about 10 fs should prevent observation of emission, because the intermediate state is a 'dark' state. This proposal is in contradiction with a number of emission data but was addressed by Cerullo et al.[110] with a model suggesting departure from a planar carotenoid configuration, leading to a conformational rearrangement upon excitation. Such a symmetry break would make the intermediate state emissive, as the symmetry selection rules would be less restrictive. The fact that this conformational change occurs upon excitation would

also explain why the intermediate state is not visible in absorption spectra. Yet, a problematic point of this explanation is that this change must occur within the proposed 10 fs lifetime of the S_2 state, and it is hard to imagine a mechanism that would modify symmetry of the conjugated backbone on such a short time scale. Moreover, the fact that S_2 emission spectra constitute a nearly perfect mirror image of the absorption spectrum is another intriguing feature that challenges the relaxation model with an intermediate state, because it suggests that absorbing and emissive states are identical. The Stokes shifts for S_2 emission are on the order of 150−300 cm^{-1} for all carotenoids regardless of their conjugation length,[37,38,40,50−52] suggesting that if the emission indeed originates from an intermediate state, its energy gap to the S_2 state must be about 300 cm^{-1} and independent of the conjugation length. Accordingly, the strong dependence of the $1B_u^-$ energy on conjugation length predicted theoretically[13] and confirmed experimentally[14,51,52] rules out the $1B_u^-$ state as the emissive state. Within the $S_2 \rightarrow 1B_u^- \rightarrow S_1 \rightarrow S_0$ model, the emission cannot be ascribed to the S_2 state, because fluorescence up-conversion measurements set a lifetime of the emissive state in the range 50−300 fs,[42,54,55,56,59] in disagreement with the ∼10 fs lifetimes suggested for the S_2 state in the framework of this model.

Another way to test if the intermediate state observed in the time-resolved data could be the $1B_u^-$ state is to monitor the spectral shift of the excited-state absorption corresponding to the intermediate state as a function of conjugation length. To account for the strong excited-state absorption, the final state must be of $1A_g^+$ symmetry if the initial state is to be the $1B_u^-$ state. Then, because the energy dependence on conjugation length is steeper for the $1B_u^-$ state than that for the $1A_g^+$ state (Figure 9), the $1B_u$−$1A_g^+$ energy gap increases with conjugation length and, consequently, the $1B_u^-$ excited-state absorption should shift toward blue with increasing conjugation length. However, an opposite result was obtained by global analysis of transient absorption data.[72] Thus, it seems that the $1B_u^-$ state is not the intermediate state observed in the time-resolved experiments.

It is also worth noting that transient absorption spectra recorded in the near-infrared region for spirilloxanthin under different experimental conditions gave qualitatively different results. Fujii et al.[72] observed distinct spectral changes in the near-infrared region attributed to the presence of an intermediate state, but this dynamics was absent when lower excitation energies were used.[67] Similarly, in studies on β-carotene, no excited-state absorption bands in the spectral region 650−850 nm were observed,[66,101] where the S_2 excited-state absorption should be present according to the relaxation model with an intermediate state.[110] Although the earlier experiments used substantially worse temporal resolution than the 15 fs used by Cerullo et al.,[110] preventing monitoring the dynamics on very short times scales, response-limited spectral bands should have been observed, which was obviously not the case.[66,101] Consequently, one can speculate that a part of the dynamics ascribed to the intermediate state could be actually induced by nonlinear effects caused by either too high excitation intensities or very short pulses having extremely high peak intensities. Thus, although the intermediate state facilitating the S_2−S_1 internal conversion would help to cure difficulties to explain the mechanism of the ultrafast S_2−S_1 relaxation, to prove or disprove this hypothesis more experiments on carotenoids with different structures and conjugation lengths including dependencies of the observed dynamics on intensities of both pump and probe pulses are needed.

Another relaxation pathway extending the original $S_2 \rightarrow S_1 \rightarrow S_0$ scheme involves the S* state, which was found in the transient absorption spectra of longer carotenoids where it exhibits a pronounced shoulder at the high-energy side of the S_1−S_N band. The S* state is more pronounced when carotenoids are bound to light-harvesting proteins of purple bacteria,[20,111−113] and the role of the S* state in these systems will be discussed in section 4.1. In solution, the S* state was detected in spirilloxanthin,[20] lycopene, β-carotene, and zeaxanthin.[115] In all cases, no dynamics occurring between the S* and S_1 states was observed, and both these states decay independently to the ground state. The S* lifetime is approximately 6 ps for all four carotenoids.[20,115] Thus, if the S* state is a separate excited state located below the S_2 state, this pathway differs significantly from the $S_2 \rightarrow 1B_u^- \rightarrow S_1 \rightarrow S_0$ model, as the S* state does not represent an intermediate state (Figure 11C). The model proposed by Gradinaru et al. for spirilloxanthin includes two separate relaxation pathways $S_2 \rightarrow S_1 \rightarrow S_0$ and $S_2 \rightarrow S^* \rightarrow S_0$ that operate in parallel. The fact that the S_1 and S* states do not interact with each other, although their energies are proposed to be rather close,[20] is quite intriguing. This puzzle can be, however, resolved in a model suggested by Wohlleben et al., who proposed a different origin for the S* state in solution. Using pump−dump−probe spectroscopy, these authors demonstrated that the S* state is not populated from the S_2 state, as the depletion of S_2 population decreased the S_1−S_N ESA but not the signal originating from the S* state.[115] On the basis of these results, the S* state was proposed to be a vibrationally hot ground state populated by impulsive Raman scattering of the pump pulse, leading to a modification of the relaxation scheme depicted in Figure 11C. This is, however, in disagreement with observation of energy transfer from the S* state to BChl-a in bacterial light-harvesting complexes[111−113] that clearly suggests that the S* state in protein environment must be higher than the Q_y state of BChl-a. Thus, to avoid this apparent contradiction, Wohlleben et al. suggested that the S* states observed in experiments performed in solution and in protein environment are of different origin. While in solution the S* state is a vibrationally hot ground state, in light-harvesting complexes the observed S* state is indeed a separate excited state.[115] Since the similarity of both spectral and temporal characteristics of the S* state in solution and protein environment makes such a situation rather unlikely, the origin of S* in solution remains to be established. The

discussion of the possible origin of the S* state in light-harvesting complexes is left for the section describing the role of the S* in light-harvesting complexes (section 4.1.).

A further modification of the $S_2 \rightarrow S^* \rightarrow S_0$ model shown in Figure 11C was proposed by Larsen et al.[116] In addition to the 'normal' relaxation pathway involving the S* state, yet another relaxation channel involving the recently discovered $S^‡$ state is operating when higher vibrational levels of the S_2 state are excited. Excess energy in the S_2 state opens a new relaxation pathway that competes with S_2 vibrational relaxation and populates the $S^‡$ state that decays directly to the ground state.[116]

Besides the relaxation pathways involving solely singlet excited states, a few studies demonstrated formation of other states on the subnanosecond time scale under certain conditions. Because of the strong S_1-S_0 vibrational coupling leading to the short S_1 lifetime, the quantum yield of intersystem crossing is very low, on the order of 10^{-6}, preventing appreciable formation of the triplet state.[133] Nevertheless, using 355 nm excitation, formation of the β-carotene triplet state on the picosecond time scale with an intersystem crossing yield of $\sim 10^{-3}$ was demonstrated.[134] No significant differences were found between different β-carotene isomers, showing that the ultrafast formation of the triplet state is not due to direct excitation of the *cis*-peak. This result suggests that UV excitation can open new relaxation channels that are not functioning when the lowest vibrational levels of the S_2 state are excited. Another indication of such new relaxation channels is offered by some measurements of excitation spectra of spheroidene and its shorter ($N = 9$) analogue 3,4-dihydrospheroidene, whose excitation spectra do not match the absorption profile below 450 nm.[76]

Formation of carotenoid radicals directly from singlet excited states was also suggested.[135] Studies of β-carotene in chlorinated solvents indicated an ultrafast electron transfer between β-carotene and the solvent, forming a β-carotene radical cation that is readily detectable by its strong absorption in the near-infrared region.[136] Using 430 nm excitation, Zhang et al.[137] demonstrated radical formation directly from the S_2 state with a time constant of 140 fs. On the contrary, it was suggested that electron transfer proceeds from either the vibrationally hot S_1 state or the intermediate $1B_u^-$ state in experiments using 30 ps pulses centered at 266, 355, and 532 nm. Although the time resolution did not allow a very precise determination of time constant of β-carotene radical formation, it was concluded that the radical is formed in less than 10 ps for all excitation wavelengths, with a yield of more than 10%.[138]

4. Excited States of Carotenoids in Pigment–Protein Complexes

Most of the biological functions of carotenoids are carried out when carotenoids are bound to specific proteins. Although a number of carotenoid-binding proteins are known to date, excited-state properties of carotenoids were studied in detail only in light-harvesting complexes. There are two main reasons for the lack of knowledge about carotenoid excited states in other carotenoid-binding proteins. First, structures of a few light-harvesting complexes are known in great detail; the conformation of a carotenoid and its interaction with the protein environment deduced from the structure facilitates the studies of excited-state properties. Second, in light-harvesting complexes, carotenoids serve as antenna pigments, making their excited states directly involved in the light-harvesting process, a vital function in all photosynthetic organisms. For other carotenoid-binding proteins, the relation between excited states properties and biological function of carotenoids is not always apparent, although, for example, carotenoid-binding proteins found in the human eye are potential candidates for involvement of carotenoid excited states in photoprotection. However, even for carotenoid-binding proteins that are not involved in light-triggered reactions, studies of carotenoid excited states can be helpful for investigating the interactions between carotenoids and protein environment, which can be of key importance for understanding the molecular functions of carotenoids in various biological tissues.

4.1. Carotenoids in Light-Harvesting Complexes from Purple Bacteria

The properties of excited states of carotenoids in pigment−protein complexes are the best understood in light-harvesting complexes in purple bacteria, because their detailed structural knowledge provides an ideal platform for experimental and theoretical investigations of energy-transfer processes between carotenoids and BChl. To date, structures of two light-harvesting complexes were resolved in great detail. In 1995, the LH2 complex from *Rhodopseudomonas* (*Rps.*) *acidophila* containing the carotenoid rhodopin glucoside was determined with 2.5 Å resolution,[139] and the 2.4 Å structure of the LH2 complex from *Rhodospirillum* (*Rs.*) *molischianum* containing lycopene followed shortly after.[140] The structure, depicted in Figure 12, revealed the BChl-a and carotenoid molecules arranged in a ring with its axis perpendicular to the membrane plane. The elementary building blocks of LH2 complexes are $\alpha\beta$-polypeptide pairs that bind two strongly coupled BChl-a molecules absorbing at around 850 nm (B850), one BChl-a molecule having an absorption band at 800 nm (B800), and one carotenoid molecule spanning the membrane. The carotenoid is in close contact with both the B800 and B850 molecules with the closest distances 5.4−9.3 Å to the central Mg atoms of the neighboring BChl-a molecules.[139] The main difference between the two LH2 structures, apart from accommodating different carotenoids, is that while the LH2 of *Rs. acidophila* exhibits 9-fold symmetry, LH2 of *Rs. molischianum* contains only eight elementary building blocks. A hydrogen bond between rhodopin glucoside and the B800 BChl was found by quantum chemical calculations on LH2 of *Rps. acidophila*.[141] The pigment arrangement of LH2 allows carotenoids to serve as efficient donors in the light-harvesting process, but it was also discovered

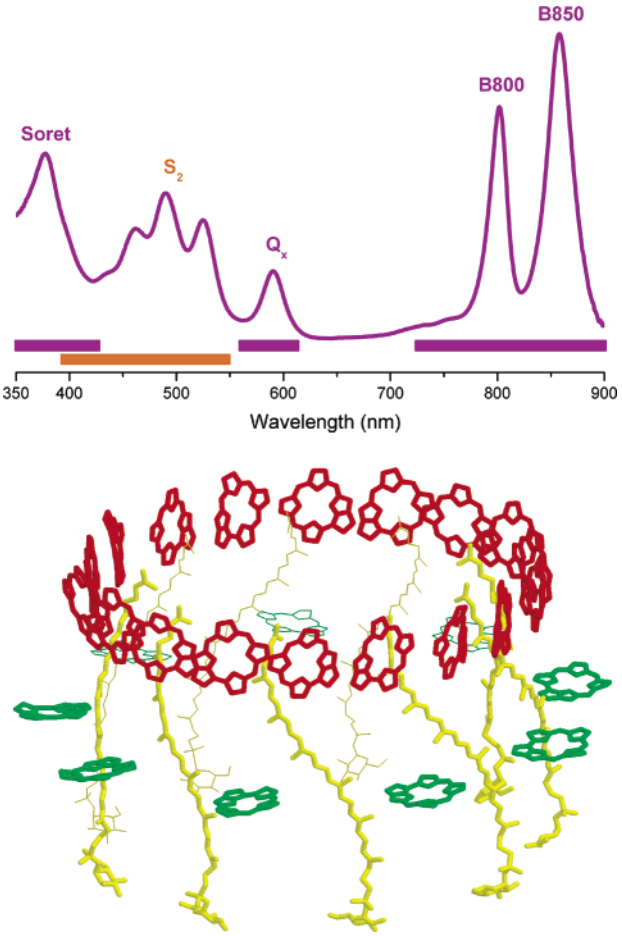

Figure 12. (Bottom) Arrangement of carotenoid and BChl-a molecules within the LH2 antenna complex of *Rps. acidophila*. The B800 BChl-a molecules are depicted in green and the tightly coupled B850 BChl-a molecules in red. The carotenoids are shown in yellow. (Top) Absorption spectrum of the LH2 complex from *Rps. acidophila*. The horizontal bars show spectral regions of BChl-a (purple) and carotenoid (orange) absorption bands.

that they are good probes of processes involving BChl-a molecules, because they are very sensitive to electric fields. The carotenoid band shifts observed in LH2 complexes were interpreted as resulting from the local electric field associated with excitation of nearby BChl-a molecules,[142] and this explanation was also supported by calculations.[143] Linear dichroism measurements showed that the transition dipole moment of rhodopin glucoside in LH2 is 9.1° off axis from the π-electron conjugated chain,[109,144] and it was concluded that this deviation is not due to perturbations by the protein environment but is rather a consequence of the single−double bond alternation in carotenoids. Moreover, intermolecular π-π stacking interactions between lycopene and the surrounding aromatic amino acid residues were found by means of quantum chemical calculations on the LH2 structure of *Rs. molischianum*.[145] These interactions were suggested to be a molecular mechanism for binding of carotenoids in LH2, and as shown later for other complexes, the role of π-π stacking interactions in carotenoid binding may be a general feature of photosynthetic proteins.[146]

Importantly, refinement of the structure of LH2 from *Rps. acidophila* to 2.0 Å was reported recently, revealing a second carotenoid molecule in the elementary building block that was not resolved in the initial structure.[147] The second rhodopin glucoside is located at the periphery of the LH2 complex, and it adopts a *cis*-configuration. Nevertheless, it was suggested that the observed *cis*-form could result from the preparation procedure and the actual in vivo configuration is likely to be *all-trans*.[147] Earlier chemical analyses determined a carotenoid/BChl ratio of 1:2 in a few LH2 complexes.[148,149] This suggests that the situation is not unique for *Rps. acidophila*, but it is likely that also other LH2 complexes possess the second carotenoid. It is, however, worth noting that spectral reconstitution resulted in a ratio of ~1:3 for *Rps. acidophila* and *Rs. molischianum*,[150] indicating that the second carotenoid on the periphery of LH2 might be removed during preparation in some cases. Since all studies of carotenoid−BChl energy transfer in LH2 complexes were so far interpreted in terms of only one carotenoid in the elementary building block (with the exception of ref 151), this finding will certainly influence our understanding of carotenoid function in LH2 complexes.

Besides the two structures described above, structural information with lower resolution is also available for other complexes. Cryo-electron microscopy studies of the LH2 complex from *Rhodobacter (Rb.) sphaeroides* revealed 9-fold symmetry of this complex and suggested that the structure is similar to the one from *Rps. acidophila*.[152] Similarly, an 8.5 Å resolution electron microscopy projection map of LH1 from *Rs. rubrum*[153] revealed a ring consisting of 16 subunits, each of which accommodates two BChl-a molecules and the carotenoid spirilloxanthin.

That carotenoids can transfer energy to BChls was known long before the X-ray structures were resolved. On the basis of fluorescence excitation spectra, carotenoid−BChl energy-transfer efficiencies of 80−100% were reported for *Rb. sphaeroides* containing spheroidene ($N = 10$),[154−156] while lower values between 35% and 70% were obtained for *Rps. acidophila* containing rhodopin glucoside ($N = 11$).[156−158] The carotenoid−BChl energy-transfer yield drops to ~30% for LH1 of *Rs. rubrum* containing spirilloxanthin ($N = 13$).[159] Less than 25% efficiency was obtained for *Rps. palustris* accommodating rhodovibrin ($N = 12$) as the dominating carotenoid.[156]

Initial suggestions regarding the mechanisms and pathways of carotenoid−BChl energy transfer in LH2 and LH1 complexes proposed energy transfer via the S_1 state, because of extremely fast deactivation of the S_2 state. The forbidden nature of the S_1 state, however, led to a suggestion that the Dexter electron exchange mechanism is active in this process.[160−162] However, the first time-resolved experiments performed in the early 1990s showed that following excitation of carotenoids, the B850 Q_y state was populated in less than 200 fs, signaling that both the S_1 and S_2 states may be efficient donors in the carotenoid−BChl energy-transfer process.[163,164] Calculations of carotenoid−BChl energy transfer for neurosporene also led to the conclusion that both the S_1 and S_2 states can be active in energy transfer.[165]

When LH2 structures to atomic resolution became available,[139,140] a number of experimental and theoretical investigations of energy-transfer mechanisms and pathways between carotenoids and BChls confirmed the initial proposal that both the S_1 and S_2 states are involved in the energy-transfer processes. It was also concluded that the precise pathways and directions of energy flow are governed mainly by the conjugation length of the involved carotenoid. In addition, new experimental approaches and improved methods of data analysis recently revealed new energy-transfer pathways that contribute to the overall carotenoid−BChl energy transfer in light-harvesting complexes of purple bacteria. A schematic representation of energy-transfer pathways within LH2 complex that are in detail described below is depicted in Figure 13.

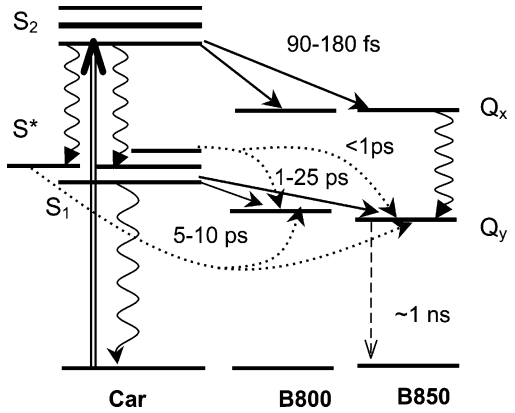

Figure 13. Schematic representation of energy levels and energy-transfer pathways between carotenoids and BChl-a in the LH2 complex. Double arrow represents excitation of the S_2 state of a carotenoid. Wavy arrows denote intramolecular relaxation processes, while the dashed arrow represents the long-lived BChl-a fluorescence. Solid arrows represent the dominating energy-transfer channels involving the S_2 and S_1 states, although the S_1 channel can be completely suppressed in some LH2 species. The dotted lines represent minor energy-transfer channels that usually contribute only fractionally to the total energy transfer: the pathway via higher vibrational levels of the S_1 state and the pathway via the S* state observed for some LH2 complexes. Energy-transfer pathways are labeled by the corresponding time constant. See text for details.

4.1.1. Energy Transfer via the S_2 State

Absorption spectra of carotenoids in LH2 and LH1 complexes resemble well those obtained for carotenoids in solution, except for a red shift of ~1000 cm^{-1} caused by interaction with the protein environment (Figure 12). The vibrational substructure of the carotenoid S_2 state in LH2 is usually very similar to that obtained in solution, although for some carotenoids the protein environment represents a confinement of the carotenoid structure, leading to a better resolution of vibrational bands of the S_2 state in protein. This situation is characteristic of rhodopin glucoside, whose glucoside ring at the end of the conjugated chain introduces a large asymmetry into the molecule, leading to a broad distribution of ground-state conformers in solution. In LH2 of *Rps. acidophila*, however, only one particular conformation is achieved, leading to better-resolved vibrational bands of the S_2 state.[92]

The first experimental data on energy transfer via the S_2 state was obtained by fluorescence up-conversion. S_2 emission decays of spheroidene in LH1 and LH2 complexes of *Rb. sphaeroides* yielded time constants of 55 and 80 fs, respectively.[54] Comparing these results with the markedly longer decays in solution (~150−250 fs), it was concluded that energy transfer via the S_2 state takes place with time constants of 90 fs for LH1 and 170 fs for LH2 (corresponding efficiencies of 65% and 47%, respectively), demonstrating that energy transfer can successfully compete with S_2-S_1 internal conversion. On the basis of spectral overlap, it was concluded that energy transfer via the S_2 state occurs to the Q_x state of Bchl.[54] Similar results were reported for the B800−B820 LH2 complex from *Rps. acidophila*, for which analysis of up-conversion kinetics supported by calculations yielded an S_2–Q_x energy-transfer rate of $(120-150\ fs)^{-1}$. The S_2–Q_x channel was concluded to be the dominating one, accounting for 60% of the total energy-transfer efficiency.[166] Later, up-conversion experiments were carried out on the wild-type B800−B850 LH2 complex of *Rps. acidophila* and a complex lacking the B800 BChls. Upon combining the results for these two LH2 complexes, Macpherson et al. addressed the question of energy acceptors in the carotenoid−BChl energy transfer.[59] An observed overall efficiency of S_2-mediated energy transfer of 51% confirmed the results obtained for the B800−B820 complex,[166] and it was in addition shown that 20% of the S_2 population transfers energy to B800 BChl while the rest (31%) goes to B850.

The fast and efficient S_2 energy-transfer pathway was also observed by transient absorption measurements. A study of the LH2 complex from *Chromatium purpuratum* accommodating the carotenoid okenone ($N = 11+$ C=O) revealed S_2-mediated energy transfer characterized by a time constant of 50−100 fs.[151] Excitation of okenone in the wavelength range 580−590 nm led to a partial excitation of the BChl Q_x band, making the estimation of energy-transfer efficiency rather difficult. The light-harvesting complex from *Chromatium vinosum* containing spirilloxanthin was studied by combination of transient absorption spectroscopy and time-resolved anti-Stokes Raman spectroscopy,[167] but due to the limited time resolution of ~0.5 ps, it was not possible to determine the time constants precisely. Nevertheless, comparison of kinetics recorded for spirilloxanthin in solution and in the protein allowed conclusion that the energy transfer via the S_2 state must occur on a time scale of ~0.2 ps. Interestingly, on the basis of anti-Stokes Raman scattering it was suggested that both the Q_x and Q_y states play a role of energy acceptors in the S_2-mediated energy transfer.[167] Improved data analysis applied to transient absorption data enabled more reliable separation of overlapping signals, usually present in transient absorption spectra. Thus, global analysis producing species associated spectra identified ~35% efficient S_2 energy transfer for spirilloxanthin in the LH1 complex of *Rs. rubrum*,[20] and S_2-mediated spheroidene−Bchl energy transfer in LH2 from *Rb. sphaeroides* yielded an efficiency of 57%,[111] in good agreement with the up-conversion data. The

same analysis, applied to transient absorption results of LH2 from a carotenoidless *Rb. sphaeroides* R26 mutant lacking the B800 BChls with incorporated spheroidene, revealed a 25% efficiency of the S_2 pathway.[112] Comparing with the 57% efficiency obtained for the wild-type B800−B850 complex,[111] it was concluded that both B800 and B850 Bchls must be acceptors in energy transfer from the carotenoid S_2 state. A more advanced method of data treatment using evolutionary target analysis determined the efficiency of the S_2 pathway in LH2 from *Rps. acidophila* to 42%.[113] Although this is less than 51% determined by means of fluorescence up-conversion, the difference is within the error limits, because the calculations require precise knowledge of the S_2-S_1 internal conversion rate in LH2. Since the S_2-S_1 internal conversion rate depends on solvent parameters (section 3.1), it is not easy to determine an accurate value for a protein environment, putting a limitation on the precision of the determined S_2 energy-transfer efficiencies.[54,59] In addition, it was shown that shaping of excitation pulses could control the ratio between S_2-S_1 internal conversion and energy transfer. For LH2 from *Rps. acidophila*, an increase, by a factor 1.4, of S_2-S_1 internal conversion was achieved by optimizing the envelope and phase of the excitation pulses,[168] demonstrating that the actual S_2 energy-transfer efficiency depends also on other parameters. Higher efficiencies of 60−70% for the S_2-mediated energy transfer were reported for the LH2 complex from *Rb. sphaeroides* G1C that has neurosporene ($N = 9$) as the main carotenoid.[169] Comparing the results on LH2 complexes containing carotenoids with $N = 9-13$, there is a certain trend, suggesting higher efficiency of the S_2 energy transfer for shorter carotenoids. This trend is supported by experiments on LH2 of the carotenoidless mutant *Rb. sphaeroides* R26 with incorporated spheroidene analogues of different conjugation lengths. With the help of S_1-S_2 internal conversion rates measured in solution, overall carotenoid−BChl energy-transfer efficiencies, and S_1-mediated energy-transfer efficiencies, the efficiencies of S_2 energy transfer were calculated. Although the LH2s with spheroidene analogues having $N = 8$ and 9 have slightly less efficient S_2 energy transfer than LH2 with spheroidene ($N = 10$), the decrease of S_2 efficiency from 50% (spheroidene) to 12% for the analogue having $N = 13$ supported the observed trend of decreasing S_2-mediated energy-transfer efficiency with increasing conjugation length.[170] Although less efficient for very long carotenoids, the S_2 energy-transfer route operates in all purple bacterial antenna complexes studied so far with efficiencies in the range 30−70%. In a number of cases it represents the dominant energy-transfer pathway between carotenoid and BChl.

The effective competition of S_2 energy transfer with the S_2-S_1 internal conversion was also rationalized theoretically. The contribution of the electron-exchange (Dexter) energy-transfer mechanism[171] to the S_2 energy transfer is negligible, and the Förster-type mechanism dominates.[165,166,172] However, contrary to the dipole−dipole interaction used in the Förster formula,[173] full Coulombic interaction is usually used to calculate couplings between carotenoids and BChl. Even without knowledge of detailed structural information, Nagae et al.[165] calculated the Coulombic couplings between the S_0-S_2 transition of neurosporene and the Q_x transition of BChl-a for a few hypothetical configurations. They concluded that S_2 energy transfer via this route can be faster than 100 fs, provided the proper orientation of donor and acceptor is realized.[165] Determination of the LH2 structure provided detailed information about the mutual orientation of pigments within LH2, allowing more precise calculations of couplings between carotenoids and BChl-a. Krueger et al. applied an advanced method, the so-called transition density cube method, to calculate full Coulombic couplings between pigments in both B800−B820[166] and B800−B850[174] LH2 complexes from *Rps. acidophila*. This method replaces the vector description of the transition dipole moments by three-dimensional transition density volumes, which is expected to give a more accurate account of the interaction between molecules.[174] The couplings of the S_0-S_2 transition of rhodopin glucoside with all possible transitions of neighboring BChl-a were calculated for the B800−B820 complex, yielding couplings larger than 100 cm^{-1} for β-B820 Q_x, B800 Q_y, and also B800 Q_y transition of BChl-a located in the neighboring building block. However, due to the small value of the spectral overlap integral for the Q_y states, only the S_2-B820 Q_x yielded an appreciable energy-transfer rate of $(240\ fs)^{-1}$.[166] Similar results were obtained for the B800−B850 complex. Although the actual couplings were slightly different from those calculated for the B800−B820 complex, the S_2-B850 Q_x channel represented the dominating route, characterized by an energy-transfer rate of $(135\ fs)^{-1}$.[174] The results of these calculations are in very good agreement with the observed depopulation rates of the S_2 state, but the absence of significant coupling of the S_2 state to the B800 Q_x contradicts the experimental observation that a substantial part of the S_2 route in *Rps. acidophila* leads toward B800.[59] On the other hand, similar calculations using full Coulombic couplings performed on the basis of the LH2 structure of *Rs. molischianum* containing the carotenoid lycopene yielded appreciable couplings of the S_0-S_2 transition with both the B850 and B800 BChls, resulting in S_2 energy-transfer times of 200 and 250 fs for the B850 and B800 acceptors, respectively.[172] Essentially the same results were obtained by calculations of the lycopene−BChl couplings by means of the collective electronic oscillators algorithm.[175] An energy-transfer rate of $(120\ fs)^{-1}$ was calculated for the S_2-Q_x channel, proposing an S_2 depopulation time of 69 fs for lycopene in LH2. It is interesting to mention that these calculations also proposed a strong coupling between the B_x (Soret) band of both B800 and B850 BChls and the S_2 state of lycopene, indicating a possibility of energy transfer from the BChl-a Soret band to lycopene,[175] but no experimental evidence for such transfer has been given so far. Also, calculations of couplings were carried out for either isolated molecules in LH2 complex and in a dielectric medium, simulating the mean field created by protein

environment. The effect of the dielectric medium on couplings involving the S_2 state were quite significant, underlining importance of protein effects.[175] Thus, while the calculations reproduce well the observed rates of S_2-mediated energy transfer and confirm the BChl-a Q_x states being the energy acceptors in the S_2-mediated energy transfer, there are still contradictions regarding the branching ratio between B850 and B800 acceptors. As no experimental studies of S_2 energy transfer in the LH2 complex from *Rs. molischianum* are currently available, it is not possible to verify the S_2 branching ratio calculated for this complex. Nevertheless, the energy transfer between lycopene and BChl-a was investigated in a LH2 mutant of *Rb. sphaeroides*. The S_2 route was found to populate both B850 and B800 BChl for both lycopene mutant and the spheroidene-containing wild type,[91] but since the structure of LH2 from *Rs. molischianum* differs from that of *Rps. acidophila* in certain aspects[140] and consequently also from that of *Rb. sphaeroides* LH2 (expected to be similar to the *Rps. acidophila* LH2[152]), direct comparison with the calculations on *Rs. molischianum* is not possible.

4.1.2. Energy Transfer via the S_1 State

Efficient energy transfer via the S_1 state requires the S_1 energies of carotenoids to be higher than those of the acceptor states. Until recently, no information about S_1 energies in LH2 and related light-harvesting complexes was available, mainly due to the fact that the most used techniques to locate S_1 energies of carotenoids, detection of S_1 fluorescence and measurements of resonance Raman profiles, were not applicable to such complex systems. However, since it was known that S_1 energies are usually insensitive to solvent properties (except carbonyl carotenoids that are not typical for purple bacterial light-harvesting complexes), it was reasonable to assume that the S_1 energies in LH2 and LH1 complexes should be very close to those determined for carotenoids in solution. Under this assumption, S_1 energies of carotenoids with $N \leq 10$ were expected to be high enough to transfer energy to the Q_y states of both B800 and B850 BChls. The first experimental evidence of this fact was provided by investigation of LH2 complexes from the *Rb. sphaeroides* R26 mutant with incorporated spheroidene analogues of different conjugation lengths. The efficiencies of S_1-mediated energy transfer were calculated from S_1 lifetimes of carotenoids in solution and in LH2, obtained from S_1-S_N ESA decays. While for conjugation lengths $N \geq 11$ the S_1 energy transfer was undetectable, a quenching of the S_1 state due to energy transfer was observed for shorter carotenoids.[170] This result was explained in terms of spectral overlap between hypothetical S_1 fluorescence and the B850 absorption band, which became small for longer carotenoids. Another direct experimental verification of the S_1-mediated energy transfer in the LH2 complex from *Rb. sphaeroides* was obtained by means of two-photon fluorescence excitation.[176] Forbidden for an one-photon transition, the S_1 state can be excited directly via a two-photon transition.[177] By measuring B850 emission after two-photon excitation of the S_1 state (achieved by exciting in the 1200−1500 nm spectral range), Krueger et al. demonstrated active participation of the spheroidene S_1 state in energy transfer. In addition, the two-photon excitation spectrum enabled determination of the spectral profile of the S_0-S_1 transition, placing the 0−0 energy of spheroidene in LH2 at 13 900 cm^{-1},[176] confirming the similarity of the S_1 energies in LH2 and in solution. It is worth noting, however, that the 0−0 band of the S_0-S_1 transition was unreasonably weak, having about 40 times less intensity than the 0−1 band. Although no clear explanation of this phenomenon was offered, later experiments suggested that it might be due to the fact that the two-photon absorption spectrum reflects the energy-transfer efficiency that does not necessarily mirror the Franck−Condon intensities of the vibrational bands. Indeed, the possibility of energy transfer from higher vibrational levels of the S_1 state of spheroidene was demonstrated later.[111,112]

Zhang et al. used three LH2 complexes, accommodating different carotenoids, to investigate the dependence of S_1-mediated energy-transfer efficiency on conjugation length of the carotenoid.[178] On the basis of measured S_1 lifetimes of neurosporene ($N = 9$), spheroidene ($N = 10$), and lycopene ($N = 11$) in solution and LH2, a dramatic decrease of S_1 energy-transfer efficiency was observed; it dropped from 94% (neurosporene) to 82% (spheroidene) and further to less than 30% (lycopene) as the conjugation length increased from 9 to 11. Similar results were obtained for spheroidene and rhodopin glucoside in LH2 complexes from *Rb. sphaeroides* and *Rps. acidophila* by means of measurements of S_1-S_N kinetics after two-photon excitation of the S_1 state.[94] These authors confirmed the ~1.8 ps S_1 lifetime of spheroidene in LH2, but for rhodopin glucoside, a longer S_1 lifetime (6−7 ps) than in solution was observed, suggesting that there is no energy transfer via the S_1 state for rhodopin glucoside.[94] A few subsequent studies confirmed this trend and established that for carotenoids with $N = 11$ the S_1 state is too low to achieve efficient energy transfer via the S_1 state, although the long S_1 lifetime of rhodopin glucoside observed by Walla et al.[94] was not confirmed by other authors. Instead, an S_1 lifetime of 3.7 ps was measured for rhodopin glucoside in LH2, while values of 4.1−4.9 ps were recorded in solution, showing that the S_1 energy-transfer efficiency is around 5% in LH2.[59] The same S_1 lifetime of 3.7 ps for rhodopin glucoside in LH2 was measured recently,[113] while a slightly longer value (4 ps) was determined by Polívka et al.[92] A study of a *Rb. sphaeroides* mutant synthesizing the longer lycopene instead of spheroidene present in wild-type LH2 proved that the efficiency of S_1 energy transfer is fully determined by the conjugation length of the carotenoid, while the protein environment plays only a negligible role. When lycopene is present in the complex, the efficiency of S_1-mediated energy transfer drops to about 20%, while more than 80% is achieved in the wild type.[91] Further evidence that carotenoids with $N = 11$ are on the edge of capability to transfer energy via the S_1 state was provided by studies of LH1 complexes from *Rs. rubrum* contain-

ing spirilloxanthin ($N = 13$). Within experimental error, no difference between S_1 lifetimes in solution and in the LH1 complex was found.[20,167] The same result was obtained for LH2 complexes from *Rb. sphaeroides* R26 reconstituted with spirilloxanthin,[112] suggesting that no S_1-mediated energy transfer is possible for spirilloxanthin because the S_1 energy is too low for efficient overlap with BChl Q_y states. It is worth noting, however, that S_1 energy transfer was reported for the B800−B830 LH2 complex of *Chromatium purpuratum* having the carotenoid okenone, which possesses 11 C=C bonds and a conjugated carbonyl group.[151] The S_1 lifetimes in CS_2 solution and in the LH2 complex were determined to be 8 and 3.8 ps, yielding quite efficient energy transfer via this route. However, since okenone contains a carbonyl group, the observed shortening of the S_1 lifetime could be caused also by a change of polarity of the environment as it was shown for other carbonyl carotenoids.[22,46]

The significance of spectral overlap for the S_1-mediated energy transfer was recently confirmed by measurements of the S_1 energies of spheroidene and rhodopin glucoside in LH2 complexes by recording the S_1-S_2 spectra (Figure 14). S_1 energies of 13 400

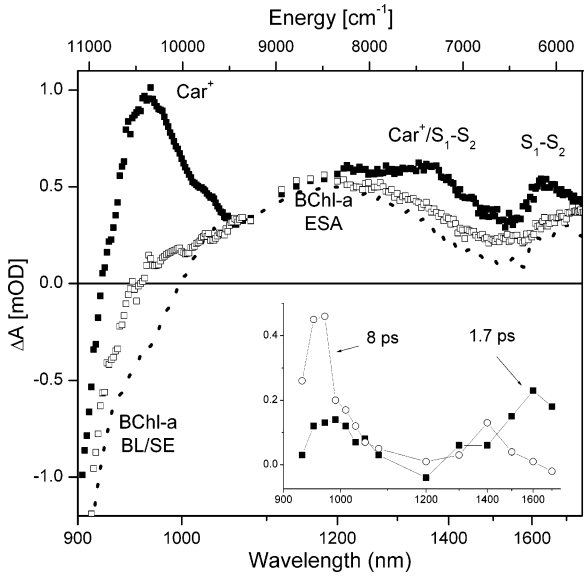

Figure 14. Near-infrared transient absorption spectra of LH2 complexes from *Rb. sphaeroides* recorded at 2 (full squares) and 20 ps (open squares). Excitation wavelength is 515 nm. The transient absorption spectrum measured after excitation of the B850 band is shown for comparison (dotted line). The B850 band was excited at 850 nm, and the transient spectrum after 850 nm excitation was normalized to have the same magnitude of B850 bleaching as the transient spectra excited in the carotenoid region. Inset shows spectral profiles of the amplitudes of the 1.7 (full squares) and 8 ps (open circles) decay components as extracted from multiexponential global fitting of the kinetics, demonstrating the different origin of the 960 nm band (carotenoid radical) and 1600 nm band (S_1-S_2 ESA).

$\pm$ 100 cm^{-1} and 12 550 $\pm$ 150 cm^{-1} were determined for spheroidene and rhodopin glucoside, respectively,[92] showing that the difference of 850 cm^{-1} makes a dramatic change in the energy-transfer pathways in these two LH2 complexes. In the case of spheroidene, the S_1 energy extracted from the S_1-S_2 spectra is the same as that determined by this method in solution, while for rhodopin glucoside the S_1 energy is 250 cm^{-1} lower than that in solution.[92] This difference was explained by confinement of rhodopin glucoside in the LH2 structure, which narrows the distribution of conformers presented in solution.

Together with the spectral overlap, calculations of the couplings between the S_0-S_1 transition and Q_y transitions of both B800 and B850 demonstrated that the observed S_1 transfer rates can be explained in terms of the same energy-transfer mechanism as for the S_2 route. Although the very small transition dipole moment of the S_0-S_1 transition led initially to a suggestion that the Dexter mechanism had to be invoked,[160−162] more detailed calculations later showed that the Dexter contribution is negligible and that higher-order Coulombic and polarization interactions dominate the S_1-mediated energy transfer.[165,172,174,175,179] In a few works, the Coulombic couplings for the S_1 state were obtained by scaling down the couplings calculated for the S_2 state, using an estimate that the transition dipole moment of the S_0-S_1 transition is about 4−6% of the S_0-S_2 transition. Although the results of this approach were promising, the calculated rates could not reproduce the measured energy-transfer rates.[172,178] To resolve this problem, an increase of S_0-S_1 Coulombic coupling via intensity borrowing from the allowed S_2 state due to S_2-S_1 mixing was proposed.[172,178] Under the assumption that the degree of mixing is inversely proportional to the square of the S_1-S_2 energy gap, Zhang et al. calculated S_1 energy-transfer rates for LH2 from *Rs. molischianum* that were reasonably close to the measured values.[178] Further improvement of the agreement between experiment and theory was obtained by calculations of Coulombic couplings by means of time-dependent density functional theory (TDDFT).[94,180] This method confirmed that small mixing between S_2 and S_1 states plays an important role in the Coulombic coupling. S_1 energy-transfer rates for LH2 complexes from three different species of purple bacteria were calculated using the Coulombic couplings obtained from TDDFT, and the obtained values (9 ps)$^{-1}$ (*Rs. molischianum*), (1.2 ps)$^{-1}$ (*Rb. sphaeroides*), and (3 ps)$^{-1}$ (*Rb. sphaeroides* G1C)[180] are very close to the experimental ones of (12 ps)$^{-1}$, (2.4 ps)$^{-1}$, and (1.4 ps)$^{-1}$.[178] For LH2 from *Rps. acidophila*, an S_1 energy-transfer time >25 ps was calculated,[180] also in a good agreement with the very low efficiency obtained experimentally.[59,113]

Regarding energy acceptors in the S_1-mediated energy-transfer route, both B800 and B850 Bchls are capable of accepting energy from carotenoids, but the S_1-B800 channel seems to be the dominating one. In experiments employing incorporation of spheroidene into LH2 from the carotenoidless *Rb. sphaeroides* R26 mutant lacking B800 BChl, the efficiency of energy transfer via the S_1 pathway reached only 35%.[112] This is significantly less than ~80% observed for the LH2 containing both B800 and B850,[91−94,178] signaling that the main pathway involves B800 as an acceptor. The same conclusion was reached for LH2 from *Rps. acidophila*. Although the S_1 efficiency

is only 4−5% in the wild-type complex,[59,113] removing the B800 BChls led to a complete absence of S_1 energy transfer.[59] Similar to the S_2-mediated energy transfer, the experimentally observed branching ratios are not fully consistent with calculations. Whereas for *Rb. sphaeroides* the calculated branching ratio, yielding ∼1:5 (B850:B800), overestimates the B800 pathway, for *Rps. acidophila* the calculated branching ratio is 3:2,[94] in obvious contradiction with experiments.[59]

In addition to the S_1-mediated energy transfer occurring from the thermalized S_1 state discussed above, a fractional energy-transfer channel from the vibrationally hot S_1 state was also proposed. This type of energy transfer was first revealed in the LHCII complex from higher plants[95] and later proved to be active also in the LH2 complex of *Rb. sphaeroides*. Using global analysis of their data, Papagiannakis et al. observed the decay of a species-associated spectrum corresponding to the vibrationally hot S_1 state, suggesting the presence of an energy-transfer channel via the hot S_1 state.[111] The contribution of this pathway to the total energy-transfer efficiency was only 5%. Interestingly, no such pathway was found when spheroidene was incorporated into the carotenoidless LH2 *Rb. sphaeroides* R26 mutant lacking B800. This was interpreted in terms of B800 being the only acceptor for this energy-transfer pathway.[112] Similarly, the energy-transfer pathway via hot S_1 state is absent in the LH2 complex from *Rps. acidophila*,[113] the LH1 complex from *Rs. rubrum*,[20] and LH2 complex from *Rb. sphaeroides* R26 reconstituted with spirilloxanthin,[112] demonstrating that this channel is of minor importance for overall energy transfer in light-harvesting complexes from purple bacteria (Figure 13).

4.1.3. Other Pathways

Another important channel involving carotenoid excited states in purple bacterial light-harvesting complexes, besides the S_1- and S_2-mediated energy transfer, is a pathway via the S* state. The initial study, which reported the discovery of the S* state in the excited-state manifold of the carotenoid spirilloxanthin in both solution and the LH1 complex of *Rs. rubrum*,[20] revealed a significant difference between the dynamics of the S* state in solution and in the LH1 complex. In solution, the S* state exhibited only one decay channel to the ground state, but in the LH1 complex the S* state was also found to be a precursor of fast (∼12 ps) formation of a spirilloxanthin triplet state. A relatively high triplet yield of 25−30% was explained to be a result of a conformational distortion of spirilloxanthin in the LH1 complex, promoting the triplet formation via singlet homofission from the S* state.[20] Further studies confirmed the triplet state formation via the S* state for other complexes containing different carotenoids. The yields of triplet formation varied from nearly 40% for rhodopin glucoside in LH2 from *Rps. acidophila*[113] to less than 10% for spheroidene in both native LH2 from *Rb. sphaeroides*[111] and incorporated into the *Rb. sphaeroides* R26 mutant.[112] Interestingly, reconstitution of LH2 from *Rb. sphaeroides* R26 with spirilloxanthin led to an observation of a triplet yield of 5−10%, markedly lower than for spirilloxanthin in LH1 of *Rs. rubrum*.[112] This observation suggests that the protein environment is a crucial factor governing the formation of the triplet via singlet homofission, and it strongly supports the conclusion that the twisted conformation of spirilloxanthin in LH1 is a necessary prerequisite for efficient homofission, since in LH2 the conformation of carotenoid is rather planar.[112] However, it turned out that the decay to the S_0 state and triplet formation are not the only possible fates of the S* state in LH2 complexes. While it is true for the LH1 complex of *Rs. rubrum*, in LH2 complexes containing either spheroidene or rhodopin glucoside, the S* state also contributes to carotenoid−BChl energy transfer. For spheroidene in LH2 of *Rb. sphaeroides*, S*-mediated energy transfer contributes 10−15% to the total spheroidene−BChl energy transfer.[111] An upper limit of 5% for the energy-transfer yield via the S* state was estimated for spheroidene incorporated into carotenoidless *Rb. sphaeroides* R26 mutant lacking B800, suggesting that B800 BChl might be crucial in this energy-transfer channel.[112] For rhodopin glucoside in *Rps. acidophila* LH2, the S*-mediated channel represents more than 10% of the total energy transfer, and it has even higher energy-transfer efficiency than the S_1 state.[113] Since the low efficiency of the S_1-mediated channel in this complex is due to the too low energy of the S_1 state, this is another piece of evidence that S* is actually located above the S_1 state.

While the importance of the S* state for the functionality of carotenoids in LH2 and LH1 complexes was conclusively demonstrated, the origin of the S* state is still a matter of debate. While in solution a vibrationally hot ground state was suggested as one of the possible origins besides the S* state being a separate excited state,[115] existence of S*−BChl-a energy transfer in light-harvesting complexes described in the previous paragraph rules out this possibility. Thus, in the protein environment, the $1B_u^-$ state is one of the possible candidates because it should be located between the S_1 and S_2 states (section 3.3), and, similar to the S* state, it is a dark state. In addition, the $1B_u^-$ state bears a double triplet character, a necessary prerequisite for singlet homofission. Recent investigations indeed proposed the $1B_u^-$ state as a likely candidate for the S* state.[111,113] Even though this is apparently the most straightforward explanation of the presence of the S* state, this assignment is still problematic. It was confirmed in a few independent experiments that there is no $S_1 \leftrightarrow S^*$ internal conversion,[20,111−113] which contradicts the hypothesis of the $1B_u^-$ state being the intermediate state in the S_2-S_1 internal conversion.[14,15,51,69] This problem could be explained if the potential-energy surfaces of the S* and S_1 states have a substantial relative shift, creating a barrier between these states.[111] Recent experiments demonstrating that the S* state has no detectable S^*-S_2 absorption[67] supports this hypothesis. Then, S* could indeed be identical to the $1B_u^-$ state, being vibrationally coupled to the ground state and located above

the S_1 state, explaining its longer lifetime as compared to the S_1 lifetime. However, although only a few carotenoids have been subjected to studies focusing on the S* state so far, it seems obvious that the lifetime of the S* state does not follow the trend known for the S_1 state. While the S_1 lifetime is changed systematically from ~9 (spheroidene) to 4.1 (rhodopin glucoside) and 1.5 ps (spirilloxanthin) as a result of increased conjugation length from 10 to 13 (Table 2), the S* lifetime does not follow this trend. The intrinsic S* lifetimes (in the absence of energy transfer) in LH2 and LH1 complexes of ~12 (spheroidene),[111] 32 (rhodopin glucoside),[113] and 8 ps (spirilloxanthin)[20] are scattered randomly without any obvious relation to the conjugation length. This makes it rather difficult to assign the S* to the $1B_u^-$ (or even $3A_g^-$) state. The energy dependence of the $1B_u^-$ state on conjugation length is predicted to be even steeper than that of the S_1 state.[13−15] Therefore, the $S_0-1B_u^-$ energy gap should decrease rapidly with conjugation length, making the S* lifetime strongly correlated with the conjugation length, which is clearly not the case. The same problem occurs if one tries to assign the S* state to the $3A_g^-$ state, although this assignment might be more reasonable due to the absence of the S* state in shorter carotenoids.

It should be mentioned that the $1B_u^-$ state was actually proposed to be active in energy transfer between carotenoids and BChl in LH2 complexes, but the suggested transfer pathway was different from that involving the S* state. With the help of an assignment of transient absorption signals of carotenoids measured for carotenoids in solution in the 840−1040 nm region to the S_2 and $1B_u^-$ states,[70] Zhang et al. performed global analysis of transient absorption data obtained in the same spectral region for the LH2 complex of *Rb. sphaeroides* G1C containing neurosporene.[169] The authors concluded that in order to explain satisfactorily all spectral components, the $1B_u^-$ state must be involved in neurosporene−BChl energy transfer. In the proposed scheme, however, the $1B_u^-$ state is treated as an intermediate state in the S_2-S_1 internal conversion and the energy transfer from the absorbing S_2 state is inefficient since the S_2 population is transferred to the $1B_u^-$ state on the sub-100 fs time scale. In this picture, the $1B_u^-$ state would transfer energy to the Q_x state of BChl-a, competing with fast (~300 fs) $1B_u^- - S_1$ internal conversion.[169]

A completely different pathway involving carotenoid excited states was recently discovered in the LH2 complex from *Rb. sphaeroides*. A distinct spectral band at 950 nm in the transient absorption spectra was assigned to the spheroidene radical cation (Figure 14), formed within the first 300 fs after excitation and decayed with 8 ps time constant.[92] It was suggested that the radical is formed with a yield of 5−8%, and its formation was rationalized by calculations on a spheroidene−BChl-a complex, indicating the presence of charge-transfer states that can be precursors of radical formation in the LH2 complex. Comparison with LH2 complexes from *Rps. acidophila* showed that the radical formation is dependent on carotenoid and/or the specific surrounding of the carotenoid, because no sign of rhodopin glucoside radical was detected. Initially, it was hypothesized that the 950 nm band could also be due to a transition involving the S* state,[92] but this possibility was ruled out due to the absence of this band in spirilloxanthin.[67]

It is apparent that detailed structural information in combination with development of time-resolved spectroscopic techniques and data analysis during the past few years vastly improved our knowledge about energy-transfer processes between carotenoids and BChl in LH2 and LH1 complexes. On the other hand, these improvements brought a number of still unanswered questions regarding the origin of the involved states, directions and efficiencies of energy transfer, and effects of protein environment. New experimental approaches are particularly important to resolve these issues, and, for example, recently introduced methods to control energy flow in LH2 complexes,[168] pump−dump−probe spectroscopies,[115,116] or femtosecond resonance Raman[66,125] hold promise to be powerful tools to disentangle the complicated network of energy-transfer pathways in these systems.

4.2. Carotenoids in LHCII and Related Proteins

The antenna complexes associated with Photosystem II (PSII) in green plants consist of a number of proteins belonging to the Lhcb gene family.[181] A higher structural complexity of these proteins, which usually bind more than one type of carotenoid in addition to Chl-a and Chl-b molecules,[182] results in a more complicated network of possible energy-transfer and internal conversion pathways. Nonetheless, the energy transfer between carotenoids and Chls was extensively studied in recent years, because in addition to the light-harvesting function, singlet excited states of carotenoids in these complexes were also suggested to play a photoprotective role, in which the 'back' energy transfer from Chl to carotenoid was the central issue. Yet, the understanding of energy-transfer pathways between carotenoids and Chl molecules in light-harvesting complexes of green plants is poorer than for their purple bacterial counterparts.

The most abundant protein of the Lhcb family is LHCII, which is located at the periphery of PSII, while minor light-harvesting proteins called CP29, CP26, and CP24 are located close to the core of the PSII supercomplex.[183] Structural knowledge of the Lhcb proteins is based on the crystal structure of LHCII, whose structure was determined with 3.4 Å resolution.[184] The structure shows that the native form of LHCII has a trimeric organization, and each of the monomeric subunits (Figure 15) binds 12 Chl molecules and 2 carotenoids. The 12 Chls usually occur in a ratio of 7 Chl-a and 5 Chl-b, but slight variation has been observed.[185] Since the structural data did not allow differentiation of Chl-a and Chl-b, the exact assignment of Chls in the LHCII structure is still matter of debate. Contrary to purple bacteria, in which the carotenoid content is species-dependent and more than 100 different carotenoids have been detected in various species,[186] only five different carotenoids are accumulated in light-

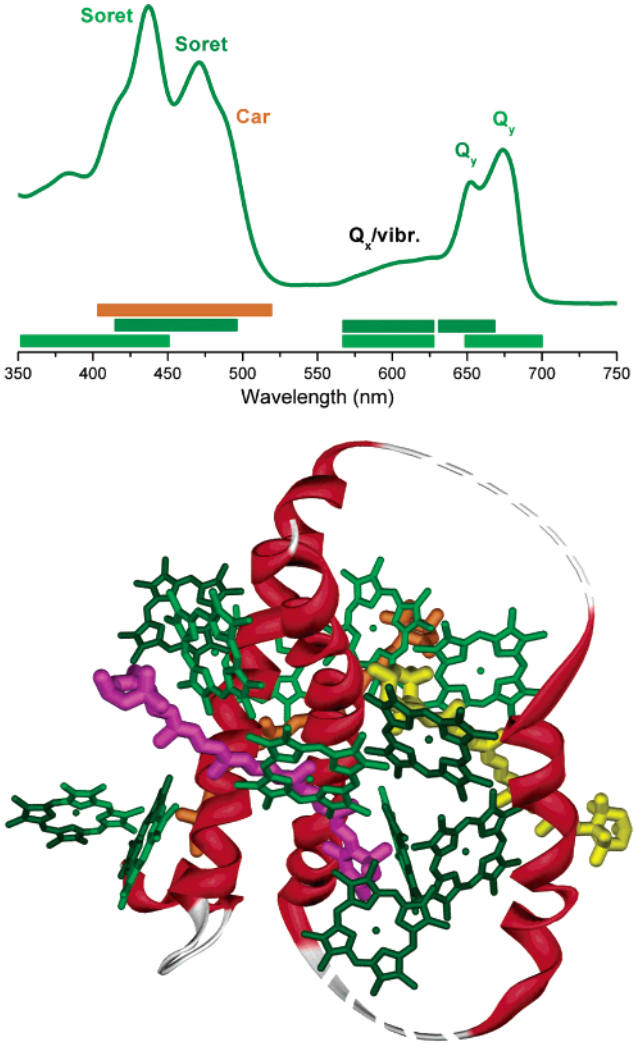

Figure 15. (Bottom) Model structure of the LHCII antenna protein based on the crystallographic data[184] and in vitro reconstitution and mutational analysis.[189] Two luteins depicted in orange (L1) and purple (L2) were revealed in the crystal structure, while neoxanthin shown in yellow was identified by biochemical studies. Chlorophyll molecules are depicted in light green (Chl-a) and dark green (Chl-b). The two chlorophyll molecules shown as half-light/half-dark green designate mixed chlorophyll sites that can accommodate both Chl-a and Chl-b. (Top) Absorption spectrum of the LHCII complex with contributions of different molecular species to the particular spectral region denoted by horizontal bars. The color code for chlorophylls is the same as in the model structure.

harvesting proteins of green plants: β-carotene, lutein, violaxanthin, neoxanthin, and zeaxanthin.[187] The two carotenoids in the LHCII structure were assigned to luteins, but later biochemical studies showed that while the L1 carotenoid site is exclusively occupied by lutein, the L2 site also binds violaxanthin though with a lutein/violaxanthin affinity of 80/20.[188] Further biochemical analysis revealed two additional carotenoid-binding sites present in LHCII: the N1 site, specific for neoxanthin,[189] and a violaxanthin-selective site V1.[190] The V1 site is easily removed during detergent treatment and seems to be occupied preferentially in plants grown at high light conditions.[190] The violaxanthin molecule occupying this site, however, is not able to transfer energy to Chl.[191] Although the sequence homology between LHCII and the other proteins of the *Lhc* family, particularly CP29, CP26, and CP24 complexes, suggests that these proteins are not structurally much different, each of the proteins has a unique carotenoid composition. It seems that all proteins except LHCII have only two carotenoid-binding sites.[28] While the L1 site is selective for lutein in all complexes, the L2 site can accommodate lutein or violaxanthin in all complexes. In CP26 and CP29 the L2 site even shows affinity to neoxanthin.[28,192] Under certain conditions the L2 site can also be occupied by zeaxanthin, and this was suggested to trigger a structural change of the protein, leading to quenching of Chl fluorescence,[28,193] which is the origin of the photoprotective mechanism called nonphotochemical quenching (NPQ). This mechanism protects against damage caused by excessive photon flux by dissipating the energy thermally in PSII.[194,195] It involves a cascade of processes triggered by high light conditions, resulting in enzymatic conversion of violaxanthin to zeaxanthin by means of the xanthophyll cycle. Although a fundamental understanding of NPQ is still lacking, it is clear that one of the crucial components is a zeaxanthin-induced quenching of Chl-a excited state, as presence of this carotenoid markedly reduces the Chl-a fluorescence lifetime.[193,196−198] Since a direct quenching by the S_1 state of zeaxanthin was suggested as one of the possible mechanisms,[79] studies of carotenoid S_1 dynamics in LHCII and related complexes became an important part of investigations of NPQ mechanisms.

Most of the studies of carotenoid−Chl energy transfer were performed on the LHCII and CP29 proteins. While LHCII is the only one whose structure is known in fine detail, the CP29 is favorable for studies of carotenoid−Chl energy transfer as it contains only 2 Chl-b molecules. This minimizes the overlap between the carotenoid S_2 state and the Chl-b Soret band peaking at around 475 nm (Figure 15). To overcome problems with the presence of a few different carotenoids with overlapping absorption spectra preventing selective excitation of only one carotenoid species, recombinant proteins that allow reconstitution with a single carotenoid species[188] were also used.[197−200] A number of studies established that the overall carotenoid−Chl energy-transfer efficiency in the Lhcb family of proteins is in the range 70−90%[5,185,197,199−204] and that the majority of the energy transfer occurs via the S_2 state (for scheme of energy-transfer pathways see Figure 16). Nevertheless, as described below, the precise assignment of pathways and donor−acceptor states involved in the energy transfer in the Lhcb proteins still remains to be revealed.

4.2.1. S_2 Pathway

The crucial requirement for the study of energy transfer in an arbitrary donor−acceptor pair by means of time-resolved spectroscopy is selective excitation of the donor. While this task is trivial for carotenoids in LH2-type complexes having only one carotenoid species with a S_0-S_2 transition well separated from the BChl Soret bands (Figure 12),

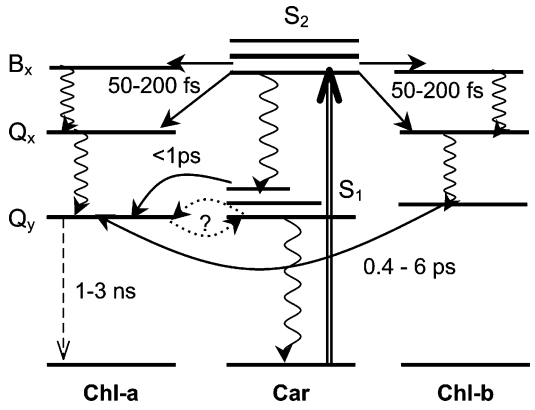

Figure 16. Scheme of energy levels and energy-transfer pathways between carotenoids and Chl molecules in the LHCII complex. The double arrow depicts excitation into the S_2 state of a carotenoid. Intramolecular relaxation processes are denoted by wavy arrows, while the dashed arrow represents the long-lived Chl-*a* fluorescence. Solid arrows represent the energy-transfer channels confirmed by time-resolved studies. The dotted lines represent possible energy-transfer channels involving energy transfer between thermalized carotenoid S_1 state and Chl-a and back energy transfer from Chl-a to the S_1 state of a carotenoid. The known energy-transfer pathways are labeled by the corresponding time constant. See text for details.

achieving such conditions in LHCII-type proteins is impossible due to the overlap of absorption spectra of different carotenoid species and Soret bands of Chl-a and Chl-b (Figure 15). Therefore, to estimate the degree of excitation of different pigments at different excitation wavelengths, sophisticated methods of fitting the Soret spectral region of LHCII-type proteins were developed. Using recombinant proteins carrying point mutations in pigment-binding residues or reconstituted with a predefined stoichiometry of carotenoid species enabled absorption spectra of individual pigments to be obtained. This information was then used to fit absorption spectra of wild-type complexes according to the known stoichiometry of pigments, which enabled spectral decomposition of the Soret region of LHCII,[185,188,189,198,205] CP29,[185,205] and CP26.[185,197,206] A similar but somewhat simpler approach relying on absorption spectra of individual pigments in solution for fitting of the Soret region of native LHCII[203,204] and CP29[203] was also employed. Yet, another method using resonance Raman spectra was applied. Since the frequency of the ground-state C=C stretching mode varies with conjugation length, measurements of resonance Raman spectra in the spectral region 430−520 nm enabled resolution of individual carotenoids.[207] Despite the complexity of the fitting, the results of all these studies are in very good agreement, except for a few inconsistencies. It is clear that neoxanthin has the highest energy of the S_2 state with a 0−0 origin of the S_0-S_2 transition in LHCII at 486−491 nm, somewhat varying between experiments.[185,198,203,205,207] Similar values have been reported for the neoxanthin S_2 state in CP26[185] and CP29,[185,200,203] suggesting that binding to either the N1 or L2 sites does not produce any significant shift of the neoxanthin absorption spectrum. For lutein in LHCII, Gradinaru et al.[203] and Ruban et al.[207] reported 0−0 origin of the S_0-S_2 transition at 495 nm. The same value was also obtained in other studies, but two different absorption spectra were assigned to luteins sitting in the L1 and L2 sites, having the 0−0 origins at 489 and 495 nm, respectively.[198,205] On the basis of shifts observed in the S_1-S_N spectra, it was suggested that the 'red' lutein corresponds to the L1 site.[198] Similarly, two luteins were resolved by Das et al.,[185] but their 0−0 origins were located at 494 and 499 nm. In CP29 and CP26, however, the two luteins exhibited identical spectra, having the 0−0 origin in the range of 494−498 nm,[185,203,205] indicating that the effect of protein environment in the L1 and L2 sites differs in these complexes. The largest discrepancy between S_2 energies obtained by different research groups occurs for violaxanthin. In LHCII, the 0−0 origins vary from ∼492 nm[185,198,205] to more than 500 nm.[203] However, it is necessary to stress that the value obtained by Gradinaru et al. refers to trimeric LHCII, for which the red-most carotenoid was later assigned to lutein having a red-shift induced by trimerization of LHCII complex.[207] The presence of the 510 nm lutein in trimeric LHCII was later also inferred from analysis of electrochromic response of carotenoids after Chl excitation.[208] For LHCII reconstituted with violaxanthin in both the L1 and L2 sites, values of 492−495 nm were found.[188,198] Again, some variations were observed for CP26 and CP29, having 0−0 energies of the violaxanthin S_2 state in the range 490−498 nm.[185,203,206] The red-most absorbing species were found when the LHCII-type complexes are reconstituted with zeaxanthin, which then have the 0−0 origin of the S_0-S_2 transition around 500 nm.[188,198,206] It is necessary to note, however, that the fitting of the very red edge of the Soret region is problematic and can suffer from some error, because of contributions from weakly absorbing states of Chl located between the Q_x and Soret transitions, not included in fitting. These states cause the plateau between 520 and 560 nm in the absorption spectrum, and their presence was also suggested in calculations.[209,210]

The first experimental evidence of fast energy transfer via the S_2 state was demonstrated in two transient absorption studies of LHCII.[202,211] The appearance of a Chl bleaching following excitation of carotenoids was assigned to an ultrafast energy transfer from the S_2 state of the carotenoids, with a time constant of 142[202] or 220 fs.[211] While the central luteins were concluded to be the energy donors in both studies, the assignment of acceptors was in contradiction. On the basis of the assumption that less than 15% of Chl-b is excited directly at 490 nm, Connely et al.[202] assigned Chl-b as the only energy acceptor in this energy-transfer pathway. On the other hand, Peterman et al.[211] reported a much higher degree of direct Chl-b excitation at 490 nm, and rapid appearance of the bleaching at around 675 nm led to the conclusion that Chl-a is a dominant energy acceptor, although some minor transfer to Chl-b could not be excluded. It is worth noting that because efficient S_2-mediated energy transfer requires a short distance between carotenoid and Chl, the assignment of Chl-b as the only acceptors is in contradiction with the initial assignment of Chl-a and

Chl-b in the crystal structure.[184] Observed efficient quenching of Chl-a triplets by carotenoids requiring very close contact of the molecules[204,212−214] is also in disagreement with Chl-b being the only acceptor for energy transfer from carotenoids.

Later, Gradinaru et al.[203] refined the picture of the S_2-mediated energy-transfer pathway in LHCII by analyzing the time evolution of the transient absorption spectrum. Using selective excitation of carotenoids at 489 and 506 nm, a fast decay of the S_2 state characterized by a time constant of 100 ± 20 fs was observed, suggesting a 60−65% energy-transfer efficiency of the S_2 channel. It was concluded that carotenoids occupying the L1 and L2 sites (lutein or violaxanthin) transfer energy to Chl-a, and Chl-b was suggested as an energy acceptor for S_2-mediated energy transfer from neoxanthin in the N1 site, the latter predominantly excited at 489 nm.[203] Yet another network of S_2 energy-transfer pathways in monomeric LHCII was proposed later using analysis of transient absorption spectra by so-called lifetime density maps.[199] This allowed separation of dynamics of the three carotenoids, yielding S_2 transfer times of 50 and 75 fs for the luteins in the L1 and L2 sites, while a slightly slower S_2 transfer (90 fs) was found for neoxanthin. In agreement with Gradinaru et al.,[203] neoxanthin was found to transfer energy exclusively to Chl-b.[199] The central luteins transferred energy from the S_2 state to both Chl-a and Chl-b with approximately a 50/50 ratio. For energy transfer to Chl-b, an interesting new channel was proposed. Analysis of dynamics of Chl-b excited-state absorption and bleaching led to the conclusion that in addition to the 'standard' channel to the Q_x state, the B_x could also be the accepting state.[199] Considering the small spectral overlap of carotenoid S_2 emission and B_x absorption, this channel would be most active for neoxanthin, which has the highest S_2 energy among the carotenoids in LHCII. The results of Croce et al.[199] were further confirmed by fluorescence up-conversion. The average lifetime of the carotenoid S_2 state measured by S_2 emission decay in LHCII trimers was 57 fs for the wild-type complex and 70 fs for the *npq2* mutant lacking violaxanthin and neoxanthin.[68] Combining these results with steady-state data, the overall carotenoid−Chl efficiency was determined to be 76% and 63% for the wild-type trimers and *npq2* mutant, respectively, with the S_2 channel representing the dominating energy-transfer pathway.[68]

Energy-transfer pathways in CP29 were found to be similar to those in LHCII. The CP29 complex has a less complex energy-transfer pattern, since it lacks the N1 site and binds only two Chl-b and six Chl-a molecules.[192] However, even without the N1 site, the CP29 can bind three different carotenoids, as the L2 site accommodates either violaxanthin or neoxanthin with a 50/50 ratio.[192] Again, contradictory results were reported as far as the energy acceptors are concerned. Similar to LHCII, a very fast S_2 decay of 70−130 fs suggests efficient S_2-mediated energy transfer.[200,203] Either exclusively Chl-a was assigned as energy acceptor[203] or transfer to both Chl-a and Chl-b was proposed.[200] In the latter case, using a CP29 mutant with an empty L2 site enabled differentiation of the channels originating from carotenoids sitting in the L1 and L2 sites. While for the L1 site the energy acceptor is the Chl-a absorbing at 680 nm, the carotenoid occupying the L2 site transfers energy to the Chl-a absorbing at 675 nm and to Chl-b with an absorption maximum at 652 nm.[200]

Despite the disagreement regarding the accepting Chl molecules, these studies provided clear evidence for very efficient S_2-mediated energy transfer in LHCII-type complexes. The problems with assignments of the accepting Chl have two origins. First, the fitting of the Soret region is a complex problem that usually does not converge to a unique solution. Therefore, estimates of direct excitation of Chl-b and Chl-a may vary slightly in different works. This problem is further enhanced by the necessity to use very short pulses in order to resolve the sub-100 fs dynamics of the S_2 state. Such short pulses have a broad spectrum, making the assessment of direct excitation even more complicated. Second, the evaluation of carotenoid−Chl energy transfer is also complicated by the fact that the Chl-b to Chl-a energy-transfer and equilibration processes among Chl-a molecules constitute a rich network of possible channels, some of them occurring on a time scale faster than 200 fs,[5,215−218] thus interfering with carotenoid−Chl energy transfer. Consequently, the exact assignment of acceptors is a difficult task, and the fact that the large mismatch between the first two studies[202,211] has converged into a relatively minor disagreement[199,200,203] demonstrates the progress in understanding of the S_2-mediated energy-transfer pathway in the LHCII-type complexes. Although no similar studies of CP26 and CP24 complexes have been carried out to date, on the basis of measured carotenoid-to-Chl energy-transfer efficiencies,[185,197] it is feasible to assume that the overall picture will be similar to that for LHCII and CP29.

4.2.2. S_1 Pathway

Knowing the energy of the lowest Q_y transition of Chl-a in LHCII-type complexes of ~14 600 cm^{-1} and S_1 energies of carotenoids estimated either from measurements in solution or the energy-gap law (Table 1), a simple comparison with LH2 complexes of purple bacteria suggests that the S_1-mediated pathway should be inefficient in the LHCII-type complexes. As demonstrated for LH2, the S_1 state should be at least 800 cm^{-1} above the acceptor state to achieve a sufficient overlap between the hypothetical S_1 emission and absorption of the acceptor. While such an arrangement often occurs in LH2, for LHCII-type complexes it implies that the S_1 energy of the carotenoid should be at least 15 400 cm^{-1}, which is higher than expected for carotenoids occurring in these complexes. The S_1 energies in solution at room temperature were measured only for violaxanthin and zeaxanthin,[81,84] yielding values below 15 000 cm^{-1} (see section 3.2 and Table 1). No studies of S_1 energies of lutein and neoxanthin in solution have been reported so far, but estimates on the basis of their S_1 lifetimes of 14 (lutein)[102] and 35 ps (neoxan-

thin)[22] suggest that the S_1 energy of lutein is lower than that of violaxanthin, while neoxanthin probably has its S_1 energy above 15 000 cm^{-1}.

Using LHCII complexes reconstituted with only one carotenoid species occupying the L1 and L2 sites, measurements of the S_1-S_2 spectra revealed that when sitting in these binding pockets, violaxanthin, lutein, and zeaxanthin have essentially the same S_1 energies of $\sim$13 900 $\pm$ 300 cm^{-1} (Table 1), preventing any energy transfer to Chl-a from the relaxed S_1 state.[198] Surprisingly, this study also showed that despite their different S_1 lifetimes in solution, all three carotenoids have also nearly the same S_1 lifetimes of $\sim$11 ps when accommodated by the L1 and L2 sites, suggesting that the protein environment in L1 and L2 sites significantly affects the excited-state properties of carotenoids and that this effect varies for different carotenoid species. This species-dependent effect of the protein environment can also be traced in the energies of both the S_0-S_2 transition and the S_1-S_N band. In both cases, the red shift, induced by interaction with the protein, is strongest for violaxanthin, smaller for lutein, and even smaller for zeaxanthin,[198] confirming the trend observed for the S_1 lifetimes—11 ps measured in protein environment is nearly the same as that in solution for zeaxanthin but significantly shorter than the violaxanthin S_1 lifetime in solution (24 ps). One possible explanation of this effect could involve the fact that the conjugation extended to the terminal rings for zeaxanthin makes the molecule rather rigid, preventing the protein to change the conformation of the molecule. For violaxanthin, the conjugation is restricted to the carbon backbone and the molecule becomes more flexible, allowing modifications of its excited-state properties through protein-induced conformational changes. In fact, the opposite effect was proposed for zeaxanthin: the rigidity of the zeaxanthin molecule was hypothesized to cause a change of protein conformation, which in turn induces favorable conditions for effective quenching of Chl-a excited states. Consequently, the L2 binding site, which allows exchange of carotenoids, was proposed to be an allosteric site facilitating the Chl-a quenching by binding of zeaxanthin.[28,193]

Besides S_1-S_2 spectra, two-photon excitation spectra were employed to locate the S_1 state of carotenoids in LHCII. Walla et al.[201] assigned a band with a 0−0 origin at 15 100 $\pm$ 300 cm^{-1} to the spectral profile of the S_1 state. Since wild-type LHCII contains lutein, violaxanthin, and neoxanthin, this value represented a 'mean' S_1 energy of carotenoids transferring energy to Chl (Table 1). By up-converting the Chl-a emission at 685 nm, these authors managed to measure directly the transfer rate of the S_1-mediated energy transfer by selectively exciting the S_1 state. An unexpectedly high rate of (250 $\pm$ 50 fs)$^{-1}$ was observed, setting the efficiency of the S_1-mediated energy transfer close to 100%. The reason for this unrealistically high S_1 energy and energy-transfer efficiency was understood in a subsequent study employing two-photon excitation. Comparing the two-photon excitation spectra of LHCII with those of lutein and β-carotene in solution, it was concluded that the energy transfer must occur from the vibrationally hot S_1 state.[95] Since the S_1 excitation spectrum is measured by detecting Chl fluorescence, it does not reflect the true S_1 spectrum but is rather an action spectrum of S_1-mediated energy transfer that obviously is appreciable only for higher vibrational levels of the S_1 state. Assuming that the 15 100 cm^{-1} spectral origin corresponds to the $v = 1$ vibrational level, the 0−0 origin would then be located at $\sim$13 800 cm^{-1}, matching perfectly the results obtained from S_1-S_2 spectra.[198] Similarly, the fast energy-transfer rate of (250 fs)$^{-1}$ is also understandable, since the energy transfer must compete with S_1 vibrational relaxation occurring on a time scale of 300−800 fs.[100,101,121−124] The resulting efficiency of the energy-transfer route employing the hot S_1 state was estimated at $\sim$50%.[95] Energy transfer from the hot S_1 state was recently confirmed by transient absorption measurements of the CP29 complex,[200] but the observed transfer rate of (700 fs)$^{-1}$ is longer than the (250 fs)$^{-1}$ observed by Walla et al.,[201] leading to only a modest efficiency of $\sim$10% (see Figure 16 for summary). The presence of an energy-transfer channel involving the hot S_1 state was also suggested on the basis of fluorescence up-conversion measurement on LHCII trimers—a component observed in the rise of the Chl-a emission having a time constant of $\sim$350 fs was ascribed to this channel.[68]

Energy transfer via the thermalized S_1 state was also reported. A 1 ps component extracted from global analysis of transient absorption spectra of CP29 and LHCII was ascribed to the S_1-mediated energy transfer.[203] The central luteins were suggested as energy donors, but this conclusion seems unlikely considering the low energy of the S_1 state of lutein in LHCII reported later.[95,198] In light of the results on CP29 assigning a 700 fs process to energy transfer via hot S_1 state, it is reasonable to assume that the $\sim$1 ps process observed by Gradinaru et al.[203] has the same origin. Nevertheless, longer time components on the time scale of picoseconds were also observed in transient absorption measurements, which cannot be rationalized by a transfer via the hot S_1 state. For LHCII, Croce et al.[199] did not find any evidence for substantial energy transfer via the thermalized S_1 state, although the 3.9 ps lifetime assigned to the S_1 state of one of the luteins might suggest the presence of energy transfer. A similar, low-amplitude component of 5 ps was also revealed in fluorescence up-conversion measurements on LHCII trimers.[68] In CP29, even longer components in the range 8−20 ps were found and assigned to energy transfer from the thermalized S_1 state of violaxanthin and/or neoxanthin bound to the L2 state. Since these two carotenoids might have higher S_1 energy, the S_1 route cannot be excluded in this case. The $\sim$13 900 cm^{-1} S_1 energy of violaxanthin determined for reconstituted LHCII[198] in fact contradicts this hypothesis, but it is possible that violaxanthin in CP29 has higher S_1 energy. On the other hand, neoxanthin seems to have the most favorable conditions for energy transfer via the thermalized S_1 state, because its S_1 state is expected to be the highest of all carotenoids in LHCII-type complexes.

To complete the list of possible energy-transfer pathways between singlet excited states of carotenoids and Chl in LHCII-type complexes, it is necessary to mention the possibility of back energy transfer from Chl-a to the S_1 state of carotenoids. This energy-transfer route was suggested by Frank et al., who proposed the so-called 'molecular gear shift mechanism' as a mechanism for NPQ.[79] In the initial proposal based on S_1 energies estimated from the energy-gap law, violaxanthin was supposed to have its S_1 energy above the Q_y transition of Chl-a serving as energy acceptor while zeaxanthin had an S_1 energy sufficiently low to act as quencher of excited Chl-a. Then, exchange of violaxanthin to zeaxanthin by means of the xanthophyll cycle would enable an increase of quencher concentration, explaining the mechanism of NPQ. Later, direct measurements of the S_1 energies in both solution[81,84] and LHCII[198] challenged this mechanism, since the S_1 energies of both violaxanthin and zeaxanthin were shown to be below the Chl-a Q_y state. Nevertheless, although the initially proposed 'molecular gear shift' would not work, the location of the zeaxanthin S_1 state below the Chl-a Q_y transition still allows direct quenching. Directly detecting the possible Chl-a quenching by the zeaxanthin S_1 state represents a nontrivial task, because the fastest component of the Chl-a lifetime observed in the quenched state has a time constant of ~500 ps.[193,196,198] If this component were due to energy transfer from Chl-a to zeaxanthin, the S_1 state of zeaxanthin would have essentially zero population due to its 10 ps lifetime, making it almost impossible to detect in a transient absorption experiment. On the other hand, such conditions would make the zeaxanthin S_1 state a very effective sink for Chl-a excitations. Therefore, although experimental data could not unambiguously assign the mechanism of quenching, a direct quenching by means of singlet energy transfer was considered as a possibility.[28,198] However, contrary to the previous suggestions,[79] the key role of zeaxanthin was not due to the intrinsic photophysical properties of zeaxanthin but rather due to its ability to promote a conformational change allowing such a transfer.[28,193,219]

Direct involvement of the zeaxanthin S_1 state in NPQ was also shown in a transient absorption study of intact thylakoid membranes of *Arabidopsis thaliana*.[220] After excitation of either Chl-b or Chl-a by ~100 fs pulses at 664 and 683 nm, respectively, an excited-state absorption in the spectral region 530−570 nm was observed directly after excitation. On the basis of the spectral profile reconstructed from a few kinetic traces measured across this region, having decays characterized by a time constant of ~10 ps, it was concluded that this signal corresponded to the S_1-S_N spectrum of zeaxanthin. Importantly, using transgenic *A. thaliana* plants, the intensity of the S_1-S_N signal was correlated to the presence of the PsbS protein that is known to be an essential part of NPQ,[221] thus confirming the relation between population of the zeaxanthin S_1 state and NPQ. Although the quenching mechanism could not be disclosed from the experimental data, either energy transfer from Chl to the zeaxanthin S_1 state or formation of a zeaxanthin−Chl heterodimer was suggested.[220] It is worth noting that this phenomenon can represent a different quenching mechanism than decrease of the Chl-a lifetime observed earlier. While the S_1-S_N signal was observed only for intact thylakoid membranes, the shortening of the Chl-a lifetime was evidently detected even in isolated monomeric LHCII-type complexes.[193,197,198] Similar zeaxanthin-induced quenching was also observed in artificial zeaxanthin−pheophorbide dyads where pyropheophorbide emission lifetime was markedly shortened when covalently linked to zeaxanthin[222,223] or in a mixture of carotenoids and Chl-a embedded in DMPC liposomes.[224] Moreover, the S_1-S_N spectrum of zeaxanthin observed for *A. thaliana*[220] is apparently blue-shifted from that recorded for LHCII reconstituted with zeaxanthin.[198] Therefore (since the detection of S_1-S_N spectrum of zeaxanthin after Chl excitation is connected with presence of PsbS protein), zeaxanthin detected in these experiments might be located outside the LHCII-type complexes, somehow interacting with the PsbS protein. One possibility could be the PsbS−zeaxanthin complex (see section 4.4) discovered recently.[225] Another hypothesis was suggested on the basis of quantum chemical calculations employing a hybrid approach consisting of time-dependent density functional theory and configuration interaction, a method capable of describing charge-transfer states.[226] This approach demonstrated the existence of a charge-transfer (CT) state in a zeaxanthin−Chl heterodimer.[226,227] For a cofacial arrangement of zeaxanthin and Chl-a with a center to center distance less than 5.5 Å, the energy of the CT state was low enough to allow quenching of the Chl-a excited state through electron transfer.[226,227] Likewise, close proximity and proper orientation of zeaxanthin and Chl-a may lead to an excitonic interaction, as proposed by van Amerongen et al.[5] In such a case, even if the S_1 energies of individual molecules are not favorable for Chl−zeaxanthin energy transfer, the excitonic interaction would cause a shortening of the Chl-a excited-state lifetime, again leading to a quenching of Chl-a fluorescence.[5]

It must be noted that besides the Chl−zeaxanthin energy transfer and formation of Chl−zeaxanthin heterodimer, other NPQ mechanisms that do not involve the S_1 state of zeaxanthin were also proposed. A quenching of Chl singlet state by electron transfer from carotenoids to Chl was suggested on the basis of observations on artificial carotenoporphyrin dyads.[228−230] Another hypothesis proposed that the essential function of zeaxanthin is to promote changes in structure and/or organization of the light-harvesting complexes that eventually lead to quenching conditions. One such mechanism involves a structural change facilitating a formation of Chl-a excitonic pairs, which then play a role of quenchers.[195,231] A long-range change involving aggregation and/or disaggregation of antenna complexes was also proposed.[213,232−234] In these processes, zeaxanthin is not directly involved in quenching but acts as a trigger of the particular process. Very recently, 'activation' of zeaxanthin, achieved by binding zeaxanthin to the

PsbS protein (see section 4.4), was proposed to be an important mechanism to trigger energy dissipation in plants.[225] Which of these mechanisms play the most important role in NPQ is not known yet. The experimental data collected recently did not lead to general consensus. Nevertheless, given the complexity of the NPQ process, it is quite possible that all of these mechanisms have a certain place and all together lead to the effective protection against excess light in higher plants.

4.3. Peridinin–Chlorophyll–Protein

The third type of light-harvesting complexes whose structure was resolved to atomic resolution is a water-soluble antenna complex from the dinoflagellate *Amphidinium carterae*. The uniqueness of the peridinin−chlorophyll-a protein complex (PCP) is in its pigment composition. As described above, in most photosynthetic antenna complexes the principal light-harvesting pigments are either Chl or BChl molecules. In contrast, the PCP utilizes the carotenoid peridinin as the main light-harvesting pigment. The 2.0 Å structure of PCP[235] revealed a trimer of protein subunits with densely packed pigments having a stoichiometry of eight peridinins and two Chl-a molecules per protein subunit. As shown in Figure 17, the pigments in each subunit are arranged as two nearly identical domains of four peridinins and one Chl-a molecule.[235] The closest distances between pigments belonging to the two different domains are larger than those between pigments within one domain. Distances between peridinins within a single domain are 4−11 Å, and the conjugated regions of the peridinins are in van der Waals contact with tetrapyrrole rings of the Chl-a molecules (3.3−3.8 Å). The distance between Mg atoms of the two Chl-a belonging to different domains is 17.4 Å. Such a tightly packed cluster of pigments creates an ideal medium for efficient energy transfer. Besides the unique pigment composition, the principal light-harvesting pigment, peridinin, belongs to the family of carotenoids having a conjugated carbonyl group that alters their excited-state properties, as the lowest S_1/ICT excited state gains a significant charge-transfer character (section 3.2). All these features make PCP quite different from other known light-harvesting complexes from bacteria and plants and have made this complex an attractive object for studies aiming at obtaining a better understanding of Nature's light-harvesting strategies.

4.3.1. Steady-State Spectroscopy

The absorption spectrum of PCP is dominated by the peridinin S_2 state that is responsible for the broad absorption band between 400 and 550 nm (Figure 17), which overlaps with the Soret band of Chl-a peaking at 435 nm. In addition, the Q_y band of Chl-a contributes to the red part of the absorption spectrum, peaking at 670 nm. The weak band located between 600 and 650 nm originates from the 0−1 vibrational transition of the Q_y band and/or the Q_x transition of Chl-a.[45,106,236−240] The lack of vibrational structure of the peridinin S_2 state, similar to that observed for peridinin in polar solvents,[21,22,24,44] suggests that the PCP protein provides a polar environment. Although the main peridinin band peaking at 490 nm is rather structureless at room temperature, a shoulder can be recognized at around 530 nm. This shoulder transforms to a distinct band located at 525 nm in the absorption spectrum measured at 77,[237,239] 10,[45] and 4 K.[237] These two bands were assigned to the 0−0 (526 nm) and 0−1 (490 nm) vibrational bands of peridinin[239] on the basis of a comparison with the peridinin absorption spectrum measured at 77 K in methanol.[241] However, analyzing the second derivative of the PCP absorption spectrum together with CD, LD, and triplet-minus-singlet spectra at 4 K, Kleima et al. obtained evidence for spectrally different peridinins having their 0−0 origins at 520, 537, and 555 nm.[237] Except for one missing spectral band, this result is in a good agreement with simulated CD and absorption spectra that, under the assumption of negligible excitonic coupling between the peridinins, gave the 0−0 origins of peridinins

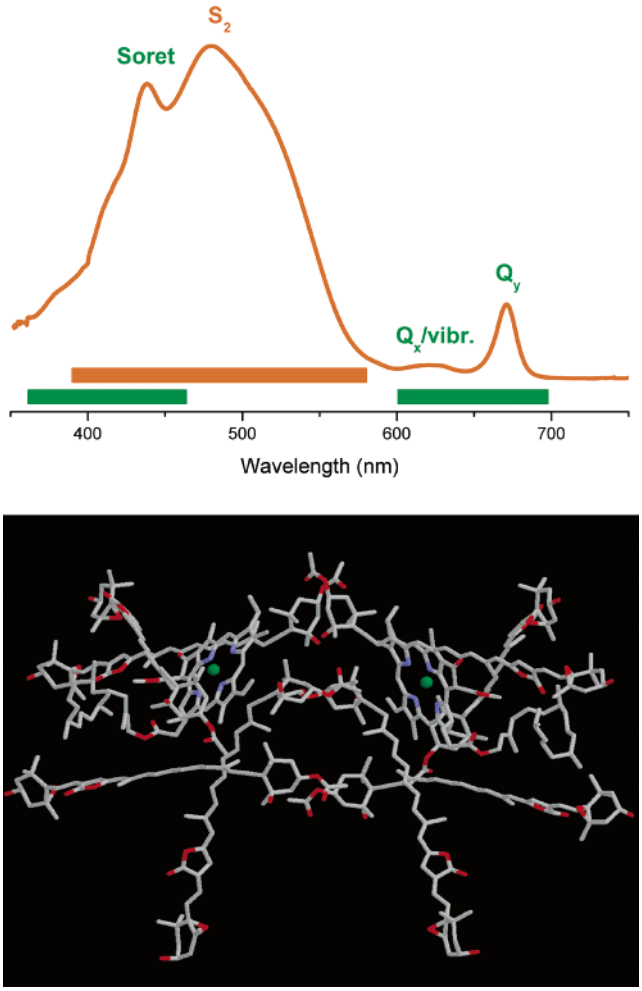

Figure 17. (Bottom) Organization of peridinin and Chl-a molecules within a monomeric unit of the PCP complex consisting of two identical domains with four peridinins and one Chl-a molecule. The central manganese atoms of the Chl-a molecules are shown as green balls, and blue parts in the molecular structure represent nitrogen atoms in the Chl-a structure. Oxygens occurring in the structure of the peridinin molecule are marked by red. (Top) Absorption spectrum of the PCP complex. The horizontal bars denote the contributions of peridinin (orange) and Chl-a (green) to the absorption spectrum.

located at 485, 518, 534, and 543 nm at 20 K.[239] Similar results were obtained by fitting the 10 K absorption spectrum of PCP using absorption spectra of individual pigments taken at 10 K in 2-MTHF.[45] The best fit was achieved for the peridinin S_2 transitions located at 545, 528, and 523 nm. For these three peridinins, the absorption spectra were identified as identical in both structural domains of PCP monomer. The fourth peridinin exhibited differences in the two domains, peaking at 485 and 465 nm, respectively.[45] These two distinct blue-shifted spectra were assigned to peridinins 612 and 622, according to the notation used in Damjanović et al.[242]

The two-photon excitation spectrum of PCP exhibited a large similarity with the one-photon absorption. Both one-photon and two-photon excitation spectra have a similar shape, except the two-photon spectrum is red-shifted as compared to its one-photon counterpart, suggesting that the S_2 state of peridinin is also two-photon allowed.[43,45] This was explained by the presence of polar groups in the peridinin structure, because for a polar molecule the two-photon transition can occur via a change of static dipole moment between the ground and excited states.[243] Thus, the large change of dipole moment of the S_2 state upon excitation together with mixing with the close-lying S_1/ICT state and deviation of peridinin from ideal C_{2h} symmetry account for the two-photon allowed S_2 state.[43,45] By measurements of the polarization ratio of absorptivities $\delta_{cir}/\delta_{lin}$, which is equal to 1 for a one-photon transition but takes values between 0 and 1.5 for two-photon absorption,[45,244] Zimmermann et al. concluded that the two-photon excitation spectrum of PCP consisted of two distinct states. The S_1/ICT state was estimated to be located at about 550−560 nm (17 850−18 120 cm^{-1}).[43] On the contrary, polarization ratio data measured later led to the conclusion that all the features in the two-photon excitation spectrum of PCP are due to the S_2 state.[45] This failure to detect the S_1/ICT state in the two-photon excitation spectrum measured up to 17 000 cm^{-1} agrees with the S_1/ICT energy obtained from S_1/ICT−S_2 spectra of PCP shown in Figure 18. The latter suggested a value of about 16 400 cm^{-1},[240] thus markedly lower than the value obtained by Zimmermann.[43] A S_1/ICT energy in the range 16 000−16 500 cm^{-1} seems to be more realistic also because the 0−0 spectral origin of the S_1/ICT in solution determined from emission spectra is in the range 16 200−16 600 cm^{-1}.[21,23,45,73] The higher S_1/ICT energy around 18 000 cm^{-1} suggested by Zimmermann et al.[43] would require a blue shift of the S_1/ICT state, despite the fact that the S_2 state is red-shifted in PCP. Such an ambivalent shift of the two lowest energy levels of peridinin seems to be unlikely, even though MNDO−PSCDI calculations on peridinin with geometry minimized according to the constraints given by the protein environment suggested a reverse ordering of the S_1/ICT and S_2 states for peridinins 612 and 622.[45] This result showed that the influence of protein environment could be more dramatic than for other light-harvesting proteins. Indeed, it was shown that hydrogen bonding

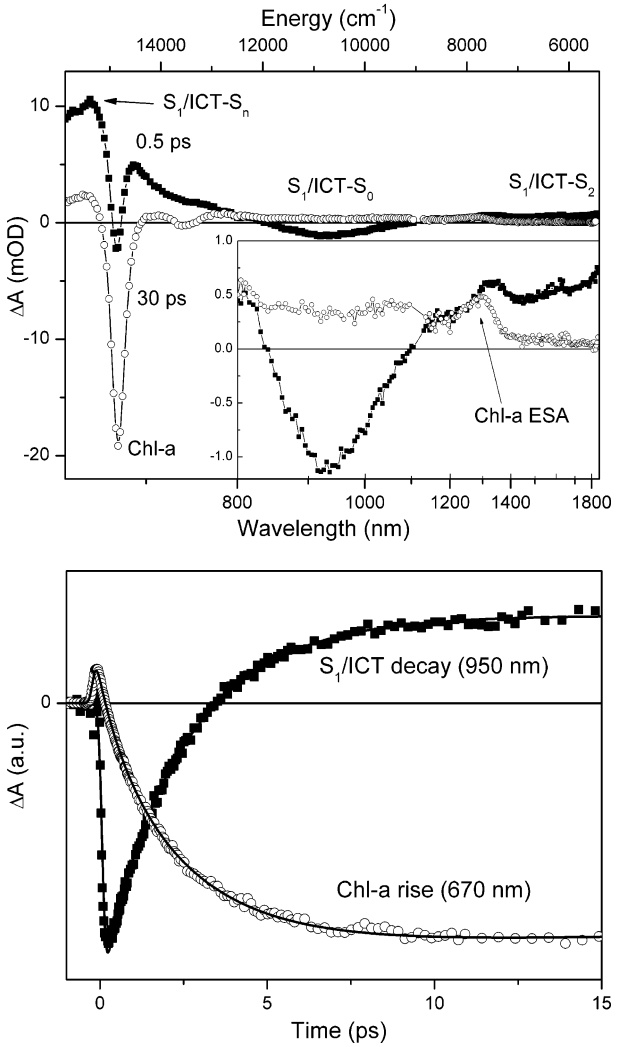

Figure 18. (Top) Transient absorption spectra of the PCP complex at 0.5 (full squares) and 30 ps (open circles) after excitation at 535 nm. The inset shows an enlargement of the 800−1800 nm spectral region. (Bottom) Kinetic traces of PCP measured after excitation at 535 nm. Probing wavelengths are indicated for each kinetic. Solid lines represent best fits obtained from a multiexponential global fitting procedure.

via the carbonyl group can alter the excited-state properties of peridinin significantly,[44] and a recent theoretical study of peridinin−protein interactions in PCP suggested a possibility that hydrogen bonding may play an important role in binding of peridinin in PCP.[146]

4.3.2. Energy-Transfer Pathways

Nearly 100% efficiency of peridinin−Chl energy transfer in the PCP complex was demonstrated long before the unique organization of pigments within the PCP complex was known.[245] Availability of a detailed structure of the PCP complex became a landmark for systematic time-resolved studies of energy-transfer pathways within PCP. The initial studies utilized the standard scheme of S_1 and S_2 states without considering the ICT character of the lowest excited state. The first transient absorption study of PCP revealed a 3 ps lifetime of the S_1 state of peridinin, suggesting efficient energy transfer via the S_1 state. Given the

overall peridinin−Chl efficiency of ~88%, it was concluded that the energy transfer via the S_1 state represents the primary route.[106] However, it must be emphasized that calculation of S_1 energy-transfer efficiency for peridinin in the PCP complex is not straightforward, because the S_1 lifetime is solvent dependent (see section 3.2) and the intrinsic S_1 lifetime (in the absence of energy transfer) of peridinin in PCP is not known. The aforementioned conclusion was based on the assumption of an intrinsic peridinin lifetime of 13 ps in PCP, close to that for peridinin in methanol.

The S_1 route being a primary channel of energy transfer in PCP was also proposed from theoretical investigations. Calculated full Coulomb couplings between peridinins and Chl-a together with the corresponding spectral overlaps only gave reasonable transfer times for S_1-mediated energy transfer.[242] While the S_2 route was found insignificant, strong couplings in the range 133−523 cm^{-1} between the S_2 states of peridinins suggested the possibility of S_2 excitons.[242] Calculations of S_2 exciton densities pinpointed peridinin 612 as having the lowest S_2 exciton density and thus the highest energy in PCP. This was suggested to direct excitations to the excitonically coupled S_2 states of the other three peridinins in the structural domain, which would then relax to the donating S_1 state.[242] The uniqueness of peridinin 612 was further suggested on the basis of MNDO−PSCDI calculations that not only confirmed that peridinin 612 has the highest energy, but it was also suggested to have reversed S_1 and S_2 states.[45] This would eliminate the fast S_2−S_1 internal conversion enabling efficient transfer between peridinin S_2 states as proposed by Damjanović et al.[242] Contrary to these results, a transient absorption study suggested that the S_2 energy-transfer pathway is active in the PCP complex.[238] This conclusion was reached using various models to fit the transient absorption data. It was shown that a model without S_2-mediated energy transfer could not explain all the features observed in the transient absorption spectra recorded in the visible spectral region, and to achieve the 88% energy-transfer efficiency, a contribution of the S_2 route as high as 25−50% was needed. S_2-mediated energy transfer was on the sub-100 fs time scale, while a transfer rate of $(2.3\ ps)^{-1}$ was calculated for S_1 energy transfer, yielding an intrinsic peridinin S_1 lifetime around 15 ps.[238] It is important to mention that the effect of excitation wavelength was also investigated, and no changes of the dynamics or spectral profiles were found when peridinin in PCP complex was excited at 500 and 520 nm. The fact that the species-associated decay spectrum of the S_2 state was very similar for both excitation wavelengths contradicts the hypothesis of peridinin 612 having higher S_2 state energy, serving as energy donor for the S_2−S_2 energy transfer among the peridinins in PCP complex.[45,242] The possibility of the ICT state of peridinin as an energy donor in the S_1-mediated energy transfer was also discussed, and it was concluded that an equilibrium between the S_1 and ICT states prevented differentiation of the contributions of these two states.[238]

The role of the ICT state in energy transfer within PCP was further addressed in a subsequent work. Inspired by previous findings that the ICT state can be monitored in the near-infrared region through its stimulated emission band centered at 950 nm,[23,44] spectroscopic investigations on PCP were focused to this region. Transient absorption spectra recorded in the broad spectral region of 630−1850 nm shown in Figure 18 demonstrated that the stimulated emission band characteristic of the ICT state is also present for peridinin in PCP.[240] Moreover, decay of the ICT stimulated emission matched perfectly the rise of the Chl-a signal, signaling direct involvement of the ICT state in peridinin−Chl energy transfer within PCP (Figure 18). Analyzing kinetics spanning the whole studied spectral region, it was concluded that the S_1 and ICT states must be strongly coupled, forming an S_1/ICT state, which plays the role of energy donor in peridinin−Chl energy transfer. The feasibility of the S_1/ICT state being one state with charge-transfer character was further confirmed by both time-resolved absorption[44] and two-photon spectroscopy[45] of peridinin in solution. Using the overall efficiency of peridinin−Chl energy transfer of 88%,[106] a model of energy-transfer pathways, depicted in Figure 19

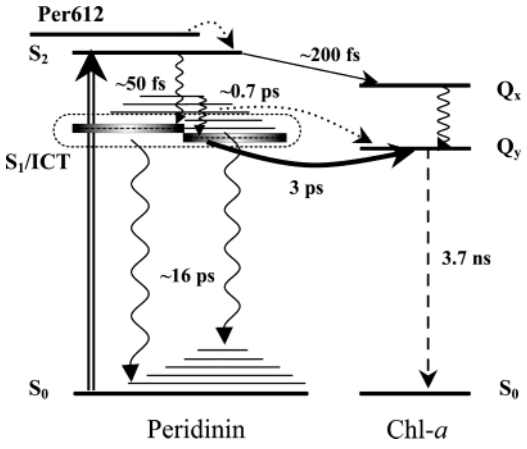

Figure 19. Scheme of energy levels and energy-transfer pathways between peridinin and Chl-*a* in the PCP complex. Intramolecular relaxation processes are denoted by wavy arrows, while the dashed arrow represents the long-lived Chl-*a* fluorescence. Solid arrows represent the main energy-transfer channels. The dotted arrows represent possible minor energy-transfer channels involving higher vibrational levels of the S_1/ICT state and the S_2−S_2 energy transfer involving peridinin 612. Excitation at 535 nm is shown as a double arrow. All processes are labeled by the corresponding time constant. See text for details.

was built. The magnitude of the Chl-a bleaching signal at 0.5 ps after excitation led to the conclusion that there must be some S_2-mediated energy transfer present, in accord with earlier suggestion of Kruger et al.[238] By modeling of the kinetics of formation of the Chl-a excited state at 670 nm, it was concluded that the S_2 pathway contributes about 25%. This rather low efficiency of the S_2 channel (compared with LH2 and LHCII complexes) is likely caused by the very short S_2 lifetime of peridinin, which was determined to be ~60 fs in methanol.[44] Given the similarity of absorption spectra of peridinin in PCP and polar solvents,[43,45,106,240] it is reasonable to assume

that the intrinsic S_2 lifetime of peridinin in PCP is similar. Then, the energy-transfer rate via the S_2 state is $\sim(200\ \text{fs})^{-1}$, which is comparable to the values observed for other light-harvesting complexes.

The rest of the energy transfer proceeds via the S_1/ICT state, and taking into account the total energy-transfer efficiency of 88%[106] and 25% efficiency of the S_2 channel, the energy-transfer time and intrinsic S_1/ICT lifetime were calculated from the 2.5 ps decay of the S_1/ICT state, yielding 3 and 16 ps, respectively.[240] In addition to the S_2 and S_1/ICT channels, a minor 700 fs component was necessary to achieve satisfactory fits of both S_1/ICT decay and Chl-a rise and was ascribed to a pathway involving higher vibrational levels of the S_1/ICT state (Figure 19). These values for the S_1/ICT energy-transfer rate and intrinsic lifetime are in very good agreement with previous results, confirming that the intrinsic S_1/ICT lifetime of peridinin is in the range of 13−16 ps,[106,238] clearly indicating that peridinin molecules are accommodated in polar surrounding in PCP. However, it should be noted that estimation of environment polarity in PCP is complicated because the S_1/ICT lifetime is also altered by hydrogen bonding via the carbonyl group.[44] Since it is known from the structure of the PCP complex that amino acid residues and water molecules in PCP offer a possibility for a rich hydrogen-bonding network,[146,235] it is possible that the intrinsic S_1/ICT lifetime of peridinin in PCP is not determined only by polarity of the surrounding but also by hydrogen bonding. Nevertheless, no matter how large the contributions from polarity and hydrogen bonding, it is apparent that the protein environment in PCP provides conditions under which the lowest excited state of peridinin gains a substantial charge-transfer character. Comparison of magnitudes of S_1/ICT stimulated emission at 950 nm and Chl-a bleaching at 670 nm showed that the gain of charge-transfer character of the S_1/ICT state increased the transition dipole moment of the S_1/ICT state, making this state more efficient in energy transfer. This is because the rate of Förster-type energy transfer is proportional to the square of the coupling between donor and acceptor, which in its turn is proportional to the transition dipole moment.[173] The PCP complex therefore represents an example of a system where energy-transfer pathways and their efficiencies are finely tuned not only by the protein structure ensuring a proper orientation of the donor and acceptor molecules, but also by the polarity and/or hydrogen-bonding capability of the environment adjusting the degree of charge-transfer character of the lowest excited state. Too low charge-transfer character of the S_1/ICT state would lead to a long intrinsic S_1/ICT peridinin lifetime, resulting in a better competition of energy transfer with the S_1/ICT−S_0 relaxation but at a price of a negligible contribution of the charge-transfer character to energy transfer. On the other hand, too high polarity could enhance the contribution of the S_1/ICT state, providing a stronger dipole moment of the donor state, but the resulting short intrinsic S_1/ICT lifetime would make the energy transfer less competitive with the S_1/ICT−S_0 relaxation. Thus, to achieve an efficient S_1/ICT energy transfer, the parameters characterizing the environment of the peridinin molecules in PCP must be perfectly balanced.[240]

It is apparent that the presence of the conjugated carbonyl group offers utilization of a special light-harvesting strategy involving a charge-transfer state as a donor. Although no studies of energy-transfer pathways in light-harvesting complexes containing carbonyl carotenoids other than PCP have been reported so far, a few earlier works provided valuable information about the efficiency of energy transfer in such light-harvesting complexes. Time-resolved fluorescence spectroscopy of the alga *Bryopsis maxima* suggested efficient energy transfer between siphonaxanthin and Chl-a.[246] The same conclusion was obtained from fluorescence excitation spectra for deep-water algae.[247] About 90% efficiency of energy transfer between fucoxanthin and Chl-a was reported for fucoxanthin−chlorophyll protein (FCP) from *Phaeodactylum tricornutum*,[248] and efficient energy transfer utilizing fucoxanthin as energy donor was also suggested by other studies.[249,250] Although these studies did not provide conclusions regarding the mechanism of energy transfer, the fact that both fucoxanthin and siphonaxanthin exhibit similar excited-state properties as peridinin[22,46] suggests that these organisms utilize a similar mechanism as PCP. Therefore, the light-harvesting strategy employing a charge-transfer state is likely to play a significant role in the total photosynthetic production on Earth, because carbonyl carotenoids, such as peridinin, fucoxanthin, siphonaxanthin, or prasinoxanthin, occur in various taxonomic groups of oceanic photosynthetic organisms, which contribute a substantial part of Earth's photosynthetic CO_2 fixation.[104] This light-harvesting strategy may be an inevitable correlate of using oxygenated carotenoids and the local protein environment to extend absorption to longer wavelengths in the green region of the visible spectrum. This may be essential for oceanic photosynthetic organisms, since the water column represents a filter for the red part of the visible light and the blue part of the spectrum is most efficiently scattered. Consequently, the photons having energy corresponding to the green light penetrate deepest in water, and it is thus vitally important for underwater photosynthetic organisms to utilize green light with highest possible efficiency. This is smartly achieved by employing carbonyl carotenoids, because their narrow S_2−S_1/ICT energy gap offers a possibility to capture efficiently green light that is not accessible by Chls while keeping the energy of the S_1/ICT state high enough to enable efficient energy transfer to the Q_y state of Chl. The less efficient S_2 channel caused by the short intrinsic S_2 lifetime resulting from the narrow S_2−S_1/ICT energy gap is compensated by high efficiency of the S_1/ICT state energy-transfer channel that is maintained by charge-transfer character of the S_1/ICT state.

4.4. Other Biological Systems Containing Carotenoids

Although carotenoids are vastly distributed in various tissues in both plant and animal kingdoms,

their spectroscopic properties are, besides the cases described in the previous sections, known only for a few additional carotenoid-binding proteins. The lack of information for the others is usually caused by an absence of structural information about these systems. Therefore, the exact localization of carotenoids in a particular tissue is unclear, making investigations of carotenoid spectroscopic properties and their relation to carotenoid functions rather complicated. Also, for carotenoid-containing systems outside photosynthesis, molecular actions of carotenoids are probably not triggered by light, and thus excited states of carotenoids are therefore not directly involved in the carotenoid function. Nevertheless, even for these systems exploration of carotenoid excited states holds promise to uncover the nature of their interactions with the surroundings which could be of vital importance for the various roles played by carotenoids in these systems.

4.4.1. Carotenoids in Other Light-Harvesting Complexes

Besides the light-harvesting complexes described in the previous sections, structural knowledge is also available for the core complex of Photosystem I (PSI-core). The 4 Å structure of the PSI-core from the cyanobacterium *Synechococcus elongatus*[251,252] was recently refined to 2.5 Å resolution.[253] This high-resolution structure revealed an aggregate of 96 Chl molecules including the reaction center special pair P700 and 22 β-carotene molecules, 17 of them in the *all-trans* configuration while the remaining five exhibited a *cis*-configuration containing either one or two *cis*-bonds. The carotenoids are grouped into six separate clusters, and all of them are in van der Waals contact with Chl-a molecules, thus providing a good basis for efficient carotenoid−Chl energy transfer.[253] Most of the experimental efforts aiming to reveal energy-transfer dynamics within the PSI-core were directed to the energy transfer and trapping among Chl-a molecules (reviewed by Gobets et al.[254]); the high-resolution structure also promoted theoretical modeling of these processes.[255−257] On the contrary, much less is known about energy transfer between carotenoids and Chl-a. The efficiency of β-carotene to Chl-a energy transfer is in the range observed also for other light-harvesting complexes, yielding a value of 85−90%.[258,259] A fluorescence up-conversion study of the PSI-core rationalized this high efficiency in terms of possible energy-transfer pathways.[259] Fast depopulation of the S_2 state characterized by a time constant of 105 fs proved that S_2-mediated energy transfer operates with substantial efficiency. By comparing the rise of Chl-a excited state after excitation of either the Soret band of Chl-a at 400 nm or β-carotene at 510 nm, an additional 1.2 ps component was revealed when β-carotene was excited selectively. This component was assigned to the energy transfer via the S_1 state of β-carotene, and from comparison with the 9 ps S_1 lifetime of β-carotene in solution,[100,101] the S_1 channel must be very efficient.[259] A subsequent transient absorption study employing 60 fs excitation pulses refined the β-carotene S_2 lifetime to ~60 fs, making the S_2-mediated channel the dominant carotenoid−Chl transfer pathway in the PSI-core, accounting for about 60% of the total 70% efficiency.[260] In agreement with the previous fluorescence up-conversion study,[259] a 3 ps component was attributed to the energy transfer via the S_1 state of β-carotene and was suggested to be responsible for the residual 10% of the total carotenoid−Chl energy-transfer efficiency. The active S_1 channel might seem surprising at first glance, as the S_1 energy of β-carotene in solution is around 14 200 cm^{-1} (Table 1), but the presence of 'red' chlorophylls in PSI absorbing above 700 nm[254] still allows a substantial spectral overlap with the hypothetical S_1 emission of β-carotene. It is thus quite likely that the 'red' chlorophylls provide acceptor states for the S_1-mediated energy transfer.[260] It is also important to realize that the observed time constants for the S_2 and S_1 channels represent an average rate of all 22 β-carotenes in the PSI-core, and the efficiencies and pathways of the particular β-carotene molecules will probably differ substantially, especially because only a fraction of them can occur in the proximity of the 'red' chlorophylls, if these are assumed to be the most likely energy acceptors.

In higher plants, PSI also contains an antenna system called LHCI that is attached to the PSI-core, forming a bigger complex usually denoted PSI-200.[254,261] The LHCI complex exhibits a high sequence homology with LHCII, suggesting that they may be structurally closely related.[261] LHCI binds both Chl-a and Chl-b and the carotenoids lutein and violaxanthin, but in contrast to the LHCII, a small amount of β-carotene is present while neoxanthin was not detected.[261−263] Energy transfer between carotenoids and Chl in isolated LHCI complexes was studied using fluorescence up-conversion and a streak camera, detecting Chl-a fluorescence after excitation in the spectral region corresponding to absorption bands of carotenoids.[264] Contrary to the PSI-core,[259] no evidence for an S_1 channel was found; only S_2-mediated energy transfer functioned in LHCI, as evidenced by carotenoid S_2 emission decaying faster (~140 fs) than in solution. Despite the absence of a slower component attributable to the S_1 channel of energy transfer, it was hypothesized that the S_1 pathway might still be operating, because the observed S_2 lifetime could not account for the observed high (80%) overall efficiency.[264] Since LHCI also accommodates the 'red' chlorophylls capable of accepting energy from the S_1 state of carotenoids, the existence of the S_1-mediated energy transfer in LHCI complexes could be anticipated. To prove or rule out this hypothesis, transient absorption studies of both wild-type LHCI complexes and their reconstituted counterparts that are now available[261,262] will be needed, because time-resolved emission cannot follow the carotenoid S_1 dynamics directly.

Carotenoids are also present in the PSII core antenna complexes CP43 and CP47. The carotenoid composition differs slightly in these two complexes, but for both, the dominant carotenoid is β-carotene and a small amount of lutein can be also bound to these complexes.[182] Fluorescence excitation spectra of CP47 suggested a rather low efficiency of carotenoid−Chl energy transfer of ~35%.[265] This low efficiency would suggest that the S_1 channel is likely

inactive in these complexes, since the Q_y states of Chl-a in these complexes are higher than in PSI-core and LHCI, preventing the S_1-mediated carotenoid−Chl energy transfer. This proposal, which was recently confirmed by time-resolved experiments, demonstrates that the S_2 channel operates efficiently and pushes the S_2 lifetime to ~80 fs in CP43 and CP47. On the other hand, no components attributable to energy transfer via the β-carotene S_1 state were found, although the possibility of a minor transfer channel via hot vibrational states of the S_1 state could not be ruled out.[266]

Carotenoids are also known to serve as energy donors in chlorosomes that are specialized antenna complexes formed exclusively by green phototrophic bacteria. They contain a large number of BChl-c, -d, or -e molecules organized in a self-aggregated rodlike structure nearly lacking protein.[267] In addition, they also contain various carotenoids whose structure and stoichiometric ratio depend on species and growing conditions.[268,269] However, exact location and function of the carotenoids in chlorosomes is still unclear. Until recently, the light-harvesting capabilities of carotenoids in chlorosomes were studied only by means of fluorescence excitation spectra. An efficiency of nearly 60% was estimated for energy transfer between carotenoids (mostly β-carotene and γ-carotene) and BChl-c in *Chloroflexus aurantiacus* at 4 K.[270] A slightly higher efficiency in the range 50−80% was found for chlorosomes from the same organism at room temperature and also in chlorosomes from *Chlorobium tepidum* containing the carotenoid chlorobactene.[271] On the other hand, for *Chlorobium phaeovibrioides* whose chlorosomes accommodate the carotenoid isorenieratene, the estimated carotenoid−BChl energy-transfer efficiency was nearly 100%.[272] A more detailed study involving time-resolved techniques is thus far available only for chlorosomes from *Chlorobium phaeobacterioides*.[273] Utilizing fluorescence excitation spectra, single-photon counting, and femtosecond transient absorption measurements in combination with comparison of wild-type and carotenoidless chlorosomes allowed construction of a better picture of energy transfer between carotenoids (mainly isorenieratene and β-isorenieratene) and BChl. The overall energy-transfer efficiency was in the range 60−70%, thus comparable with previous studies on other species. The S_2 lifetime of isorenieratene in chlorosomes was as short as 50 fs, while the time constant corresponding to the S_1 decay was ~10 ps. Because both isorenieratene and β-isorenieratene have conjugated systems similar to β-carotene (they differ in the structure of terminal rings), one should also expect similar excited-state lifetimes. Consequently, the observed lifetimes of S_2 and S_1 states suggested that the S_2 channel represents by far the dominating energy-transfer pathway, while the S_1 energy transfer is probably completely absent.[273]

Very little is known about energy-transfer capabilities of carotenoids in other light-harvesting systems. Fluorescence excitation spectra of FMO-reaction center core complex from *Chlorobium tepidum* revealed carotenoid to BChl-a energy-transfer efficiency of 23% at 6 K.[274] Carotenoids are also present in antenna reaction center (ARC) complexes of heliobacteria.[275] This youngest family of photosynthetic bacteria discovered in 1983 by Gest and Favinger[276] contains previously unknown BChl species called Bchl-g and the carotenoid 4,4′-diaponeurosporene. Although nothing is known about location, functions, and energy-transfer ability of this carotenoid to date, its presence underlines the unique pigment composition of ARC from heliobacteria, because 4,4′-diaponeurosporene contains only 30 carbon atoms instead of the 40 that normally build the skeleton of a carotenoid molecule.[277]

4.4.2. Other Carotenoid-Binding Proteins of Plants and Cyanobacteria

Besides light-harvesting proteins and reaction centers, carotenoids have also been found in other proteins from higher plants and algae. Two of them deserve attention since they are proposed to play important roles in photoprotection and, consequently, the dynamics of their excited states may be directly related to their functions. The first of these proteins is a small protein called PsbS, which is a member of LHC protein family that was shown to be essential for regulation of photosynthetic light harvesting. This protein was found to be necessary for the nonphotochemical quenching in higher plants, while light-harvesting capacity was not affected by the presence of PsbS.[221] Although it was initially suggested that PsbS binds both Chl and carotenoids,[278] later it was shown that recombinant PsbS did not bind any pigments, suggesting that if PsbS were to bind pigments in its natural form, the binding mechanisms must be different from other proteins from LHC the family.[279] Indeed, it was recently shown that the isolated PsbS protein is able to bind exogenous zeaxanthin, leading to the formation of a zeaxanthin−PsbS complex, causing a new, red-shifted absorption band of zeaxanthin located at around 535 nm.[225] Interestingly, absorbance changes at 535 nm were earlier associated with activation of nonphotochemical quenching in higher plants[195] and the particular absorbance change was, on the basis of resonance Raman spectroscopy, associated with a change of a zeaxanthin molecule.[280] Thus, the binding of zeaxanthin to PsbS was described as an activation of zeaxanthin that is a necessary condition for efficient energy dissipation in light-harvesting complexes.[225] As described in section 4.2, the presence of PsbS was correlated to a direct population of the S_1 state of zeaxanthin after excitation of either Chl-a or Chl-b for intact thylakoids of *A. thaliana*.[220] Since the transient absorption spectrum of the zeaxanthin S_1 state populated in this experiment differed from that observed for zeaxanthin in solution or LHCII complexes,[198] it is possible that the zeaxanthin−PsbS complex is directly involved in quenching of Chl excited states.

Another interesting carotenoid-binding protein is a water-soluble orange carotenoid protein (OCP) isolated from certain species of cyanobacteria.[281,282] The structure of the OCP from cyanobacterium *Arthrospira maxima* was recently determined with

2.1 Å resolution.[283] The high-resolution structure revealed that OCP forms a homodimer with one carotenoid, 3-hydroxyechinenone, per monomer. This carotenoid belongs to the family of carotenoids possessing a conjugated carbonyl group, and its carbonyl group is located at the end of the conjugated chain consisting of 11 C=C bonds. Hydrogen bonding between 3-hydroxyechinenone and tyrosine and tryptophan residues via the conjugated carbonyl group was inferred from the structure. Interestingly, the binding site of 3-hydroxyechinenone in OCP is lined by a large number of methionine residues.[283] Although the exact function remains unknown, increasing OCP levels during exposure to intense light suggested its possible involvement in photoprotection.[283] Various hypotheses for the OCP function were suggested, ranging from a carotenoid transport protein[281] to involvement in effective singlet oxygen quenching.[283] OCP can be also converted to another form called RCP, which is characterized by a red-shifted absorption spectrum. The OCP to RCP conversion is achieved either by proteolysis and caused by exposure of a part of 3-hydroxyechinenone to solvent or by acidification of OCP to approximately pH 3.5.[283]

Preliminary results on excited-state dynamics of 3-hydroxyechinenone in OCP revealed a significant effect of protein environment on excited-state dynamics of 3-hydroxyechinenone.[284] Absorption spectra of 3-hydroxyechinenone in *n*-hexane and methanol display a 0−0 origin of the S_2 state at ∼475 nm; this is shifted to ∼495 nm in OCP. Interestingly, the vibrational structure of the S_2 state is better resolved in OCP, suggesting that confinement of 3-hydroxyechinenone in the protein prevents the wider distribution of conformers. In solution, the S_1 lifetime of 3-hydroxyechinone is ∼6 ps in methanol, *n*-hexane, and CS_2 (Table 3), suggesting that neither polarity nor polarizability affects S_1 lifetime. This suggests that the location of the carbonyl group at one end of the long conjugated backbone of 3-hydroxyechinenone minimizes the polarity-induced effects, although the typical asymmetric broadening of the absorption spectrum is still present. While the S_1 lifetime is the same in all solvents used, it is significantly shortened to 2.6 ps in OCP, demonstrating a dramatic effect of protein environment on the S_1 lifetime. The large protein-induced change is further emphasized in transient absorption spectra. While in solution the S_1-S_N band of hydroxyechinenone peaks at 570 nm in both *n*-hexane and methanol, this band is shifted to nearly 650 nm in OCP, making the protein-induced shift of the S_1-S_N band in OCP the largest observed so far.[284] This large shift may be partially due to the presence of the methionine residues in the binding pocket, which creates a polarizable medium that could cause a substantial shift of both S_0-S_2 and S_1-S_N transitions. A deeper understanding of these effects awaits future investigations.

To complete the list of carotenoid-binding proteins related to photosynthesis, it is necessary to mention the presence of carotenoids in reaction centers. Carotenoids have two main roles in reaction centers. First, they quench triplet states of Chl by triplet−triplet energy transfer to prevent interaction of Chl triplets with molecular oxygen, leading to formation of singlet oxygen.[285] This function is not limited to reaction centers and is also active in antenna complexes where the same carotenoid molecule can perform the light harvesting and triplet quenching as they are well separated in time.[106,156,170,211,212] Second, carotenoids serve as alternative electron donors in the PSII reaction center under conditions when the primary electron-donation pathway is blocked.[286−289] Both these processes do not involve singlet excited states (although formation of both carotenoid triplets and radicals directly from the singlet states was actually observed (see section 3.5), but no evidence for such a process in reaction centers was found) and occur on a time scale much slower (microseconds to milliseconds) than the dynamics of singlet excited states of carotenoids. Therefore, we limit ourselves to underlining their importance for proper functioning of reaction centers (but see Note Added in Proof), while detailed description of these processes can be found in the aforementioned references.

4.4.3. Animal Carotenoid-Binding Proteins

Animals, including humans, have a large number of carotenoids in various tissues. Since animals cannot synthesize carotenoids de novo, they are acquired from exogenous sources, and some of them are incorporated into proteins, whose functions are much less understood than in plants. Studies of spectroscopic properties of carotenoid-binding proteins from animals are limited to two systems. The first protein is the xanthophyll-binding protein (XBP) isolated from human macula and retina.[290] It has been known for a long time that the yellow spot (macula lutea) of the human retina contains large amounts of the two xanthophylls, lutein and zeaxanthin.[291,292] About 50% of the total amount of the xanthophylls in the retina is concentrated in the macula, where zeaxanthin dominates over lutein by a ratio of 2:1.[292] At the center of the macula (the fovea), the zeaxanthin is actually a 50:50 mixture of zeaxanthin and its stereoisomer *meso*-zeaxanthin (Figure 20), which is

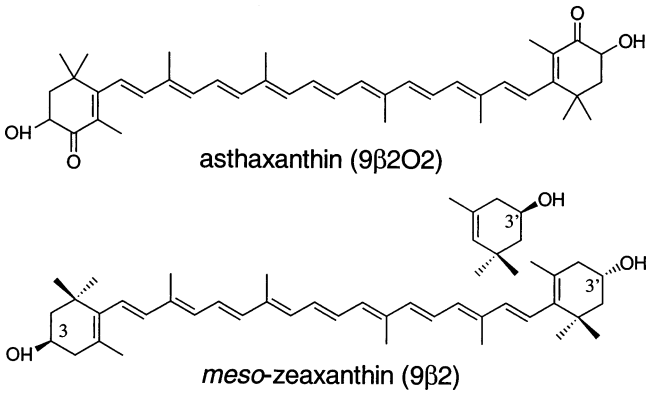

Figure 20. Molecular structures of two carotenoids occurring in animal carotenoid-binding proteins. To visualize the difference between *meso*-zeaxanthin and zeaxanthin, the terminal β-ring of zeaxanthin is also shown for comparison. While the hydroxyl group of zeaxanthin is located in the 3′R position, for *meso*-zeaxanthin this hydroxyl group is oriented in the 3′S position. At the opposite side of the molecule at the 3 position, the hydroxyl group is in the 3R position for both zeaxanthin and *meso*-zeaxanthin.

presumably a metabolite of lutein or zeaxanthin since *meso*-zeaxanthin is not synthesized by plants and cannot be thus acquired from exogenous sources.[291] The concentration of xanthophylls increases progressively toward the center of the macula, and in the fovea, the concentrations of these xanthophylls are ~1000-fold higher than in other human tissues.[7] In the peripheral part of the retina, the concentration of carotenoids is lower and lutein dominates over zeaxanthin by a ratio of 2:1.[7] It was recently proposed that carotenoids in human retina are bound to a specific protein, called XBP.[290] Transient absorption spectroscopy was employed to study dynamics of the S_1 state of the carotenoids in both carotenoid-enriched and native XBP.[293] The results from the native XBP and the enriched XBP were then compared to those for carotenoids in organic solvents and in detergent micelles. Both steady-state and transient absorption spectra show that the incorporation of xanthophylls into the protein causes a red shift of the spectra, which is stronger for lutein than for zeaxanthin. The S_1-S_N spectra of the native XBP protein confirmed the presence of both xanthophylls in native XBP as they clearly consisted of contributions from lutein and (meso)zeaxanthin. While the S_1 lifetime of lutein does not exhibit any changes when measured in solution, micelles, or XBP, the S_1 lifetime of *meso*-zeaxanthin changed from 9 ps in solution to 12 ps in XBP. The most pronounced effect was found for vibrational relaxation in the S_1 state, which is significantly slower for xanthophylls in XBP compared to micelles and solution. This effect was most pronounced for *meso*-zeaxanthin and was attributed to a specific carotenoid-binding site in XBP, confirming the importance of this zeaxanthin stereoisomer in the human eye.[293] Although the time-resolved experiments provided strong support for specific binding of carotenoids in XBP, the physiological functions of XBP still remain to be clarified. In view of the probable photoprotective role of carotenoids against degenerative eye diseases, this protein may play a central role in this function.

The second animal carotenoid-binding protein studied by spectroscopic methods is the astaxanthin-binding protein, β-crustacyanin, responsible for the color of lobster shells. Its crystal structure was recently resolved with 3.2 Å resolution, and the whole pigment−protein complex was found to consist of eight β-crustacyanin units, each of which binds two astaxanthin molecules in a dimer consisting of two basic building blocks called α-crustacyanin.[294] The intriguing feature of β-crustacyanin is a large red shift of the absorption spectrum of astaxanthin, from 472 nm in solution to 630 nm in the protein.[295] With the help of the structural data, this large spectral shift of the absorption spectrum was explained in terms of a specific interaction of astaxanthin with the protein. The carotenoid astaxanthin possesses two carbonyl groups located symmetrically at terminal rings involved in conjugation (Figure 20). In the protein, hydrogen bonding via these two carbonyl groups together with protein-induced coplanarization of the terminal rings with the conjugated backbone leads to significant perturbation of the central part of the conjugated chain and consequently to a red shift.[294,295] No time-resolved studies of either β-crustacyanin or astaxanthin have been reported so far, but the availability of the high-resolution structure of β-crustacyanin and quantum chemical calculations on astaxanthin[296,297] provides a good platform for investigations of dynamical properties of astaxanthin excited states. Such work can extend our knowledge of coloration mechanisms of crustaceans and can serve as an interesting model system for investigations of interactions between carotenoids and proteins.

5. Carotenoids in Artificial Systems

The capability of carotenoids to serve as light-harvesting agents in photosynthetic antenna complexes on the one side and their potential to play a role of electron donors in some photosynthetic reaction centers on the other side encouraged a number of investigations of carotenoids in artificial systems aiming to mimic either antenna complexes or reaction centers. Construction of carotenoporphyrin (CarP) dyads in the early 1980s, in which a carotenoid molecule is covalently linked to a porphyrin molecule, demonstrated the possibility of carotenoids playing both antenna (singlet−singlet energy transfer from carotenoid to porphyrin) and photoprotective (quenching of porphyrin triplets) functions in such a system.[298] Later, extension of these dyads to triads containing an additional electron acceptor (quinone) capable of taking one electron from a porphyrin led to a successful mimicking of an electron-transfer chain.[299] In the triad, excitation of the porphyrin promoted electron transfer from the excited porphyrin to the quinone (Q) and the oxidized porphyrin was consequently reduced by electron transfer from a carotenoid molecule, producing a charge-separated state Car^+PQ^-. These carotenoid-based triads or even pentads[300] were proven to be excellent models for an artificial reaction center, and various modifications of these systems have been the subject of a number of investigations during the last 20 years.[301−312] The modifications were done either in the central porphyrin site that was replaced by pyropheophorbide[305] or in the choice of the final electron acceptor as imide[307−309,312] or fullerene[301,303,304,306] used instead of quinone. Electron-transfer processes in these molecules were also studied theoretically,[313] and the functionality of the carotenoid-based triads was demonstrated by their incorporation into a lipid membrane. The CarPQ triads were able to carry out light-driven generation of a proton gradient across the membrane,[310] light-driven ATP synthesis,[311] or light-driven active transport of Ca^{2+} ions.[302] Since the electron-transfer reactions in these triads do not involve singlet excited states of carotenoids, the photochemistry of these supramolecular systems will not be described here, and a detailed account on the dynamics of the electron-transfer steps can be found in the references above. Nevertheless, it was demonstrated that direct excitation of the carotenoid moiety in these molecules resulted in carotenoid−porphyrin energy transfer.

5.1. Energy Transfer in Carotenoid-Based Artificial Antennae

Energy transfer was studied especially for carotenoporphyrin dyads. In the pioneering study of carotenoporphyrin dyads by Bensasson et al.,[298] the importance of the mutual orientation of carotenoid and porphyrin for efficient energy transfer was clearly demonstrated. While for a linear arrangement the energy-transfer efficiency was negligible, a folded arrangement in which the carotenoid molecule bends over the porphyrin heterocycle allowing a close contact between the conjugated systems of both chromophores resulted in a carotenoid-to-porphyrin energy-transfer efficiency of 25%.[298] Later, measurements of energy transfer in a dyad consisting of a carotenoid with conjugation length of 11 and a free-base porphyrin yielded an efficiency of 30−35%, and it was concluded that the energy-transfer route utilizes the S_1 state of the carotenoid.[307] This result was further supported by employing a zinc−porphyrin with a higher acceptor state, where no carotenoid−porphyrin energy transfer was observed.[308] Similar results were obtained for carotenoid−pyropheophorbide dyads containing fucoxanthin as energy donor. On the basis of fluorescence excitation spectra it was concluded that the energy-transfer efficiency is in the range 28−42% depending on the substituents on the pyropheophorbide moiety.[222] Due to the known energetics of the donor and acceptor states (the S_1 energy of fucoxanthin was known from measurements of S_1 emission, see Table 1), the S_1-mediated energy transfer was suggested as the dominant route. However, energy-transfer efficiencies of 8−15% were also obtained when zeaxanthin was attached to the pyropheophorbide moiety, although the S_1 state of zeaxanthin was supposed to be lower than the acceptor state, suggesting the possibility of an active S_2-route. This hypothesis was confirmed later using femtosecond transient absorption spectroscopy. Debreczeny et al.[314] reported energy transfer via the S_1 state of fucoxanthin in a series of carotenoid−pyropheophorbide dyads yielding an efficiency of 12−44%. The S_1 lifetime of fucoxanthin, measured by the decay of the S_1-S_N absorption, was 67 ps without the presence of the pyropheophorbide moiety, and it was shortened to 38 ps when covalently linked to the pyropheophorbide acceptor, signaling energy transfer via the S_1 state. The S_1-mediated energy transfer was further confirmed by measurements of the rise of pyropheophorbide bleaching at 682 nm perfectly matching the decay of the fucoxanthin S_1 state. The shortening of the carotenoid S_1 lifetime from 67 to 38 ps represented the best case of five different pyropheophorbide acceptors, corresponding to an efficiency of 44% and a S_1-mediated energy-transfer rate of $(86\ \text{ps})^{-1}$.[314] When fucoxanthin was replaced by zeaxanthin, attachment of the carotenoid to the pyropheophorbide moiety did not affect the S_1 lifetime of zeaxanthin, showing that no energy transfer via the S_1 state of zeaxanthin took place. Nevertheless, in accord with the previous study,[222] energy transfer utilizing the S_2 route was observed for the zeaxanthin−pyropheophorbide dyad as a shortening of the S_1-S_N absorption rise time, reflecting the S_2-S_1 relaxation of zeaxanthin. While no changes of the rise time were detected in the case of fucoxanthin, it changed from 203 to 184 fs in going from zeaxanthin to the zeaxanthin−pyropheophorbide dyad, indicating competition of the S_2-S_1 relaxation with the S_2-mediated energy transfer in the dyad. The efficiency of the S_2 pathway was 4−15% depending on the type of pyropheophorbide acceptor, and on the basis of some calculations, the Q_y state of pyropheophorbide was suggested as the energy acceptor.[314]

The S_1 pathway was also observed in similar dyads containing pyropheophorbide as acceptor and either fucoxanthin or peridinin as energy donors.[315] Since the S_1 energies of both these carotenoids are well above the Q_y state of pheophorbide (Table 1), the S_1-mediated energy transfer occurred with efficiencies of 24% and 54% for fucoxanthin and peridinin, respectively. The higher efficiency for the peridinin−pyropheophorbide dyad was rationalized in terms of a longer S_1 lifetime of peridinin.[315] Since the charge-transfer character and corresponding strong dependence of the lowest peridinin excited state on solvent polarity (see section 3.2) was discovered later, we can now see that the mildly polar solvent toluene used in this study indeed justifies this conclusion. A subsequent study of these dyads in different solvents showed that in the polar solvent ethanol the energy-transfer efficiency dropped significantly for the peridinin−pyropheophorbide dyad,[316] and it was hypothesized that in polar solvents the dyad took a different conformation that was not favorable for efficient energy transfer. In light of the current knowledge of peridinin excited-state dynamics (see section 3.2), it is also possible that the decrease of energy-transfer efficiency instead reflected the shortening of the S_1/ICT lifetime of peridinin in polar solvents, making the energy transfer less competitive with S_1/ICT internal conversion.

The opposite situation, when solely the S_2 pathway is active in energy transfer, was observed recently for a dyad consisting of a modified β-carotene covalently linked to a purpurin.[317] Experiments employing fluorescence up-conversion revealed S_2 lifetimes of 150 and 40 fs for the carotenoid model and the carotenopurpurin dyad, respectively. This shortening of the S_2 lifetime yielded an efficiency of 73% for S_2-mediated energy transfer, higher than that for most of the natural photosynthetic light-harvesting antennae. On the other hand, no change of the carotenoid S_1 lifetime was observed in the carotenopurpurin dyad, signaling the absence of the S_1 route in this dyad.[317] This result, together with those for the dyads described in the previous paragraph, mimic nicely the energy-transfer pathways in natural systems, where light-harvesting complexes such as LHCII accommodating non-carbonyl carotenoids mainly utilize the S_2-mediated transfer but antennae employing carbonyl carotenoids such as peridinin or fucoxanthin employ predominantly the S_1 route (see section 4).

Recently, another type of artificial antenna complex based on carotenoids was reported. Two 8′-apo-β-carotene molecules were linked as axial ligands to a

phthalocyanine derivative via its central silicon atom.[318] Fluorescence excitation spectra revealed an overall carotenoid−phthalocyanine energy-transfer efficiency exceeding 95%, and contrary to the dyads discussed above, both S_1 and S_2 pathways operate with a substantial efficiency. Using fluorescence up-conversion, the efficiency of the S_2-mediated pathway was found to be 35% since the S_2 lifetime decreased from 82 fs for the carotenoid alone to 53 fs for the carotenoids linked to the Si−phthalocyanine. The S_1 route was explored by monitoring the rise of Si−phthalocyanine emission in the 670−690 nm spectral region. A 2.6 ps rise component was ascribed to energy transfer via the S_1 state of the carotenoid. Given the S_1 lifetime of the 8′-apo-β-carotene of 24 ps in solution (see also Table 2), the efficiency of this energy-transfer channel was concluded to be 90%, contributing 58% to the total energy-transfer efficiency in this system.[318] Later, the relaxation pathways disclosed by fluorescence up-conversion were further verified by transient absorption measurements of this antenna system. In the transient absorption study, the artificial antenna system containing 8′-apo-β-carotene ($N = 9$) described above was compared to another system in which two 6′-apo-β-carotene ($N = 10$) molecules were attached to Si−phthalocyanine.[114] The S_2 lifetimes were shortened from 73 ($N = 9$) and 66 fs ($N = 10$) in solution to 55 fs in the triad, resulting in ∼30% efficiency of the S_2 energy-transfer channel for both systems. On the other hand, the energy transfer via the S_1 state is strikingly different. While for the triad containing the shorter carotenoid the S_1 lifetime is 4 ps, thus markedly shorter than 25 ps observed in *n*-hexane solution, only a small change of the S_1 lifetime, from 11.5 ps in *n*-hexane to 8.8 ps in the triad, was revealed for the longer carotenoid. The resulting efficiencies of the S_1-mediated energy transfer yield 84% and 23% for the triads containing carotenoid with $N = 9$ and 10, respectively. The dramatic difference between S_1-mediated energy-transfer efficiency explains the large discrepancy between total energy-transfer efficiencies of 92% and 30% that were calculated from fluorescence excitation spectra of both triads. Thus, the transient absorption measurements confirmed the energy-transfer scheme constructed on the basis of fluorescence up-conversion. In addition, however, it also revealed an additional feature that could not be detected by the fluorescence up-conversion technique. By analysis of the transient absorption spectra in the visible region, Kodis et al. have shown that the recently discovered S* state (see section 3.3) is populated when a carotenoid is attached to Si−phthalocyanine.[114] While no S* state was detected for both carotenoids in *n*-hexane solution, the presence of the S* state was unequivocally demonstrated for both triads. While the spectral position of the band corresponding to the S* ESA is different for the two triads (506 nm for $N = 9$, 525 nm for $N = 10$), dynamics of the S* state is virtually identical in both systems. About 20% of the initially excited S_2 population goes to the S*, whose lifetime is 26 ps, independent of the triad. Nevertheless, an important difference was found when probing energy transfer via formation of the Si−phthalocyanine bleaching at 690 nm. While for the longer carotenoid no rise component matching the S* lifetime was found, in the case of the carotenoid with $N = 9$, a clear rise component having a time constant of 26 ps was detected. Thus, for the triad with the shorter carotenoid the S* state also represents an energy donor, while in the other case the S* state exhibits only one relaxation pathway toward the ground state. As pointed out by Kodis et al.,[114] this situation resembles well the behavior of spheroidene ($N = 10$) and spirilloxanthin ($N = 13$) in LH2 complexes, where the former is capable of transfering energy via the S* state while the latter is inactive.[111−113] The appearance of the S* state in artificial and natural antenna complexes is also worth comparison. Since for spheroidene and both carotenoids used in the triads there was no signature of the S* state when carotenoids are dissolved in solution, in both LH2 and artificial antenna it is the interaction with environment that directs the S_2 population toward the S* state. It was suggested that the S* state is stabilized due to a strong electronic coupling to nearby pigments, since such a situation occurs in both LH2, where carotenoid and Bchl molecules are very close, and in the artificial system where the coupling is achieved by covalent bonding of carotenoid to the Si−phthalocyanin.[114] Contrary to LH2, in which the S* state is also an efficient precursor of ultrafast triplet formation,[20,111−113] no triplet formation from the S* state was observed for artificial systems.[114] This observation is in a good agreement with the hypothesis that deviation of carotenoid from a planar *all-trans* conformation caused by protein environment is an important factor governing the S* to triplet conversion,[112] as no such deformation of a carotenoid molecule occurs in the artificial triads.

In addition to the very efficient energy transfer, a significant quenching of the Si−phthalocyanine excited state was observed for both triads when they were dissolved in polar solvents. After excitation of Si−phthalocyanine at 680 nm, the Si−phthalocyanine excited-state decayed with a time constant of 6 ps in tetrahydrofuran,[318] and an even shorter lifetime of 2.5 ps was found when dissolved in benzonitrile,[114] although a nanosecond lifetime was observed in toluene.[318] The quenching was ascribed to the formation of a charge-separated state that in a polar solvent is low enough to quench the Si−phthalocyanine excited state. This hypothesis was further confirmed by observation of the carotenoid radical in the near-infrared region, whose formation time matched the decay of Si−phthalocyanine excited state.[114,318] The charge-separated state, which is formed with an efficiency of nearly 100%, has a very short lifetime, recombining back to the ground state with a time constant of 25 (triad with $N = 9$ in tetrahydrofuran),[318] 10.5 (triad with $N = 9$ in benzonitrile),[114] and 17 ps (triad with $N = 10$ in benzonitrile).[114] A similar ultrafast formation of a short-lived carotenoid radical was recently observed also in light-harvesting complexes of purple bacteria (section 4.1 and Figure 14).[92] Although the detailed mechanisms behind the ultrafast electron-transfer

reactions in light-harvesting antennae are still unknown, these results demonstrate the potential importance of the carotenoid radical formation in these systems, since electron-transfer quenching was suggested to be one of the possible photoprotective mechanisms leading to the dissipation of excess energy in photosynthetic organisms.[226−230]

5.2. Ultrafast Electron Transfer at a Carotenoid–Semiconductor Interface

Besides artificial reaction centers and light-harvesting antennae, carotenoids were also investigated as prospective sensitizers for the so-called Grätzel solar cells. The heart of the Grätzel cell is a dye−semiconductor interface in which the semiconductor is represented predominantly by TiO_2 nanoparticles while a large number of various dyes were investigated as potential sensitizers. Excitation of the dye promotes ultrafast electron injection into the conduction band of TiO_2. After being injected, the electron is further transported through the spongelike network of TiO_2 nanoparticles into an outer electrical circuit to perform work.[319]

The sensitizer is usually attached to the surface of the TiO_2 nanoparticles via a carboxylic group, which is not present in naturally occurring carotenoids. Therefore, various chemically prepared carotenoic acids were used as sensitizers. The feasibility of attachment of a carotenoid to the surface of the TiO_2 semiconductor was first demonstrated for *all-trans*-retinoic acid (ATRA), a short carotenoid-like molecule having a backbone consisting of five C=C bonds terminated by carboxylic group.[320] Excitation of a colloidal solution of ATRA−TiO_2 system at 355 nm produced a new, long-lived (up to 10 ns) spectral band in the transient absorption spectrum centered at 600 nm. This band was formed within the first 200 ps and ascribed to the ATRA radical cation resulting from efficient electron injection from the S_1 state of ATRA. Formation of the carotenoid cation radical as a result of electron injection was further confirmed for a few different carotenoids attached to TiO_2 nanoparticles by means of EPR spectroscopy.[321]

A functional solar cell consisting of the ITO working electrode coated with TiO_2 film sensitized by 8′-apo-β-caroten-8′-oic acid (ACOA) was recently constructed.[322] The absorption spectrum of ACOA attached to the TiO_2 surface was substantially blue shifted as compared to solution, suggesting partial aggregation of ACOA on the surface.[323] At the absorption maximum (426 nm), incident photon-to-photocurrent conversion efficiency (IPCE) reached 34%, further confirming the ability of carotenoids to act as sensitizers in Grätzel-type solar cells. Similarly, Langmuir−Blodgett films of carotenoids deposited directly on ITO electrodes were also proven to generate photocurrents on the order of a few nA/cm^{-2}.[324,325]

Deeper insight into the electron-transfer processes at the carotenoid−TiO_2 interface was obtained by time-resolved spectroscopy measurements applied to a system consisting of TiO_2 nanoparticles sensitized by ACOA in a colloidal solution.[326] The concentrations of TiO_2 and ACOA were set to ensure a ratio of less than one ACOA molecule per particle to avoid aggregation of ACOA molecules at the surface. Excitation of the attached ACOA molecule into its S_2 state resulted in ultrafast formation of the ACOA radical cation formed as a product of electron injection into the TiO_2 conduction band. On the basis of kinetics recorded at various wavelengths corresponding to formation of the ACOA radical cation, ACOA bleaching, and the S_1-S_N transition, it was concluded that the radical cation is formed directly from the S_2 state with an efficiency of ~40%. The remaining 60% underwent internal conversion to the S_1 state. Interestingly, however, although the S_1 state was thermodynamically favorable for donating electrons to the TiO_2 conduction band, no electron injection from the S_1 state was observed, as confirmed by the same S_1 lifetime of ACOA both in solution and attached to TiO_2.[326] The formed radical cation was stable, decaying by electron recombination on a broad range of time scales extending from nanoseconds to milliseconds, thus rationalizing the relatively high IPCE observed earlier.[322] Interestingly, two channels of electron recombination forming either ACOA ground state or ACOA triplet state were detected. Such ambivalent electron recombination was also observed for other electron-transfer systems containing carotenoids,[303,327−329] and it was explained by the fact that electron recombination to the ground state involved a higher driving force in the Marcus inverted region, making the recombination to form the carotenoid triplet state kinetically more favorable.[303,326] An analogous injection−recombination scheme was recently concluded on the basis of femtosecond transient absorption spectroscopy of ATRA attached to TiO_2 nanoparticles in colloidal solution,[330] despite large differences between excited-state properties of ACOA and ATRA. Electron injection from the initially excited state of ATRA occurs with a time constant of 350 fs, while no S_1 injection from the S_1 state of ATRA was detected, although a slower, 1.8 ps injection was hypothesized to occur from a $^1n\pi^*$ state occurring below the absorbing S_2 state.[330] Contrary to ACOA, however, the ATRA−TiO_2 system exhibits much faster electron recombination with the dominant recombination pathway forming the triplet state of ATRA with time constant of 19 ps while the less-favorable recombination to the ground state occurs with a 140 ps time constant.[330]

6. Acknowledgment

We thank Tõnu Pullerits, Donatas Zigmantas, Arkady Yartsev, Helena Hörvin Billsten, Gabor Benkö, and Jie Pan from our department for many fruitful discussions and important contributions to the work surveyed in this review article. Robert Smith is gratefully acknowledged for critical reading of the manuscript. We also thank our collaborators, Harry Frank, Ronald Christensen, Rienk van Grondelle, Emmanouil Papagiannakis, John Kennis, Jennifer Herek, Roberto Bassi, Roger Hiller, and Richard Cogdell for many helpful discussions during the past few years and for sharing their results prior to publication. We thank Roberto Bassi for providing us with Figure 15 and Tõnu Pullerits for making

Figure 12. The research at Lund University is supported by the Swedish Research Council, the Knut and Alice Wallenberg Foundation, and the Crafoord Foundation. T.P thanks Delegationen för Energiförsörjning i Sydsverige (DESS) and the Swedish Energy Agency Administration (Energimyndigheten) for financial support.

7. Note Added in Proof

Energy transfer from a carotenoid to BChl in reaction center was recently demonstrated. In the reaction center of *Rb. sphaeroides*, carotenoid spheroidenone transfers energy to BChl-a with 75% efficiency utilizing the S_1 route.[331]

8. References

(1) Frank H. A.; Cogdell R. J. In *Carotenoids in Photosynthesis*; Young, A. J., Britton, G., Eds.; Chapman and Hall, 1993; p 252.
(2) Frank, H. A.; Cogdell, R. J. *Photochem. Photobiol.* **1996**, *63*, 257.
(3) Koyama, Y.; Kuki, M.; Andersson, P. O.; Gillbro, T. *Photochem. Photobiol.* **1996**, *63*, 243.
(4) Ritz, T.; Damjanović, A.; Schulten, K.; Zhang, J.-P.; Koyama, Y. *Photosynth. Res.* **2000**, *66*, 125.
(5) van Amerongen, H.; van Grondelle, R. *J. Phys. Chem. B* **2001**, *105*, 604.
(6) Edge, R.; Truscott, T. G. In *Photochemistry of Carotenoids*; Frank, H. A., Young, A. J., Britton, G., Cogdell, R. J., Eds.; Kluwer Academic Publishers: Dordrecht, The Netherlands, 1999; p 223.
(7) Landrum, J. T.; Bone, R. *Arch. Bioch. Biophys.* **2001**, *385*, 21.
(8) Nishino, H. *J. Cell. Biochem.* **1997**, *27*, 86.
(9) Dutton, H. J.; Manning, W. M.; Duggar, B. M. *J. Phys. Chem.* **1943**, *47*, 308.
(10) Govindjee, In *Photochemistry of Carotenoids*; Frank, H. A., Young, A. J., Britton, G. Cogdell, R. J., Eds.; Kluwer Academic Publishers: Dordrecht, The Netherlands, 1999; p 1.
(11) Schulten, K.; Karplus, M. *Chem. Phys. Lett.* **1972**, *14*, 305.
(12) Hudson, B. S.; Kohler, B. E. *Chem. Phys. Lett.* **1972**, *14*, 299.
(13) Tavan, P.; Schulten, K. *Phys. Rev. B* **1987**, *36*, 4337.
(14) Sashima, T.; Koyama, Y.; Yamada, T.; Hashimoto, H. *J. Phys. Chem. B* **2000**, *104*, 5011.
(15) Furuichi, K.; Sashima, T.; Koyama, Y. *Chem. Phys. Lett.* **2002**, *356*, 547.
(16) Orlandi, G.; Zerbetto, F.; Zgierski, M. Z. *Chem. Rev.* **1991**, *91*, 867.
(17) Hudson, B. S.; Kohler, B. E.; Schulten, K. In *Excited States*; Lim, E. C., Ed.; Academic Press: New York, 1982; Vol. 6, p 1.
(18) Wasielewski, M. R.; Kispert, L. D. *Chem. Phys. Lett.* **1986**, *128*, 238.
(19) Christensen, R. In *Photochemistry of Carotenoids*; Frank, H. A., Young, A. J., Britton, G. Cogdell, R. J., Eds.; Kluwer Academic Publishers: Dordrecht, The Netherlands, 1999; p 137.
(20) Gradinaru, C. C.; Kennis, J. T. M.; Papagiannakis, E.; van Stokkum, I. H. M.; Cogdell, R. J.; Fleming, G. R.; Niederman, R. A.; van Grondelle, R. *Proc. Natl. Acad. Sci. U.S.A.* **2001**, *98*, 2364.
(21) Bautista, J. A.; Connors, R. E.; Raju, B. B.; Hiller, R. G.; Sharples, F. P.; Gosztola, D.; Wasielewski, M. R.; Frank, H. A. *J. Phys. Chem. B* **1999**, *103*, 8751.
(22) Frank, H. A.; Bautista, J. A.; Josue, J.; Pendon, Z.; Hiller, R. G.; Sharples, F. P.; Gosztola, D.; Wasielewski, M. R. *J. Phys. Chem. B* **2000**, *104*, 4569.
(23) Zigmantas, D.; Polívka, T.; Hiller, R. G.; Yartsev, A.; Sundström, V. *J. Phys. Chem. A* **2001**, *105*, 10296.
(24) Sundström, V.; Pullerits, T.; van Grondelle, R. *J. Phys. Chem. B* **1999**, *103*, 2327.
(25) Hu, X.; Ritz, T.; Damjanović, A.; Schulten, K. *J. Phys. Chem. B* **1997**, *101*, 3854.
(26) Krueger, B. P.; Scholes, G. D.; Yu, J.-Y.; Fleming, G. R. *Acta Phys. Pol., A* **1999**, *95*, 63.
(27) Fraser, N. J.; Hashimoto, H.; Cogdell, R. J. *Photosynth. Res.* **2001**, *70*, 249.
(28) Bassi, R.; Caffari, S. *Photosynth. Res.* **2000**, *64*, 243.
(29) Britton, G. In *Carotenoids*; Britton, G., Liaaen-Jensen, S., Pfander, H., Eds.; Birkhäuser Verlag: Basel, 1995; p 13.
(30) Schulten, K.; Ohmine, I.; Karplus, M. *J. Chem. Phys.* **1976**, *64*, 4422.
(31) Tavan, P.; Schulten, K. *J. Chem. Phys.* **1979**, *70*, 5407.
(32) Tavan, P.; Schulten, K. *J. Chem. Phys.* **1986**, *85*, 6602.
(33) Fuss, W.; Haas, Y.; Zilberg, S. *Chem. Phys.* **2000**, *259*, 273.
(34) Schlücker, S.; Szeghalmi, A.; Schmitt, M.; Popp, J.; Kiefer, W. *J. Raman Spectrosc.* **2003**, *34*, 413.
(35) Christensen, R.; Kohler, B. *Photochem. Photobiol.* **1973**, *18*, 293.
(36) Hemley, R.; Kohler, B. E. *Biophys. J.* **1977**, *20*, 377.
(37) Christensen, R. L.; Goyette, M.; Gallagher, L.; Duncan, J.; DeCoster, B.; Lugtenburg, J.; Jansen, F. J.; van der Hoef, I. *J. Phys. Chem. A* **1999**, *103*, 2399.
(38) Frank, H. A.; Desamero, R. Z. B.; Chynwat, V.; Gebhard, R.; van der Hoef, I.; Jansen, F. J.; Lugtenburg, J.; Gosztola, D.; Wasielewski, M. R. *J. Phys. Chem. A* **1997**, *101*, 149.
(39) Andersson, P.-O.; Bachilo, S. M.; Chen, R.-L.; Gillbro, T. *J. Phys. Chem.* **1995**, *99*, 16199.
(40) Frank, H. A.; Josue, J. S.; Bautista, J. A.; van der Hoef, I.; Jansen, F. J.; Lugtenburg, J.; Wiederrecht, G.; Christensen, R. L. *J. Phys. Chem. B* **2002**, *106*, 2083.
(41) Knoll, K.; Schrock, R. R. *J. Am. Chem. Soc.* **1989**, *111*, 7989.
(42) Macpherson, A. N.; Gillbro, T. *J. Phys. Chem. A* **1998**, *102*, 5049.
(43) Zimmermann, J.; Linden, P. A.; Vaswani, H. M.; Hiller, R. G.; Fleming, G. R. *J. Phys. Chem. B* **2002**, *106*, 9418.
(44) Zigmantas, D.; Hiller, R. G.; Yartsev, A.; Sundström, V.; Polívka, T. *J. Phys. Chem. B* **2003**, *107*, 5339.
(45) Shima, S.; Ilagan, R. P.; Gillespie, N.; Sommer, B. J.; Hiller, R. G.; Sharples, F. P.; Frank, H. A.; Birge, R. R. *J. Phys. Chem. A* **2003**, *107*, 8052.
(46) Zigmantas, D.; Hiller, R. G.; Frank, H. A.; Sundström, V.; Polívka, T. *Phys. Chem. Chem. Phys.*, submitted for publication.
(47) He, Z.; Gosztola, D.; Deng, Y.; Gao, G.; Wasielewski, M. R.; Kispert, L. D. *J. Phys. Chem. B* **2000**, *104*, 6668.
(48) Takaichi, S.; Furihata, K.; Harashima, K. *Arch. Microbiol.* **1991**, *155*, 473.
(49) Mimuro, M.; Nishimura, Y.; Takaichi, S.; Yamano, Y.; Ito, M.; Nagaoka, S.; Yamazaki, I.; Katoh, T.; Nagashima, U. *Chem. Phys. Lett.* **1993**, *213*, 576.
(50) Fujii, R.; Onaka, K.; Kuki, M.; Koyama, Y.; Watanabe, Y. *Chem. Phys. Lett.* **1998**, *288*, 847.
(51) Fujii, R.; Ishikawa, T.; Koyama, Y.; Taguchi, M.; Isobe, Y.; Nagae, H.; Watanabe, Y. *J. Phys. Chem. A* **2001**, *105*, 5348.
(52) Onaka, K.; Fujii, R.; Nagae, H.; Kuki, M.; Koyama, Y.; Watanabe, Y. *Chem. Phys. Lett.* **1999**, *315*, 75.
(53) Strickler, S. J.; Berg, R. A. J. *J. Chem. Phys.* **1962**, *37*, 814.
(54) Ricci, M.; Bradforth, S. E.; Jimenez, R.; Fleming, G. R. *Chem. Phys. Lett.* **1996**, *259*, 381.
(55) Akimoto, S.; Yamazaki, I.; Takaichi, S.; Mimuro, M. *Chem. Phys. Lett.* **1999**, *313*, 63.
(56) Akimoto, S.; Yamazaki, I.; Sakawa, T.; Mimuro, M. *J. Phys. Chem. A* **2002**, *106*, 2237.
(57) Andersson, P.-O.; Gillbro, T. *J. Chem. Phys.* **1995**, *103*, 2509.
(58) Andersson, P.-O.; Takaichi, S.; Cogdell, R. J.; Gillbro, T. *Photochem. Photobiol.* **2001**, *74*, 549.
(59) Macpherson, A. N.; Arellano, J. B.; Fraser, N. J.; Cogdell, R. J.; Gillbro, T. *Biophys. J.* **2001**, *80*, 923.
(60) Mimuro, M.; Akimoto, S.; Takaichi, S.; Yamazaki, I. *J. Am. Chem. Soc.* **1997**, *119*, 1452.
(61) van Stokkum, I. H. M.; Scherer, T.; Brouwer, A. M.; Verhoeven, J. W. *J. Phys. Chem.* **1994**, *98*, 852.
(62) Polívka, T.; Zigmantas, D.; Frank, H. A.; Bautista, J. A.; Herek, J. L.; Koyama, Y.; Fujii, R.; Sundström, V. *J. Phys. Chem. B* **2001**, *105*, 1072.
(63) Zhang, J.-P.; Skibsted, L. H.; Fujii, R.; Koyama, Y. *Photochem. Photobiol.* **2001**, *73*, 219.
(64) Rondonuwu, F. S.; Watanabe, Y.; Fujii, R.; Koyama, Y. *Chem. Phys. Lett.* **2003**, *376*, 292.
(65) Polli, D.; Cerullo, G.; Lanzani, G.; De Silvestri, S.; Hashimoto, H.; Cogdell, R. J. *Synth. Met.* **2003**, *139*, 893.
(66) Yoshizawa, M.; Aoki, H.; Ue, M.; Hashimoto, H. *Phys. Rev. B* **2003**, *67*, 174302.
(67) Papagiannakis, E.; Stokkum, I. H. M.; van Grondelle, R.; Niederman, R. A.; Zigmantas, D.; Sundström, V.; Polívka, T. *J. Phys. Chem. B* **2003**, *107*, 11216.
(68) Holt, N. E.; Kennis, J. T. M.; Dall'Osto, L.; Bassi, R.; Fleming, G. R. *Chem. Phys. Lett.* **2003**, *379*, 305.
(69) Sashima, T.; Nagae, H.; Kuki, M.; Koyama, Y. *Chem. Phys. Lett.* **1999**, *299*, 187.
(70) Zhang, J.-P.; Inaba, T.; Watanabe, Y.; Koyama, Y. *Chem. Phys. Lett.* **2000**, *332*, 351.
(71) Rondonuwu, F. S.; Watanabe, Y.; Zhang, J.-P.; Furuichi, K.; Koyama, Y. *Chem. Phys. Lett.* **2002**, *357*, 376.
(72) Fujii, R.; Inaba, T.; Watanabe, Y.; Koyama, Y.; Zhang, J. P. *Chem. Phys. Lett.* **2003**, *369*, 165.
(73) Mimuro, M.; Nagashima, M.; Takaichi, S.; Nishimura, Y.; Yamazaki, I.; Katoh, T. *Biochim. Biophys. Acta* **1992**, *1098*, 271.
(74) Thrash, R. J.; Fang, H. L. B.; Leroi, G. E. *J. Chem. Phys.* **1977**, *67*, 5930.
(75) Cosgrove, S. A.; Guite, M. A.; Burnell, T. B.; Christensen, R. L. *J. Phys. Chem.* **1990**, *94*, 8118.
(76) deCoster, B.; Christensen, R. L.; Gebhard, R.; Lugtenburg, J.; Farhoosh, R.; Frank, H. A. *Biochim. Biophys. Acta* **1992**, *1102*, 107.
(77) Engelman, R.; Jortner, J. *J. Mol. Phys.* **1970**, *18*, 145.

(78) Chynwat, V.; Frank, H. A. *Chem. Phys.* **1995**, *194*, 237.
(79) Frank, H. A.; Cua, A.; Chynwat, V.; Young, A.; Gosztola, D.; Wasielewski, M. R. *Photosynth. Res.* **1994**, *41*, 389.
(80) Frank, H. A.; Cua, A.; Chynwat, V.; Young, A.; Gosztola, D.; Wasielewski, M. R. *Biochim. Biophys. Acta* **1996**, *1277*, 243.
(81) Polívka, T.; Herek, J. L.; Zigmantas, D.;Åkerlund, H.-E.; Sundström, V. *Proc. Natl. Acad. Sci. U.S.A.* **1999**, *96*, 4914.
(82) Zhang, J.-P.; Chen, C.-H.; Koyama, Y.; Nagae, H. *J. Phys. Chem. B* **1998**, *102*, 1632.
(83) Bondarev, S. L.; Knyukshto, V. N. *Chem. Phys. Lett.* **1994**, *225*, 346.
(84) Frank, H. A.; Bautista, J. A.; Josue, J. S.; Young, A. J. *Biochemistry* **2000**, *39*, 2831.
(85) Josue, J. S.; Frank, H. A. *J. Phys. Chem. A* **2002**, *106*, 4815.
(86) Robert, B. In *Photochemistry of Carotenoids*; Frank, H. A., Young, A. J., Britton, G. Cogdell, R. J., Eds.; Kluwer Academic Publishers: Dordrecht, The Netherlands, 1999; p 189.
(87) Gaier, K.; Angerhofer, A.; Wolf, H. C. *Chem. Phys. Lett.* **1991**, *187*, 103.
(88) Hashimoto, H.; Koyama, Y.; Mori, Y. *Jpn. J. Appl. Phys.* **1997**, *36*, 916.
(89) Sashima, T.; Shiba, M.; Hashimoto, H.; Nagae, H.; Koyama, Y. *Chem. Phys. Lett.* **1998**, *290*, 36.
(90) Noguchi, T.; Hayashi, H.; Tasumi, M.; Atkinson, G. H. *J. Phys. Chem.* **1991**, *95*, 3167.
(91) Billsten, H. H.; Herek, J. L.; Garcia-Asua, G.; Hashøj, L.; Polívka, T.; Hunter, C. N.; Sundström, V. *Biochemistry* **2002**, *41*, 4127.
(92) Polívka, T.; Zigmantas, D.; Herek, J. L.; He, Z.; Pascher, T.; Pullerits, T.; Cogdell, R. J.; Frank, H. A.; Sundström, V. *J. Phys. Chem. B* **2002**, *106*, 11016.
(93) Lindal, T.-R.; Liaaen-Jensen, S. *Acta Chem. Scand.* **1997**, *51*, 1128.
(94) Walla, P. J.; Linden, P. A.; Hsu, C.-P.; Scholes, G. D.; Fleming, G. R. *Proc. Natl. Acad. Sci. U.S.A.* **2000**, *97*, 10808.
(95) Walla, P. J.; Linden, P. A.; Ohta, K.; Fleming, G. R. *J. Phys. Chem. A* **2002**, *106*, 1909.
(96) Jones, P. F.; Jones, W. J.; Davies, B. H. *J. Photochem. Photobiol. A* **1992**, *68*, 59.
(97) Bettermann, H.; Bouschen, W.; Ulrich, L.; Domnick, G.; Martin, H. D. *J. Mol. Struct.* **1999**, *480*, 101.
(98) Beck, M.; Stiel, H.; Leupold, D.; Winter, B.; Pop, D.; Vogt, U.; Spitz, C. *Biochim. Biophys. Acta* **2001**, *1506*, 260.
(99) Stiel, H.; Leupold, D.; Beck, M.; Will, I.; Sandner, W.; Lokstein, H. *J. Biochem. Biophys. Methods* **2001**, *48*, 239.
(100) Billsten, H. H.; Zigmantas, D.; Sundström, V.; Polívka, T. *Chem. Phys. Lett.* **2002**, *355*, 465.
(101) de Weerd, F. L.; van Stokkum, I. H. M.; van Grondelle, R. *Chem. Phys. Lett.* **2002**, *354*, 38.
(102) Frank, H. A.; Chynwat, V.; Desamero, R. Z. B.; Farhoosh, R.; Erickson, J.; Bautista, J. A. *Pure Appl. Chem.* **1997**, *69*, 2117.
(103) Bautista, J. A.; Chynwat, V.; Cua, A.; Jansen, F. J.; Lugtenburg, J.; Gosztola, D.; Wasielewski, M. R.; Frank, H. A. *Photosynth. Res.* **1998**, *55*, 49.
(104) Hiller, R. G. In *Photochemistry of Carotenoids*; Frank, H. A., Young, A. J., Britton, G., Cogdell, R. J., Eds.; Kluwer Academic Publishers: Dordrecht, The Netherlands, 1999; p 81.
(105) Akimoto, S.; Takaichi, S.; Ogata, T.; Nishimura, Y.; Yamazaki, I.; Mimuro, M. *Chem. Phys. Lett.* **1996**, *260*, 147.
(106) Bautista, J. A.; Hiller, R, G.; Sharples, F. P.; Gosztola, D.; Wasielewski, M.; Frank, H. A. *J. Phys. Chem. A* **1999**, *103*, 2267.
(107) Vaswani, H. M.; Hsu, C.-P.; Head-Gordon, M.; Fleming, G. R. *J. Phys. Chem. B* **2003**, *107*, 7940.
(108) O'Neil, M. P.; Wasielewski, M. R.; Khaled, M. M.; Kispert, L. D. *J. Chem. Phys.* **1991**, *95*, 7212.
(109) Dolan, P. M.; Miller, D.; Cogdell, R. J.; Birge, R. R.; Frank, H. A. *J. Phys. Chem. B* **2001**, *105*, 12134.
(110) Cerullo, G.; Polli, D.; Lanzani, G.; De Silvestri, S.; Hashimoto, H.; Cogdell, R. J. *Science* **2002**, *298*, 2395.
(111) Papagiannakis, E.; Kennis, J. T. M.; van Stokkum, I. H. M.; Cogdell, R. J.; van Grondelle, R. *Proc. Natl. Acad. Sci. U.S.A.* **2002**, *99*, 6017.
(112) Papagiannakis, E.; Das, S. K.; Gall, A.; Stokkum, I. H. M.; Robert, B.; van Grondelle, R.; Frank, H. A.; Kennis, J. T. M. *J. Phys. Chem. B* **2003**, *107*, 5642.
(113) Wohlleben, W.; Buckup, T.; Herek, J. L.; Cogdell, R. J.; Motzkus, M. *Biophys. J.* **2003**, *85*, 442.
(114) Kodis, G.; Herrero, C.; Palacios, R.; Mariño-Ochoa, E.; Gould, S.; de la Garza, L.; van Grondelle, R.; Gust, D.; Moore, T. A.; Moore, A. L.; Kennis, J. T. M. *J. Phys. Chem. B* **2004**, *108*, 414.
(115) Wohlleben, W.; Buckup, T.; Herek, J. L.; Motzkus, M. *J. Phys. Chem. B*, in press.
(116) Larsen, D. S.; Papagiannakis, E.; van Stokkum, I. H. M.; Vengris, M.; Kennis, J. T. M.; van Grondelle, R. *Chem. Phys. Lett.* **2003**, *381*, 733.
(117) Jiang, Y.; Kurimoto, Y.; Shimamura, T.; Ko-Chi, N.; Ohashi, N.; Mukai, Y.; Koyama, Y. *Biospectroscopy* **1996**, *2*, 47.
(118) Tsukida, K. *Methods Enzymol.* **1992**, *213*, 291.
(119) Fujii, R.; Chen, C.-H.; Mizoguchi, T.; Koyama, Y. *Spectrochim. Acta, Part A* **1998**, *54*, 727.
(120) Hengartner, U.; Bernhard, K.; Mayer, K.; Englert, G.; Glinz, E. *Helv. Chim. Acta* **1992**, *75*, 1848.
(121) Cerullo, G.; Lanzani, G.; Zavelani-Rossi, M.; De Silvestri, S. *Phys. Rev. B* **2001**, *63*, 241104.
(122) Siebert, T.; Engel, V.; Materny, A.; Kiefer, W.; Schmitt, M. *J. Phys. Chem. A* **2003**, *107*, 8355.
(123) Yoshizawa, M.; Aoki, H.; Hashimoto, H. *Phys. Rev. B* **2001**, *6318*, 180301.
(124) McCamant, D. W.; Kim, J. E.; Mathies, R. A. *J. Phys. Chem. A* **2002**, *106*, 6030.
(125) McCamant, D. W.; Kukura, P.; Mathies, R. *J. Phys. Chem. A* **2003**, *107*, 8208.
(126) Okamoto, H.; Nakabayashi, T.; Tasumi, M. *J. Phys. Chem. A* **1997**, *101*, 3488.
(127) Siebert, T.; Maksimenka, R.; Materny, A.; Engel, V.; Kiefer, W.; Schmitt, M. *J. Raman Spectrosc.* **2002**, *33*, 844.
(128) Hayashi, H.; Brack, T. L.; Noguchi, T.; Tasumi, M.; Atkinson, G. H. *J. Phys. Chem.* **1991**, *95*, 6797.
(129) Nakabayashi, T.; Okamoto, H.; Tasumi, M. *J. Phys. Chem. A* **1997**, *101*, 3494.
(130) Zerbetto, G.; Zgierski, M. Z.; Negri, F.; Orlandi, G. *J. Chem. Phys.* **1987**, *87*, 2505.
(131) Nagae, H.; Kuki, M.; Zhang, J.-P.; Sashima, T.; Mukai, Y.; Koyama, Y. *J. Phys. Chem. A* **2000**, *104*, 4155.
(132) Woywood, C.; Livingwood, W. C.; Frederick, J. H. *J. Chem. Phys.* **2001**, *114*, 1645.
(133) Nielsen, B. R.; Mortensen, A.; Jørgensen, K.; Skibsted, L. H. *J. Agric. Food Chem.* **1996**, *44*, 2106.
(134) Hashimoto, H.; Koyama, Y.; Hirata, Y.; Mataga, N. *J. Phys. Chem.* **1991**, *95*, 3072.
(135) Jeevarajan, A. S.; Kispert, L. D.; Avdievitch, N. I.; Forbes, M. D. E. *J. Phys. Chem.* **1996**, *100*, 669.
(136) Jeevarajan, J. A.; Wei, C. C.; Jeevarajan, A. S.; Kispert, L. D. *J. Phys. Chem.* **1996**, *100*, 5637.
(137) Zhang, J.-P.; Fujii, R.; Koyama, Y.; Rondonuwu F. S.; Watanabe, Y.; Mortensen, A.; Skibsted, L. H. *Chem. Phys. Lett.* **2001**, *348*, 235.
(138) Gurzadyan, G. G.; Steenken, S. *Phys. Chem. Chem. Phys.* **2002**, *4*, 2983.
(139) McDermott, G.; Prince, S. M.; Freer, A. A.; Hawthornwaite-Lawless, A. M.; Papiz, M. Z.; Cogdell, R. J.; Isaacs, N. W. *Nature* **1995**, *374*, 517.
(140) Koepke, J.; Hu, X.; Muenke, C.; Schulten, K.; Michel, H. *Structure* **1996**, *4*, 581.
(141) He, Z.; Sundström, V.; Pullerits, T. *FEBS Lett.* **2001**, *496*, 36.
(142) Herek, J. L.; Polívka, T.; Pullerits, T.; Fowler, G. J. S.; Hunter, C. N.; Sundström, V. *Biochemistry* **1998**, *37*, 7057.
(143) He, Z.; Sundström, V.; Pullerits, T. *Chem. Phys. Lett.* **2001**, *334*, 159.
(144) Georgakopoulou, S.; Cogdell, R. J.; van Grondelle, R.; van Amerongen, H. *J. Phys. Chem. B* **2003**, *107*, 655.
(145) Wang, Y.; Hu, X. *J. Am. Chem. Soc.* **2002**, *124*, 8445.
(146) Mao, L.; Wang, Y.; Hu, X. *J. Phys. Chem. B* **2003**, *107*, 3963.
(147) Papiz, M. Z.; Prince, S. M.; Howard, T.; Cogdell, R. J.; Isacs, N. W. *J. Mol. Biol.* **2003**, *326*, 1523.
(148) Germeroth, L.; Lottspeich, F.; Robert, B.; Michel, H. *Biochemistry* **1993**, *32*, 5615.
(149) Evans, M. B.; Cogdell, R. J.; Britton, G. *Biochim. Biophys. Acta* **1988**, *935*, 292.
(150) Arellano, J. B.; Bangar Raju, B.; Naqvi, K. R.; Gillbro, T. *Photochem. Photobiol.* **1998**, *68*, 84.
(151) Andersson, P. O.; Cogdell, R. J.; Gillbro, T. *Chem. Phys.* **1996**, *210*, 195.
(152) Walz, T.; Jamieson, S. J.; Bowers, C. M.; Bullough, P. A.; Hunter, C. N. *J. Mol. Biol.* **1998**, *282*, 833.
(153) Karrasch, S.; Bullough, P. A.; Ghosh, R. *EMBO J.* **1995**, *14*, 631.
(154) Cogdell, R. J.; Hipkins, M. F.; MacDonald, W.; Truscott, T. G. *Biochim. Biophys. Acta* **1981**, *634*, 191.
(155) van Grondelle, R.; Kramer, H.; Rijgersberg, C. *Biochim. Biophys. Acta* **1982**, *682*, 208.
(156) Angerhofer, A.; Bornhäuser, F.; Gall, A.; Cogdell, R. J. *Chem. Phys.* **1995**, *194*, 259.
(157) Angerhofer, A.; Cogdell, R. J.; Hipkins, M. *Biochim. Biophys. Acta* **1986**, *848*, 333.
(158) Chadwick, B.; Zhang, C.; Cogdell, R. J.; Frank, H. *Biochim. Biophys. Acta* **1987**, *893*, 444.
(159) Rademaker, H.; Hoff, A. J.; van Grondelle, R.; Duysens, L. N. M. *Biochim. Biophys. Acta* **1980**, *592*, 240.
(160) Naqvi, K. R. *Photochem. Photobiol.* **1980**, *31*, 523.
(161) van Grondelle, R. *Biochim. Biophys. Acta* **1985**, *811*, 147.
(162) Cogdell, R. J.; Frank, H. A. *Biochim. Biophys. Acta* **1987**, *895*, 63.
(163) Shreve, A. P.; Trautman, J. K.; Frank, H. A.; Owens, T. G.; Albrecht, A. C. *Biochim. Biophys. Acta* **1991**, *1058*, 280
(164) Trautman, J. K.; Shreve, A. P.; Violette, C. A.; Frank, H. A.; Owens, T. G.; Albrecht, A. C. *Proc. Natl. Acad. Sci. U.S.A.* **1990**, *87*, 215.
(165) Nagae, H.; Kakitani, T.; Katoh, T.; Mimuro, M. *J. Chem. Phys.* **1993**, *98*, 8012.

(166) Krueger, B. P.; Scholes, G. D.; Jimenez, R.; Fleming, G. R. *J. Phys. Chem. B* **1998**, *102*, 2284.
(167) Okamoto, H.; Ogura, M.; Nakabayashi, T.; Tasumi, M. *Chem. Phys.* **1998**, *236*, 309.
(168) Herek, J. L.; Wohlleben, W.; Cogdell, R. J.; Zeidler, D.; Motzkus, M. *Nature* **2002**, *417*, 533.
(169) Zhang, J.-P.; Inaba, T.; Watanabe, Y.; Koyama, Y. *Chem. Phys. Lett.* **2001**, *340*, 484.
(170) Desamero, R. Z. B.; Chynwat, V.; van der Hoef, I.; Jansen, F. J.; Lugtenburg, J.; Gosztola, D.; Wasielewski, M. R.; Cua, A.; Bocian, D. F.; Frank, H. A. *J. Phys. Chem. B* **1998**, *102*, 8151.
(171) Dexter, D. L. *J. Chem. Phys.* **1953**, *21*, 836.
(172) Damjanović, A.; Ritz, T.; Schulten, K. *Phys. Rev. E* **1999**, *59*, 3293.
(173) Förster, T. In *Modern Quantum Chemistry*; Sinanoglu, O., Ed.; Academic Press: New York, 1965; p 93.
(174) Krueger, B. P.; Scholes, G. D.; Fleming, G. R. *J. Phys. Chem. B* **1998**, *102*, 5378.
(175) Tretiak, S.; Middleton, C.; Chernyak, V.; Mukamel, S. *J. Phys. Chem. B* **2000**, *104*, 9540.
(176) Krueger, B. P.; Yom, J.; Walla, P. J.; Fleming, G. R. *Chem. Phys. Lett.* **1999**, *310*, 57.
(177) Shreve, A. P.; Trautman, J. K.; Owens, T. G.; Albrecht, A. *Chem. Phys. Lett.* **1990**, *170*, 51.
(178) Zhang, J.-P.; Fujii, R.; Qian, P.; Inaba, T.; Mizoguchi, T.; Koyama, Y.; Onaka, K.; Watanabe, Y. *J. Phys. Chem. B* **2000**, *104*, 3683.
(179) Scholes, G. D.; Harcourt, R. D.; Fleming, G. R. *J. Phys. Chem. B* **1997**, *101*, 7302.
(180) Hsu, C.-P.; Walla, P. J.; Head-Gordon, M.; Fleming, G. R. *J. Phys Chem. B* **2001**, *105*, 11016.
(181) Green, B. R.; Pichersky, E.; Kloppstech, K. *Trends Biochem. Sci.* **1991**, *16*, 181.
(182) Bassi, R.; Pineau, B.; Dainese, P.; Marquardt, J. *Eur. J. Biochem.* **1993**, *212*, 297.
(183) Boekema, E. J.; van Roon, H.; Breemen, J. F. L.; Dekker, J. P. *Eur. J. Biochem.* **1999**, *266*, 444.
(184) Kühlbrandt, W.; Wang, D. N.; Fujiyoshi, Y. *Nature* **1994**, *367*, 614.
(185) Das, S. K.; Frank, H. A. *Biochemistry* **2002**, *41*, 13087.
(186) Takaichi, S. In *Photochemistry of Carotenoids*; Frank, H. A., Young, A. J., Britton, G. Cogdell, R. J., Eds.; Kluwer Academic Publishers: Dordrecht, The Netherlands, 1999; p 39.
(187) Dellapenna, R. In *Photochemistry of Carotenoids*; Frank, H. A., Young, A. J., Britton, G., Cogdell, R. J., Eds.; Kluwer Academic Publishers: Dordrecht, The Netherlands, 1999; p 21.
(188) Croce, R.; Weiss, S.; Bassi, R. *J. Biol. Chem.* **1999**, *274*, 29613.
(189) Croce, R.; Remelli, R.; Varotto, C.; Breton, J.; Bassi, R. *FEBS Lett.* **1999**, *456*, 1.
(190) Ruban, A. V.; Lee, P. J.; Wentworth, M.; Young, A. J.; Horton, P. *J. Biol. Chem.* **1999** *274*, 10458.
(191) Caffari, S.; Croce, R.; Breton, J.; Bassi, R. *J. Biol. Chem.* **2001**, *276*, 35924.
(192) Bassi, R.; Croce, R.; Cugini, D.; Sandonna, D. *Proc. Natl. Acad. Sci. U.S.A.* **1999**, *96*, 10056.
(193) Crimi, M.; Dorra, D.; Bösinger, C. S.; Giuffra, E.; Holzwarth, A. R.; Bassi, R. *Eur. J. Biochem.* **2001**, *268*, 260.
(194) Demmig-Adams, B.; Adams, W. W. *Trends Plant Sci.* **1996**, *1*, 21.
(195) Horton, P.; Ruban, A. V.; Walters, R. G. *Annu. Rev. Plant Physiol. Plant Mol. Biol.* **1996**, *47*, 655.
(196) Richter, M.; Goss, R.; Wagner, B.; Holzwarth, A. R. *Biochemistry* **1999**, *38*, 12718.
(197) Frank, H. A.; Das, S. K.; Bautista, J. A.; Bruce, D.; Vasilev, S.; Crimi, M.; Croce, R.; Bassi, R. *Biochemistry* **2001**, *40*, 1220.
(198) Polívka, T.; Zigmantas, D.; Sundström, V.; Formaggio, E.; Cinque, G.; Bassi, R. *Biochemistry* **2002**, *41*, 439.
(199) Croce, R.; Müller, M. G.; Bassi, R.; Holzwarth, A. R. *Biophys. J.* **2001**, *80*, 901.
(200) Croce, R.; Müller, M. G.; Caffari, S.; Bassi, R.; Holzwarth, A. *Biophys. J.* **2003**, *84*, 2517.
(201) Walla, P. J.; Yom, J.; Krueger, B. P.; Fleming, G. *J. Phys. Chem. B* **2000**, *104*, 4806.
(202) Connelly, J. P.; Müller, M. G.; Bassi, R.; Croce, R.; Holzwarth, A. *Biochemistry* **1997**, *36*, 281.
(203) Gradinaru, C. C.; van Stokkum, I. H. M.; Pascal, A. A.; van Grondelle, R.; van Amerongen, H. *J. Phys. Chem. B* **2000**, *104*, 9330.
(204) Peterman, E. J. G.; Gradinaru, C.; Calkoen, F.; Borst, J. C.; van Grondelle, R.; van Amerongen, H. *Biochemistry* **1997**, *36*, 12208.
(205) Croce, R.; Cinque, G.; Holzwarth, A.; Bassi, R. *Photosynth. Res.* **2000**, *64*, 221.
(206) Croce, R.; Canino, G.; Ros, F.; Bassi, R. *Biochemistry* **2002**, *41*, 7334.
(207) Ruban, A. V.; Pascal, A.; Robert, B. *FEBS Lett.* **2000**, *477*, 181.
(208) Gradinaru, C. C.; van Grondelle, R.; van Amerongen, H. *J. Phys. Chem. B* **2003**, *107*, 3938.
(209) Parusel, A. B. J.; Grimme, S. *J. Phys. Chem. B* **2000**, *104*, 5395.
(210) Sundholm, D. *Chem. Phys. Lett.* **2000**, *317*, 545.
(211) Peterman, E. J. G.; Monshouwer, R.; van Stokkum, I. H. M.; van Grondelle, R.; van Amerongen, H. *Chem. Phys. Lett.* **1997**, *264*, 279.
(212) Peterman, E. J. G.; Dukker, F. M.; van Grondelle, R.; van Amerongen, H. *Biophys. J.* **1995**, *69*, 2670.
(213) Naqvi, K. R.; Melø, T. B.; Raju, B. B.; Jávorfi, T.; Simidijev, I.; Garab, G. *Spectrochim. Acta, Part A* **1997**, *53*, 2659.
(214) Barzda, V.; Peterman, E. J. G.; van Grondelle, R.; van Amerongen, H. *Biochemistry* **1998**, *37*, 546.
(215) Connelly, J. P.; Müller, M. G.; Hucke, M.; Gatzen, G.; Mullineaux, C. V.; Ruban, A. V.; Horton, P.; Holzwarth, A. R. *J. Phys. Chem. B* **1997**, *101*, 1902.
(216) Trinkunas, G.; Connely, J. P.; Müller, M. G.; Valkunas, L.; Holzwarth, A. R. *J. Phys. Chem. B* **1997**, *101*, 7313.
(217) Cinque, G.; Croce, R.; Holzwarth, A. R.; Bassi, R. *Biophys. J.* **2000**, *79*, 1706.
(218) Croce, R.; Müller, M. G.; Bassi, R.; Holzwart, A. R. *Biophys. J.* **2003**, *84*, 2508.
(219) Moya, I.; Silvestri, M.; Cinque, G.; Bassi, R. *Biochemistry* **2001**, *40*, 12552.
(220) Ma, Y.-Z.; Holt, N. E.; Li, X.-P.; Niyogi, K.; Fleming, G. R. *Proc. Natl. Acad. Sci. U.S.A.* **2003**, *100*, 4377.
(221) Li, X.-P.; Björkman, O.; Shih, C.; Grossman, A. R.; Rosenquist, M.; Jansson, S.; Niyogi, K. K. *Nature* **2000**, *403*, 391.
(222) Shinoda, S.; Osuka, A.; Nishimura, Y.; Yamazaki, I. *Chem. Lett.* **1995**, 1139.
(223) Shinoda, S.; Tsukube, H.; Nishimura, Y.; Yamazaki, I.; Osuka, A. *J. Org. Chem.* **1999**, *64*, 3757.
(224) He, Z.; Kispert, L. D.; Metzger, R. M.; Gosztola, D.; Wasielewski, M. R. *J. Phys. Chem. B* **2000**, *104*, 6302.
(225) Aspinall-O'Dea, M.; Wentworth, M.; Pascal, A.; Robert, B.; Ruban, A.; Horton, P. *Proc. Natl. Acad. Sci. U.S.A.* **2002**, *99*, 16331.
(226) Dreuw, A.; Fleming, G. R.; Head-Gordon, M. *Phys. Chem. Chem. Phys.* **2003**, *5*, 3247.
(227) Dreuw, A.; Fleming, G. R.; Head-Gordon, M. *J. Phys. Chem. B* **2003**, *107*, 6500.
(228) Hermant, R. M.; Lidell, P. A.; Lin, S.; Alden, R. G.; Kang, H. K.; Moore, A. L.; Moore, T. A.; Gust, D. *J. Am. Chem. Soc.* **1993**, *115*, 2080.
(229) Cardozo, S. L.; Nicodem, D. E.; Moore, T. A.; Moore, A. L.; Gust, D. *J. Braz. Chem. Soc.* **1996**, *7*, 19.
(230) Fungo, F.; Otero, L.; Durantini, E.; Thompson, W. J.; Silber, J. J.; Moore, T. A.; Moore, A. L.; Gust, D.; Sereno, L. *Phys. Chem. Chem. Phys.* **2003**, *5*, 469.
(231) Crofts, A. R.; Yerkes, C. T. *FEBS Lett.* **1994**, *352*, 265−270.
(232) Young, A. J.; Phillip, D.; Ruban, A. V.; Horton, P.; Frank, H. A. *Pure Appl. Chem.* **1997**, *69*, 2125.
(233) Grudziński, W.; Krupa, Z.; Garstka, M.; Maksymiec, W.; Swartz, T. E.; Gruszecki, W. I. *Biochim. Biophys. Acta* **2002**, *1554*, 108.
(234) Garab, G.; Cseh, Z.; Kovács, L.; Rajagopal, S.; Várkonyi, Z.; Wentworth, M.; Mustárdy, L.; Dér, A.; Ruban, A. V.; Papp, E.; Holzenburg, A. Horton, P. *Biochemistry* **2002**, *41*, 15121.
(235) Hofmann, E.; Wrench, P.; Sharples, F. P.; Hiller, R. G.; Welte, W.; Diederichs, K. *Science* **1996**, *272*, 1788.
(236) Kleima, F. J.; Hofmann, E.; Gobets, B.; van Stokkum, I. H. M.; van Grondelle, R.; Diederichs, K.; van Amerongen, H. *Biophys. J.* **2000**, *78*, 344.
(237) Kleima, F. J.; Wendling, M.; Hofman, E.; Peterman, E. J. G.; van Grondelle, R.; van Amerongen, H. *Biochemistry* **2000**, *39*, 5184.
(238) Krueger, B. P.; Lampoura, S. S.; van Stokkum, I. H. M.; Papagiannakis, E.; Salverda, J. M.; Gradinaru, C. C.; Rutkauskas, D.; Hiller, R. G.; van Grondelle, R. *Biophys. J.* **2001**, *80*, 2843.
(239) Carbonera, D.; Giacometti, G.; Segre, U.; Hofmann, E.; Hiller, R. G. *J. Phys. Chem. B* **1999**, *103*, 6349.
(240) Zigmantas, D.; Hiller, R. G.; Sundström, V.; Polívka, T. *Proc. Natl. Acad. Sci. U.S.A.* **2002**, *99*, 16760.
(241) Koka, P.; Song, P.-S. *Biochim. Biophys. Acta* **1977**, *495*, 220.
(242) Damjanović, A.; Ritz, T.; Schulten, K. *Biophys. J.* **2000**, *79*, 1695.
(243) Dick, B.; Hohlneicher, G. *J. Chem. Phys.* **1982**, *76*, 5755.
(244) Drucker, R. P.; McClain, W. M. *Chem. Phys. Lett.* **1974**, *61*, 2609.
(245) Song, P. S.; Koka, P.; Berzelin, B. B.; Haxo, F. T. *Biochemistry* **1976**, *15*, 422.
(246) Nakayama, K.; Mimuro, M.; Nishimura, Y.; Yamazaki, I.; Okada, M. *Biochim. Biophys. Acta* **1994**, *1188*, 117.
(247) Kageyama, A.; Yokohama, Y.; Shimura, S.; Ikawa, T. *Plant Cell Physiol.* **1977**, *18*, 477.
(248) Trautman, J. K.; Shreve, A. P.; Owens, T. G.; Albrecht A. C. *Chem. Phys. Lett.* **1990**, *166*, 369.
(249) Katoh, T.; Mimuro, M. *Photosynth. Res.* **1992**, *34*, 117.
(250) Grevby, C.; Sundqvist, C. *J. Plant Physiol.* **1992**, *140*, 414.
(251) Krauss, N.; Schubert, W.-D.; Klukas, O.; Fromme, P.; Witt, H. T.; Saenger, W. *Nat. Struct. Biol.* **1996**, *3*, 965.
(252) Schubert, W. D.; Klukas, O.; Krauss, N.; Saenger, W.; Fromme, P.; Witt, H. T. *J. Mol. Biol.* **1997**, *272*, 741.
(253) Jordan, P.; Fromme, P.; Witt, H. T.; Klukas, O.; Saenger, W.; Krauss, N. *Nature* **2001**, *411*, 909.

(254) Gobets, B.; van Grondelle, R. *Biochim. Biophys. Acta* **2001**, *1507*, 80.
(255) Byrdin, M.; Jordan, P.; Krauss, N.; Fromme, P.; Stehlik, D.; Schlodder, E. *Biophys. J.* **2002**, *83*, 433.
(256) Damjanović, A.; Vaswani, H. M.; Fromme, P.; Fleming, G. R. *J. Phys. Chem. B* **2002**, *106*, 10251.
(257) Sener, M. K.; Lu, D.; Ritz, T.; Park, S.; Fromme, P.; Schulten, K. *J. Phys. Chem. B* **2002**, *106*, 7948.
(258) van der Lee, J.; Bald, D.; Kwa, S. L. S.; van Grondelle, R.; Rögner, M.; Dekker, J. P. *Photosynth. Res.* **1993**, *35*, 311.
(259) Kennis, J. T. M.; Gobets, B.; van Stokkum, I. H. M.; Dekker, J. P.; van Grondelle, R.; Fleming, G. R. *J. Phys. Chem. B* **2001**, *105*, 4485.
(260) de Weerd, F. L.; Kennis, J. T. M.; Dekker, J. P.; van Grondelle, R. *J. Phys. Chem. B* **2003**, *107*, 5995.
(261) Croce, R.; Morosinotto, T.; Castelleti, S.; Breton, J.; Bassi, R. *Biochim. Biophys. Acta* **2002**, *1556*, 29. The 4 Å structure of PSI-LHCI complex appeared recently: Ben-Shem, A.; Frowlow, F.; Nelson, N. *Nature* **2003**, *426*, 630.
(262) Castelleti, S.; Morosinotto, T.; Robert, B.; Caffari, S.; Bassi, R.; Croce, R. *Biochemistry* **2003**, *42*, 4226.
(263) Schmid, V. H. R.; Potthast, S.; Wiener, M.; Bergauer, V.; Paulsen, H.; Storf, S. *J. Biol. Chem.* **2002**, *277*, 37307.
(264) Gobets, B.; Kennis, J. T. M.; Ihalainen, J. A.; Brazzoli, M.; Croce, R.; Stokkum, I. H. M.; Bassi, R.; Dekker, J. P.; van Amerongen, H.; Fleming, G. R.; van Grondelle, R. *J. Phys. Chem. B* **2001**, *105*, 10132.
(265) van Dorssen, R. J.; Breton, J.; Plijter, J. J.; Satoh, K.; van Gorkom, H. J.; Amesz, J. *Biochim. Biophys. Acta* **1987**, *893*, 267.
(266) de Weerd, F. L.; Dekker, J. P.; van Grondelle, R. *J. Phys. Chem. B* **2003**, *107*, 6214.
(267) Blankenship, R. E.; Olson, J. M.; Miller, M. In *Anoxygenic Photosynthetic Bacteria*; Blankenship, R. E., Madigan, M. T., Bauer, C. E., Eds.; Kluwer Academic Publishers: Dordrecht, The Netherlands, 1995; p. 399.
(268) Oelze, J.; Golecki, J. R. In *Anoxygenic Photosynthetic Bacteria*; Blankenship, R. E., Madigan, M. T., Bauer, C. E., Eds.; Kluwer Academic Publishers: Dordrecht, The Netherlands, 1995; p. 259.
(269) Borrego, C. M.; Garcia-Gil, L. J. *Photosynth. Res.* **1995**, *45*, 21.
(270) van Dorssen, R. J.; Vasmel, H.; Amesz, J. *Photosynth. Res.* **1986**, *9*, 33.
(271) Melø, T. B.; Frigaard, N.-U.; Matsura, K.; Naqvi, K. R. *Spetrochim. Acta, Part A* **2000**, *56*, 2001.
(272) Otte, S. C. M.; van der Heiden, J. C.; Pfennig, N.; Amesz, J. *Photosynth. Res.* **1991**, *28*, 77.
(273) Pšenčík, J.; Ma, Y.-Z.; Arellano, J. B.; Garcia-Gil, J.; Holzwart, A. R.; Gillbro, T. *Photosynth. Res.* **2002**, *71*, 5.
(274) Francke, C.; Otte, S. C. M.; Miller, M.; Amesz, J.; Olson, J. M. *Photosynth. Res.* **1996**, *50*, 71.
(275) Neerken, S.; Amesz, J. *Biochim. Biophys. Acta* **2001**, *1507*, 278.
(276) Gest, H.; Favinger, J. L. *Arch. Microbiol.* **1983**, *136*, 11.
(277) Takaichi, S.; Inoue, K.; Akaike, M.; Kobayashi, M.; Ohoka, H.; Madigan M. T. *Arch. Microbiol.* **1997**, *168*, 277.
(278) Funk, C.; Schroeder, W. P.; Napiwotzki, A.; Tjus, S. E.; Renger, G.; Andersson, B. *Biochemistry* **1995**, *34*, 11133.
(279) Dominici, P.; Caffari, S.; Armenante, F.; Ceoldo, S.; Crimi, M.; Bassi, R. *J. Biol. Chem.* **2002**, *277*, 22750.
(280) Ruban, A. V.; Pascal, A. A.; Robert, B.; Horton, P. *J. Biol. Chem.* **2002**, *277*, 7785.
(281) Holt, T. K.; Krogmann, D. W. *Biochim. Biophys. Acta* **1981**, *637*, 408.
(282) Wu, Y. P.; Krogmann, D. W. *Biochim. Biophys. Acta* **1997**, *1322*, 1.
(283) Kerfeld, C. A.; Sawaya, M. R.; Brahmandam, V.; Cascio, D.; Ho, K. K.; Trevithick-Sutton, C. C.; Krogmann, D. W.; Yeates, T. O. *Structure* **2003**, *11*, 55.
(284) Polívka, T.; Kerfeld, C. A.; Sundström, V. Unpublished data.
(285) de Winter, A.; Boxer, S. G. *J. Phys. Chem. B* **1999**, *103*, 8786.
(286) Hanley, J.; Deligiannakis, Y.; Pascal, A.; Faller, P.; Rutherford, A. W. *Biochemistry* **1999**, *38*, 8189.
(287) Faller, P.; Pascal, A.; Rutherford, A. W. *Biochemistry* **2001**, *40*, 6431.
(288) Telfer, A.; Frolov, D.; Barber, J.; Robert, B.; Pascal, A. *Biochemistry* **2003**, *42*, 1008.
(289) Tracewell, C. A.; Cua, A.; Stewart, D. H.; Bocian, D. F.; Brudwig, G. W. *Biochemistry* **2001**, *40*, 193.
(290) Yemelyanov, A. Y.; Katz, N. B.; Bernstein, P. S. *Exp. Eye Res.* **2001**, *72*, 381.
(291) Bone, R. A.; Landrum, J. T.; Friedes, L. M.; Gomez, C. M.; Kilburn, M. D.; Menendez, E.; Vidal, I.; Wang, W. I. *Exp. Eye Res.* **1997**, *64*, 211.
(292) Handelman, G. J.; Snodderly, D. M.; Adler, A. J.; Russet, M. D.; Dratz, E. A. *Methods Enzymol.* **1992** *213*, 220.
(293) Billsten, H. H.; Bhosale, P.; Yemelyanov, A.; Bernstein, P. S.; Polívka, T. *Photochem. Photobiol.* **2003**, *78*, 138.
(294) Cianci, M.; Rizkallah, P. J.; Olczak, A.; Raftery, J.; Chayen, N. E.; Zagalsky, P. F.; Helliwell, J. R. *Proc. Natl. Acad. Sci. U.S.A.* **2002**, *99*, 9795.
(295) Krawczyk, S.; Britton, G. *Biochim. Biophys. Acta* **2001**, *1544*, 301.
(296) Weesie, R. J.; Merlin, J. C.; de Groot, H. J. M.; Britton, G.; Lugtenburg, J.; Jansen, F. J. H. M.; Cornard, J. P. *Biospectroscopy* **1999**, *5*, 358.
(297) Guo, J.-D.; Luo, Y.; Himo, F. *Chem. Phys. Lett.* **2002**, *366*, 73.
(298) Bensasson, R. V.; Land, E. J.; Moore, A. L.; Crouch, R. L.; Dirks, G.; Moore, T. A.; Gust, D. *Nature* **1981**, *290*, 329.
(299) Moore, T. A.; Gust, D.; Mathis, P.; Mialocq, J.-C.; Chachaty, C.; Bensasson, R. V.; Land, E. J.; Doizi, D.; Liddell, P. A.; Lehman, W. R.; Nemeth, G. A.; Moore, A. L. *Nature* **1984**, *307*, 630.
(300) Gust, D.; Moore, T. A.; Moore, A. L.; Macpherson, A. N.; Lopez, A.; DeGraziano, J. M.; Gouni, I.; Bittersmann, E.; Seely, G. R.; Gao, F.; Nieman, R. A.; Ma, X. C.; Demanche, L. J.; Hung, S.-C.; Luttrull, D. K.; Lee, S.-J.; Kerrigan, P. K. *J. Am. Chem. Soc.* **1993**, *115*, 11141.
(301) Bahr, J. L.; Kuciauskas, D.; Liddell, P. A.; Moore, A. L.; Moore, T. A.; Gust, D. *Photochem. Photobiol.* **2000**, *72*, 598.
(302) Bennett, I. M.; Farfano, H. M. V.; Bogani, F.; Primak, A.; Liddell, P. A.; Otero, L.; Sereno, L.; Silber, J. J.; Moore, A. L.; Moore, T. A.; Gust, D. *Nature* **2002**, *420*, 398.
(303) Kuciauskas, D.; Liddell, P. A.; Lin, S.; Stone, S. G.; Moore, A. L.; Moore, T. A.; Gust, D. *J. Phys. Chem. B* **2000**, *104*, 4307.
(304) Kuciauskas, D.; Liddell, P. A.; Moore, A. L.; Moore, T. A.; Gust, D. *J. Am. Chem. Soc.* **1998**, *120*, 10880.
(305) Liddell, P. A.; Barrett, D.; Makings, L. R.; Pessiki, P. J.; Gust, D.; Moore, T. A. *J. Am. Chem. Soc.* **1986**, *108*, 5350.
(306) Liddell, P. A.; Kuciauskas, D.; Sumida, J. P.; Nash, B.; Nguyen, D.; Moore, A. L.; Moore, T. A.; Gust, D. *J. Am. Chem. Soc.* **1997**, *119*, 1400.
(307) Osuka, A.; Yamada, H.; Maruyama, K.; Mataga, N.; Asahi, T.; Ohkouchi, M.; Okada, T.; Yamazaki, I.; Nishimura, Y. *J. Am. Chem. Soc.* **1993**, *115*, 9439.
(308) Osuka, A.; Yamada, H.; Maruyama, K.; Mataga, N.; Asahi, T.; Yamazaki, I.; Nishimura, Y, *Chem. Phys. Lett.* **1991**, *181*, 419.
(309) Osuka, A.; Yamada, H.; Shinoda, S.; Nozaki, K.; Ohno, T. *Chem. Phys. Lett.* **1995**, *238*, 37.
(310) Steinberg-Yfrach, G.; Liddell, P. A.; Hung, S.-C.; Moore, A. L.; Gust, D.; Moore, T. A. *Nature* **1997**, *385*, 239.
(311) Steinberg-Yfrach, G.; Rigaud, J. L.; Durantini, E. N.; Moore, A. L.; Gust, D.; Moore, T. A. *Nature* **1998**, *392*, 479.
(312) Tan, Q.; Kuciauskas, D.; Lin, S.; Stone, S.; Moore, A. L.; Moore, T. A.; Gust, D. *J. Phys. Chem. B* **1997**, *101*, 5214.
(313) Parusel, A. *J. Mol. Model.* **1998**, *4*, 366.
(314) Debreczeny, M. P.; Wasielewski, M. R.; Shinoda, S.; Osuka, A. *J. Am. Chem. Soc.* **1997**, *119*, 6407.
(315) Osuka, A.; Kume, T. *Tetrahedron Lett.* **1998**, *39*, 655.
(316) Osuka, A.; Kume, T.; Haggquist, G. W.; Jávorfi, T.; Lima, J. C.; Melo, E.; Naqvi, K. R. *Chem. Phys. Lett.* **1999**, *313*, 499.
(317) Macpherson, A. N.; Liddell, P. A.; Kuciauskas, D.; Tatman, D.; Gillbro, T.; Gust, D.; Moore, T. A.; Moore, A. L. *J. Phys. Chem. B* **2002**, *106*, 9424.
(318) Mariño-Ochoa, E.; Palacios, R.; Kodis, G.; Macpherson, A. N.; Gillbro, T.; Gust, D.; Moore, T. A.; Moore, A. L. *Photochem. Photobiol.* **2002**, *76*, 116.
(319) *Grätzel, M.; Moser, J.-E. Solar Energy Conversion. In Electron Transfer in Chemistry*; Balzani, V., Gould, I., Eds.; Wiley-VCH: Weinheim, 2001; Vol. V, p 589 and references therein.
(320) Sahyun, M. R. V.; Serpone, N. *J. Photochem. Photobiol. A* **1998**, *115*, 231.
(321) Konovalova, T. A.; Kispert, L. A.; Konovalov, V. V. *J. Phys. Chem. B* **1999**, *103*, 4672.
(322) Gao, F. G.; Bard, A. J.; Kispert, L. D. *J. Photochem. Photobiol. A* **2000**, *130*, 49.
(323) Gruszecki, W. In *Photochemistry of Carotenoids*; Frank, H. A., Young, A. J., Britton, G., Cogdell, R. J., Eds.; Kluwer Academic Publishers: Dordrecht, The Netherlands, 1999; p 363.
(324) Fungo, F.; Otero, L.; Durantini, E. N.; Silber, J. J.; Sereno, L.; Mariño-Ochoa, E.; Moore, T. A.; Moore, A. L.; Gust, D. *J. Phys. Chem. B* **2001**, *105*, 4873.
(325) Sereno, L.; Silber, J. J.; Otero, L.; del Valle Bohorquez, M.; Moore, A. L.; Moore, T. A.; Gust, D. *J. Phys. Chem.* **1996**, *100*, 814.
(326) Pan, J.; Benkö, G.; Xu, Y.; Pascher, T.; Sun, L.; Sundström, V.; Polívka, T. *J. Am. Chem. Soc.* **2002**, *124*, 13949.
(327) Weng, Y.-X.; Li, L.; Liu, Y.; Wang, L.; Yang, G.-Z. *J. Phys. Chem. B* **2003**, *107*, 4356.
(328) Weng, Y.-X.; Li, L.; Liu, Y.; Wang, L.; Yang, G.-Z.; Sheng, J.-Q. *Chem. Phys. Lett.* **2002**, *355*, 294.
(329) Carbonera, D.; Di Valentin, M.; Corvaja, C.; Agostini, G.; Giacometti, G.; Liddell, P. A.; Kuciauskas, D.; Moore, A. L.; Moore, T. A.; Gust, D. *J. Am. Chem. Soc.* **1998**, *120*, 4398.
(330) Zhang, L.; Yang, J.; Wang, L.; Yang, G.-Z.; Weng, Y.-X. *J. Phys. Chem. B* **2003**, *107*, 13688.
(331) Lin, S.; Katilius, E.; Taguchi, A. K. W.; Woodbury, N. W. *J. Phys. Chem. B* **2003**, *107*, 14103.

CR020674N